Aus dem Fachbereich Medizin
der Johann Wolfgang Goethe-Universität
Frankfurt am Main

betreut am
Zentrum für Molekularen Medizin
Institut für Kardiovaskuläre Pharmakologie
Direktor: Prof. Dr. med. Stefan Offermanns
und am
Max-Planck-Institut für Herz- und Lungenforschung

Role of Orphan G-protein-coupled receptor GPRC5B in smooth muscle contractility and differentiation

Dissertation
zur Erlangung des Doktorgrades der theoretischen Medizin
des Fachbereichs Medizin
der Johann Wolfgang Goethe-Universität
Frankfurt am Main

vorgelegt von
Jorge Carvalho
M.Sc.Biochemie

aus Vila Real (Portugal)

Frankfurt am Main, 2019

Dekan:	Prof. Dr. Josef Pfeilschifter
Referentin:	Prof. Dr. Nina Wettschureck
Korreferentin:	Prof. Dr. Stefanie Dimmeler
2. Korreferent:	Prof. Dr. Ralf Brandes
Tag der mündlichen Prüfung:	02.06.2020

SUMMARY

G protein coupled receptors (GPCRs) are the largest family of cell-surface receptors encoded in the human genome. They mediate the cellular responses to a wide variety of stimuli, ranging from light, odorants, and metabolic cues to hormones, neurotransmitters, and local mediators. Upon ligand binding, the GPCR undergoes conformational changes resulting in the activation of heterotrimeric G-proteins belonging to the families G_s, $G_{i/o}$, $G_{q/11}$, $G_{12/13}$, which in turn mediate the downstream signaling. While most of the 360 non-olfactory GPCRs are well studied, approximately 120 GPCRs are still considered “orphan”, meaning that their mechanism of activation and biological function is unknown. GPCRs have been functionally described in the regulation of almost all organ systems, and their dysregulation has been implicated in the pathogenesis of a multitude of diseases. In the vascular system, the contractile tone of vessels is crucially regulated by GPCRs. Substances that act through $G_{12/13}$- and $G_{q/11}$-coupled GPCRs are associated with facilitation of contraction, while G_s-coupled GPCRs are usually associated with the induction of relaxation. Furthermore, while $G_{q/11}$ pathway activation promotes proliferation and dedifferentiation of vascular smooth muscle cells (VSMC), $G_{12/13}$ and G_s signaling pathways promote expression of contractile proteins and differentiation.

The functional properties of VSMC depend on the anatomical location, and a recent single-cell expression analysis showed that VSMC from different vascular beds have different patterns of GPCR expression. Interestingly, smooth muscle cells (SMCs) from resistance arteries not only express various GPCRs for known modulators of vascular tone, but also a number of orphan GPCRs. These results suggest a potential role of orphan GPCRs in the modulation of blood pressure. Orphan GPCR GPRC5B was one of the GPCRs enriched in resistance arteries, and this receptor was also upregulated in dedifferentiated aortal SMC. The function of GPRC5B in these types of SMC is currently unknown. In vitro studies suggested that GPRC5B negatively regulates obesity, inflammation, insulin secretion and fibrotic activity, but there are no data available with respect to its function in regulation of vascular tone or other SMC functions.

Our study aimed at the identification of the specific functions of GPRC5B in SMC. To do so, we generated a SMC-specific GPRC5B-deficient mouse line by crossing Gprc5b$^{fl/fl}$ mice with smooth muscle-specific, tamoxifen-inducible Myh11-CreERT2 mice. We found that SMC-specific deletion of GPRC5B did neither affect myogenic tone in pressure myography, nor the response to the contractile agonists in wire myography. In contrast, vessel relaxation in response to prostacyclin analogues cicaprost and iloprost, which act on the prostacyclin receptor IP, were increased. These results suggested a selective improvement of IP receptor signaling. The IP receptor is coupled to G_s protein, it promotes vasorelaxation and acts as a restraint on platelet activation. Using overexpression of IP and GPRC5B in HEK cells, we found that GPRC5B physically interacts with the IP receptor and controls IP trafficking and membrane localization. Furthermore, we found that membrane IP receptor expression was increased in GPRC5B-deficient human aortic SMC and in resistance vessels of SMC-specific GPRC5B. To investigate the importance of increased IP-mediated signaling in SMC in vivo, we measured blood pressure in two mouse models of hypertension. We found that SMC-deletion of *Gprc5b* resulted in a significant reduction of blood pressure compared with control mice, which suggested that *Gprc5b* negatively regulated relaxation in hypertensive disease by decreasing IP mediated relaxation. In line with this notion we found that application of the IP antagonist Cay10441 largely abrogated the beneficial effect of GPRC5B inactivation in this hypertension model. Another important function of the IP receptor is the regulation of SMC differentiation, which led us to investigate the differentiation state of GPRC5B-deficient SMC. We found that deletion of GPRC5B enhanced expression of contractile genes and reduced expression of proliferative markers. This improved differentiation was, at least partially, due to increased IP signaling in SMC. Moreover, in a mouse model of atherosclerosis SMC-specific deletion of *Gprc5b* reduced plaque area and contributed to a more stable fibrous cap by promoting differentiation.

In conclusion, deletion of GPRC5B in SMC significantly improved contractility and differentiation by increasing IP receptor membrane availability and signaling.

ZUSAMMENFASSUNG

G-Protein-gekoppelte Rezeptoren (GPCRs) stellen die größte Familie der im menschlichen Genom kodierten Zelloberflächenrezeptoren dar. Sie vermitteln die zellulären Reaktionen auf so diverse Stimuli wie Licht, Gerüche, Metaboliten, Hormone, Neurotransmittern und lokalen Mediatoren. Nach Ligandenbindung an den GPCR kommt es zu Aktivierung heterotrimerer G-Proteine der Familien G_s, $G_{i/o}$, $G_{12/13}$ und $G_{q/11}$, welche dann die nachgeschalteten Signale vermitteln. Während die meisten der 360 nicht-olfaktorischen GPCRs gut erforscht worden sind, gibt es noch ungefähr 120 “verwaiste” (engl. „orphan“) GPCRs für die sowohl der Aktivierungsmechanismus als auch die biologische Funktion unbekannt sind. GPCRs sind bei der Steuerung fast aller Organsysteme von Bedeutung, und ihre Dysfunktion ist mit der Pathogenese einer Vielzahl von Krankheiten in Verbindung gebracht worden. Im vaskulären System sind GPCRs unabdingbar für die Regulation des Gefäßtonus. Substanzen, die über $G_{12/13}$- und $G_{q/11}$-gekoppelte GPCRs agieren, werden mit der Förderung von Kontraktionen in Verbindung gebracht, während Aktivierung G_s-gekoppelter GPCRs gewöhnlich zu Relaxierung führt. Darüber hinaus führt Aktivierung des $G_{q/11}$-Signalweges zu Proliferation und Dedifferenzierung von vaskulären glatten Muskelzellen (im Folgenden “SMCs” für “smooth muscle cells”), während die Signalwege $G_{12/13}$ und G_s die Expression von kontraktilen Proteinen und die Differenzierung fördern.

Die funktionalen Eigenschaften von vaskulären SMCs hängen von ihrer anatomischen Verortung ab, und eine kürzlich erfolgte Einzelzell-Expressionsanalyse zeigte, dass aus verschiedenen vaskulären Betten stammende SMCs verschiedene GPCR-Expressionsmuster aufweisen. Interessanteweise exprimieren SMCs aus Widerstandsarterien nicht nur verschiedene GPCRs für bekannte Modulatoren des vaskulären Tonus, sondern auch eine Anzahl von “orphan”-GPCRs. Diese Ergebnisse legen eine potentielle Rolle von “orphan”-GPCRs bei der Modulation des Blutdruckes nahe. GPRC5B war einer derjenigen „orphan“-GPCRs, die in Widerstandsarterien angereichert waren, und zusätzlich war dieser Rezeptor in dedifferenzierten Aorten-SMCs hochreguliert. Die Funktion von GPRC5B in diesen Arten von SMCs ist momentan noch unbekannt.

Unsere Untersuchungen zielen auf eine Identifizierung der spezifischen Funktionen von GPRC5B in SMCs ab. Dafür generierten wir eine SMC-spezifische, Tamoxifen-induzierbare GPRC5B-defiziente Mauslinie, indem wir Gprc5b$^{fl/fl}$-Mäuse mit Myh11-CreERT2-Mäusen kreuzten. Myographische Untersuchungen zeigten, dass die Deletion von GPRC5B in SMCs weder Einfluss auf den myogenen Tonus noch auf die Antwort auf kontraktile Agonisten hatte. Im Gegensatz dazu war die durch Prostazyklinrezeptor (IP)-Agonisten induzierte Gefäßrelaxation verstärkt, was auf eine selektive Verbesserung der IP-Rezeptor-Signalweiterleitung hindeutete. In Überexpressionsstudien in HEK-Zellen konnten wir zeigen, dass GPRC5B physisch mit dem IP-Rezeptor interagiert und dessen Lokalisierung in der Zellmembran kontrolliert. In Übereinstimmung damit fanden wir in GPRC5B-defizienten humanen Aorten-SMCs und in Widerstandsgefäßen von SMC-spezifischen GPRC5B-*Knockout*mäusen eine erhöhte Verfügbarkeit von IP-Rezeptoren. Um die Bedeutung erhöhter IP-vermittelter Signalweiterleitungsaktivität in SMCs *in vivo* zu untersuchen, führten wir Blutdruckmessungen in zwei Mausmodellen des Bluthochdruckes durch. Wir fanden, dass die Deletion von *Gprc5b* in SMCs im Vergleich zu Kontrollmäusen eine signifikante Reduktion des Blutdruckes zur Folge hatte und dass die Applikation des IP-Antagonisten Cay10441 diesen günstigen Effekt weitgehend aufhob. Da der IP-Rezeptor auch dafür bekannt ist, die Dedifferenzierung von SMCs zu hemmen, untersuchten wir zusätzlich den Differenzierungszustand von GPRC5B-defizienten SMCs. Es zeigte sich, dass die Deletion von GPRC5B die Expression von kontraktilen Genen verstärkte und die Expression proliferativer Marker abschwächte. Dieser Differenzierungsphänotyp von SMCs war, zumindest teilweise, auf eine erhöhte Signalweiterleitungsaktivität von IP in SMCs zurückzuführen. Darüber hinaus reduzierte die SMC-spezifische Deletion von *Gprc5b* in einem Atherosklerose-Mausmodell die Ausbreitung von Plaques und trug durch seine Differenzierungs-fördernde Wirkung zu einer stabileren fibrösen Kappe bei.

Aus diesen Arbeiten schlussfolgern wir, dass die Deletion von GPRC5B in SMCs über eine Steigerung der Membranverfügbarkeit des IP-Rezeptores die Kontraktionsfähigkeit und Differenzierung deutlich verbessert.

TABLE OF CONTENTS

I. ABBREVIATIONS

7TM	Seven-helix transmembrane domain
ACTA2	α-smooth muscle actin
AngII	Angiotensin II
apo-E	Apolipoprotein E
AR	Adrenergic receptors
AT_1R	Angiotensin II receptor
ATP	Adenosine triphosphate
BP	Blood pressure
cAMP	Cyclic adenosine monophosphate
CaSR	Calcium-sensing receptor
CCNA2	Cyclin A2
Col1	Collagen type I
Col3	Collagen type III
COX-1	Cyclooxygenase 1
CRD	Cysteine rich domain
Da	Dalton
DAPI	4’,6-diamidin-2-phenylindol
DIT	Diffuse intimal thickening
DOCA	Deoxycorticosterone acetate
EC	Endothelial cell
ECD	Extracellular domain
ECM	Extracellular matrix
EP2	Prostaglandin E2 receptor
EP4	Prostaglandin E4 receptor
ER	Endoplasmic reticulum
Erk1/2	Extracellular signal-regulated kinase 1/2
ETA	Endothelin-1 receptor
FZDs	Frizzled GPCRs
$GABA_B$	Gamma-amino-butyric acid type B
GAP	GTPase-activating proteins
GDP	Guanosine diphosphate

GEF	Guanine nucleotide exchange factor
GO	Gene Ontology
GPCR	G-protein-coupled receptor
GTP	Guanosine triphosphate
Gα	G-protein α subunit
Gβγ	G-protein βγ subunit
hAoSMC	Human aortic SMC
HEK	Human embryonic kidney
HEK293T	Human embryonic kidney
IP	Prostacyclin receptor
kd	Knock down
KO	Knockout
KLF4	Krüppel-like factor 4
LDL-R	Low-density lipoprotein receptor
MAPK	Mitogen-activated protein kinase
MAPKs	Mitogen-activated protein kinase
mGluR	Metabotropic glutamate receptors
MLC20	Myosin light chain at the Ser-19
MLCK	Myosin light chain kinase
MLCP	Myosin light chain phosphatase
MMP	Metalloproteinase
MRTF	Myocardin related transcription factor
MYH11	Smooth muscle myosin heavy chain
MYOCD	Myocardin
PCNA	Proliferating cell nuclear antigen
PCR	Polymerase chain reaction
PGH2	Prostaglandin H2
PGI_2	Prostaglandin I2
PIT	Pathological intimal thickening
PKA	Protein kinase A
PLC-β	Phospholipase C-β
RAAS	Renin-angiotensin-aldosterone system
RhoA	Ras homolog gene family member A

$S1P_1$	Sphingosine 1-phosphate receptor 1
$S1P_3$	Sphingosine 1-phosphate receptor 3
SER	Serum response elements
SMao	Aotic smooth muscle cells
SMmes	Mesenteric smooth muscle cells
SMMHC	Smooth muscle myosin heavy chain
SMsk	Skeletal smooth muscle cells
SMTN	Smoothelin
SNP	Sodium nitroprusside
SNS	Sympathetic nervous system
SRF	Serum response factor
TAGLN	Transgelin
TAS	Taste receptors
TCF	Ternary complex factor
TIMP	Tissue inhibitors of MMP
TP	Thromboxane receptor
TXA_2	Thromboxane A2
VSMC	Vascular smooth muscle cells
VTF	Venus flytrap domain
α-AR	α-adrenergic-receptor
αSMA	α-smooth muscle actin
β-AR	β-adrenergic receptor

II. INTRODUCTION

1. Vascular smooth muscle cells

Vascular smooth muscle cells (VSMCs) are an important cellular component of the blood vessel wall. They provide structural integrity and regulate the diameter of the blood vessels through their dynamic contraction or relaxation in response to vasoactive stimuli such as hormones, metabolites and neurotransmitters. This adaptation of the vascular diameter is very important to maintain adequate transport of oxygenated blood, nutrients, hormones and metabolites, immune cells and waste products to and from all tissues/organs in the body. In addition to their role in the acute regulation of vascular tone, VSMC have the ability to adapt expression of proteins involved in contraction and extracellular matrix (ECM) synthesis depending on extrinsic and intrinsic cues during developmental stages as well as in response to disease or injury [1, 2]. This phenotypic modulation allows SMC to transiently adopt a more proliferative, migratory and matrix synthesizing phenotype (also known as SMC dedifferentiation), which allows the vessel to adapt to hemodynamic changes or to contribute to the vascular response to injury and inflammation. However, chronic dysregulation of this process is known to contribute to vascular diseases and can be detrimental in atherosclerosis and restenosis [1, 3]. Elucidating the molecular mechanisms underlying VSMC migration and proliferation is crucial in the development of therapeutic agents to control the disease process of these vascular lesions.

1.1. Role in Physiology - Contractility

Vascular tone refers to the degree of vessel constriction relative to a maximally dilated state and is determined by a balance between local vasodilator and vasoconstrictor molecules [3]. There are three main types of blood vessels: arteries, veins, and capillaries [4, 5] (Figure 1). The artery is a blood vessel that conducts blood away from the heart. The heart pumps blood into these elastic tubes, which recoil, ensuring fast and efficient blood flow to the tissues. This requires a strong, elastic and thick wall on the composition of these vessels that can withstand the high pressure of blood ejected from the heart [6, 7]. The wall of an artery, no matter what its size, is composed of three distinct tissue layers. From the most interior layer to the outer, these layers are the tunica intima, tunica media and

tunica externa. The tunica intima is predominantly populated with endothelial cells (ECs) (endothelium) sitting on elastic tissues. The tunica media is composed of VSMCs intermingled with elastic fibers, and as the arteries became smaller, the number of elastic fibers decreases while the number of VSMCs increases in the composition of this tunica. The outermost layer, the tunica externa or adventitia, consists mainly of collagen and elastic fibers that act as a supportive element protecting the vessel from overexpansion [8-10] (Figure 1).

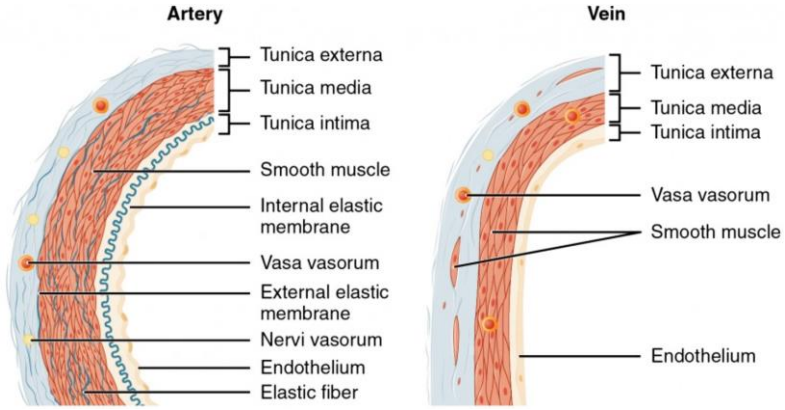

Figure 1 – Schematic representation of an artery (left) and a vein (right). (Adapted from Anatomy & Physiology, provided by OpenStax CNX).

The VSMCs, which maintain vascular homeostasis, display diversity in function and phenotype depending on their location within the arterial tree, contributing to its functional characteristics. The strength/size of the muscle layer is related to the function of the artery. According to this feature, the arteries can be divided in elastic arteries, muscular arteries and resistance arteries (Figure 2) [7, 11]. Arteries such as aorta, large aortal branches, and pulmonary artery contain a high amount of elastin in all three of their layers and thereby are designed as elastic (conducting) arteries. The elastic connective tissue enables the expansion of the artery as blood enters the lumen, withstanding the high pressure of blood ejected from the heart, and also enables recoiling of the vascular wall, driving the blood through the arterial system, maintaining the gradient pressure. Due to the large diameter of the lumen, which provides low resistance to blood flow and promotes the conduction of blood to smaller branches, these arteries are also known as conducting arteries, having no main role in the blood pressure and flow regulation under normal physiological conditions (Figure 2). Femoral, radial and mesenteric arteries have a thin tunica intima and an increased number of SMCs in the thick

tunica media which provides resistance to blood flow. These arteries are described as muscular arteries. They have a decreased amount of elastin which restricts the expansion ability, in contrast, the thick SMC layer allows them to play a leading role in vasoconstriction by regulating the mean arterial pressure and tissue perfusion. Muscular arteries also exhibit a substantial intrinsic myogenic tone response to circulating hormones and endothelial substances [12-14] (Figure 2). Arterioles and small arteries (skin vessels, inner organs, skeletal muscle, etc.) are referred as resistance vessels. They play a critical role in the regulation of vascular resistance via modulation of the contractile tone in the SMCs, a hallmark feature of this kind of vessels, via vasoconstriction and vasodilation [15, 16]. Resistance vessels represent the primary site of both resistance and regulation of blood pressure as well as blood flow within the organ [17]. Resistance arteries consist of the same three layers as other types of arteries, but the thickness is greatly diminished. However, relative to the vessel size, the tunica media, restricted to one or two smooth muscle cell layers, is relatively thick [18-20] (Figure 2).

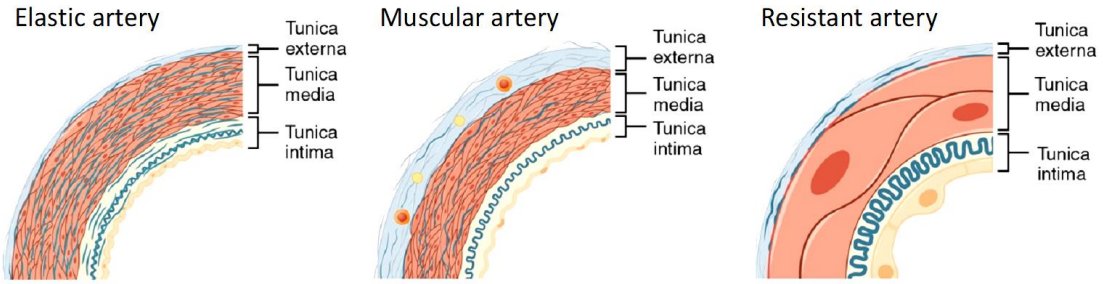

Figure 2 – Types of Arteries. Comparison of the walls of an elastic artery, a muscular artery, and a resistance artery. (Adapted from Anatomy & Physiology, provided by OpenStax CNX).

1.2. Role in Physiology - Differentiation

In addition to their role in vascular tone regulation, VSMC have important functions during growth and in response to injury [21]. It is known, from morphological and biochemical studies, that there are two distinct phenotypes of VSMCs in the vessel wall, 1) the differentiated contractile and 2) the synthetic proliferative phenotype, which differ in terms of gene expression [22, 23]. The differentiated state of contractile VSMCs is characterized by the expression of contractility proteins, contractility-regulating proteins, receptors for

contractile/relaxant mediators, and signaling proteins responsible for contraction and maintenance of vascular tone. The most discriminatory markers expressed in the contractile phenotype are α-smooth muscle actin (αSMA/ACTA2) [24], smooth muscle myosin heavy chain (SMMHC/ MYH11) [25], smoothelin (SMTN) [26] and transgelin (TAGLN/SM-22α) [27]. In addition, contractile VSMCs secrete different levels of ECM components (increased collagens, elastins and proteoglycans) and matrix-modifying enzymes (decreased matrix metalloproteinases [MMPs] and increased tissue inhibitors of matrix metalloproteinases [TIMPs]) [28-32]. Synthetic VSMCs, in contrast, are characterized by high proliferation rates, significant migration activity and extensive ECM synthesis/degradation capabilities. The expression of SMC-related genes for contractile proteins (ACTA2/TAGLN) is decreased with concomitantly increased expression of pro-inflammatory cytokines, matrix metalloproteinases (MMPs) and proliferative markers such as proliferating cell nuclear antigen (PCNA) [33, 34] and cyclin A2 (CCNA2) [1, 21, 35]. Differentiated SMCs proliferate at extremely low rates and produce only small amounts of ECM proteins. These processes are greatly accelerated during development of the vascular system, during vessel remodeling, following vessel injury, and in atherogenesis [1, 36, 37]. In these circumstances, VSMC can in fact, acquire a broad spectrum of different phenotypes. This remarkable plasticity must be considered a necessary part of the SMC differentiation program, which can change relatively rapid and can be reversible.

1.2.1. Regulation of SMC differentiation

Different physiological or pathological stimuli modulate the VSMC phenotype, ranging from the contractile state to maintain vascular tone to the synthetic or proliferative state in response to vascular injury [38, 39]. During the last years an enormous effort has be made to study the mechanisms that contribute to transcriptional regulation of SMC marker genes. At the molecular level, the VSMC phenotype is driven by transcription factors - including serum response factor (SRF) [40] and Krüppel-like factor 4 (KLF4) [37]. The widely expressed transcription factor SRF, which belongs to the MADS box transcription factor superfamily, binds to serum response elements (SRE), which are characterized by CArG-box elements within the promoters of contraction-related genes,

regulating their transcription [41]. The target spectrum of the SRF does not only consist of SMC differentiation marker genes such as αSMA, MYH11, but also of growth-related genes involved in smooth muscle proliferation and dedifferentiation, as example the proto-oncogene c-FOS [42] and the early growth response 1 (EGR1) [43]. Two families of transcriptional co-factors differentially modulate the transcription of these distinct SRF target genes through their mutually exclusive binding to SRF, 1) the myocardin family, consisting of myocardin (MYOCD) itself and myocardin related transcription factors (MRTFs) A and B, and 2) the ternary complex factor (TCF) family of Ets-domain proteins [40]. While transcription co-factors of the myocardin family promote VSMC differentiation, competitive binding of TCFs induces transcription of early response growth genes as well as VSMC dedifferentiation and proliferation. RhoA-mediated signaling promotes nuclear translocation of MRTFs and induces smooth muscle differentiation, while dedifferentiation is driven by phosphorylation and activation of TCFs through the extracellular signal-regulated kinase 1/2 (Erk1/2) pathway [44-46] (Figure 3).

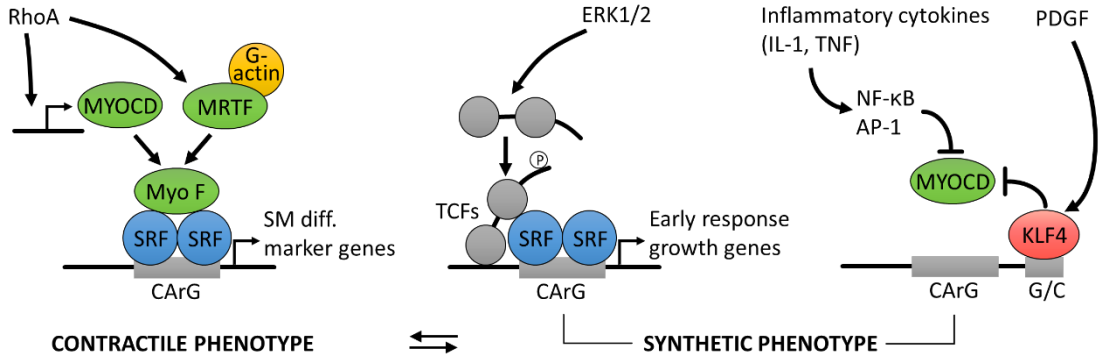

Figure 3 – Molecular mechanisms underlying VSMC plasticity. Transcriptional control of VSMC plasticity. Ternary complex factors (TCFs), myocardin related transcription factor A (MRTF), myocardin (MYOCD), myocardin family of transcriptional cofactors (Myo F), activator protein 1 (AP-1). (Adapted from [39] and [47]).

The Krüppel-like factor 4 (KLF4), a transcription factor involved in pluripotency [48] and induced in post injury VSMCs, represses the expression of contraction-related genes through several mechanisms. It can 1) interact with enhancers in smooth muscle growth genes, 2) inhibit smooth muscle differentiation genes, and 3) bind to G/C repressor elements inhibiting SRF

binding to CArG-box repressing MYOCD expression. For both SRF-MYOCD and SRF-KLF4 systems, SRF serves as a platform for myogenic cofactors that compete for a common docking site, thereby mediating VSMC phenotypic switching [49] (Figure 3).

The ability for VSMC to dedifferentiate and redifferentiate enables vascular development, repair and adaptation to chronically altered hemodynamics. This phenotypic plasticity is therefore considered as a requirement for vascular remodeling processes [50].

1.3. Role of VSMC in disease

Dysregulation of VSMC plasticity results in pathological vascular remodeling, a typical hallmark of vascular diseases like atherosclerosis, hypertension and neointima. These diseases have common features, mainly thickening of the vessel wall and narrowing of the vascular lumen, which is due, among other reasons, to the activation of migration, growth, changes in cell morphology and protein synthesis in VSMCs.

1.3.1. Atherosclerosis

Atherosclerosis is the main pathological process underlying several diseases such as myocardial infarction, heart failure and stroke. It is characterized as a chronic progressive inflammatory disorder described by the formation of plaques containing lipids, cells, debris and scar tissue in the intima of arteries [51]. The development and expansion of plaques is a continuous process, driven by uptake of circulating lipoproteins, recruitment of inflammatory cells from blood, migration of dedifferentiated SMCs into lesions and secretion of matrix from SMCs. The macrophages and dedifferentiated VSMCs are the key players in this process [52] (Figure 4). Some in vivo studies suggest that VSMCs are the most abundant cells in atherosclerotic lesions and they contribute the majority of total foam cells [53]. Additionally, a great number of lineage tracing studies demonstrated that 30% to 70% of all plaque cells are derived from recruitment and proliferation of VSMCs, which indicates the great plasticity of VSMC in atherogenesis [37, 54-56]. These VSMC-derived cells do not have detectable levels of common SMC markers (ACTA2, MYH11), instead, some cells (>30%) are positive for multiple markers that have been previously used to study macrophages in

atherosclerosis, including LGALS3/Mac2, CD11b, F4/80, and CD68 [37, 57, 58]. These VSMC-to-macrophage transdifferentiated cells promote atherosclerosis by having reduced ability to clear lipids, dying cells and necrotic debris, and by exacerbating inflammation [54, 59]. However, VSMC-entry into the plaque may also have beneficial effects, in particular if smooth muscle identity is maintained. In this case, plaque-SMC have been suggested to promote plaque repair and protect the fibrous cap from rupture [60]. Notably, most of αSMA cells within the fibrous cap are positive for VSMC-lineage label [51, 61].

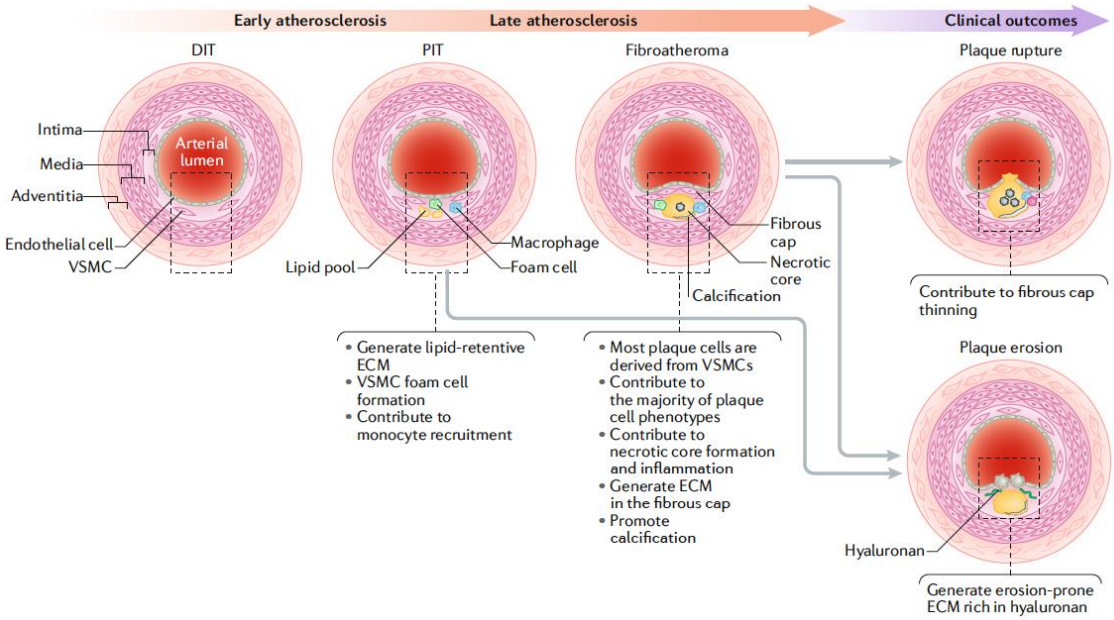

Figure 4 – Overview of the role of VSMCs in atherosclerosis. Vascular smooth muscle cells (VSMCs) are a major source of plaque cells and extracellular matrix (ECM) at all stages of atherosclerosis and contribute to numerous processes throughout the disease. DIT, diffuse intimal thickening; PIT, pathological intimal thickening. (Adapted from [47]).

1.3.2. Hypertension

Arterial hypertension or hypertension is an asymptomatic medical condition characterized by persistent high blood pressure (BP). It is defined by systolic BP ≥130 mmHg and/or diastolic BP ≥80 mmHg and is one of the key risk factors for cardiovascular diseases. BP is controlled by several parameters of the cardiovascular system, including blood volume, cardiac output, as well as the arterial tone, which is affected by both intravascular volume and neurohumoral systems [62]. The maintenance of normal BP levels is a complex process that

includes the renin–angiotensin–aldosterone system (RAAS), the roles of natriuretic peptides, the endothelium, the sympathetic nervous system (SNS) and the immune system. Disturbance of any of these factors may directly or indirectly result in blood pressure dysregulation [63]. These changes might be beneficial: In a stressful situation for example, the body can trigger a sequence of hormonal changes and physiological responses as a survival mechanism which results in a temporary increase of the blood pressure by narrowing of the blood vessels and by causing the heart to beat faster [64]. However, in chronic high BP as well as in disease states, these adaptive changes do not return to baseline levels, instead they initiate pathological vascular alterations which result in vascular remodeling [65].

Vascular remodeling is a heterogeneous process and differs depending on the vessel type, specific disease severity or progression [66]. The remodeling process is characterized essentially by wall thickening, driven by proliferation, migration and hypertrophy of VSMCs with consequently increased of chemokine and cytokine production as well as ECM production and degradation [67, 68]. Highly differentiated VSMCs, which normally express genes and proteins important for the regulation of vascular tone, become under pathological conditions hypercontractile and undergo phenotypic dedifferentiation, assuming a proliferative/migratory phenotype [1, 69]. The molecular mechanisms underlying the cellular phenotypic switch in hypertension are complex and diverse. It is known that some vasoactive stimuli (Angiotensin II (AngII), norepinephrine (NE)), growth factors (IGF-1, EGF, PDGF), mechanical forces (stretch, shear stress, pressure), induce changes in expression and function of genes important in vascular hypertrophy in hypertension [70-72]. Moreover, signaling pathways that regulate contraction/relaxation such as IP_3-PKC-DAG and ROCK-SRF/myocardin are dysregulated and signaling pathways not typically associated with contraction, such as MAPKs, tyrosine kinases, and transcription factors are activated [73-76]. In fact, it has been acknowledged that the SRF/MYOCD pathway represents an essential mechanism underlying the regulation of aortic VSMC properties and arterial stiffness [73, 74]. In the early stages of hypertension, the vascular remodeling due the increased blood pressure is beneficial and allows the vessel to adapt to transient hemodynamic

changes, however in a long term contributes to chronic remodeling and vascular dysfunction in which VSMCs are critically involved [76].

2. G-protein-coupled receptors

G-protein-coupled receptors (GPCRs), also known as seven-transmembrane domain receptors, are the largest family of membrane receptors in eukaryotes [77]. The genes encoding GPCRs account for approximately 4% of the protein-coding human genome [78]. The human genome encodes approximately 800 GPCRs, the majority of them olfactory receptors. For most of the approximately 360 non-olfactory GPCRs endogenous ligand and biological function are well studied. Due the ability to bind ligands with high specificity and affinity, GPCRs are the most common target for therapeutic drugs, about 36% of currently marketed drugs target human GPCRs [79, 80]. However, for more than 120 GPCRs the endogenous ligand remains unidentified, leaving these GPCRs as “orphan” receptors without known ligands and functions [81-83]. GPCRs have regulatory functions in almost all organ system. GPCRs transduce signals of numerous physicochemical stimuli including neurotransmitters, hormones, local mediators, metabolic or olfactory cues, and light [84], and thereby control key physiological functions such as neurotransmission, hormone and enzyme release from endocrine and exocrine glands, immune responses, cardiac and smooth muscle contraction, vision and olfaction [85-87]. Dysregulation of GPCR signaling has been implicated in the pathogenesis of a multitude of diseases [88-92].

The G protein-mediated signaling system consists of a receptor, a heterotrimeric G protein, and an effector, which allows convergence and divergence at the interfaces of receptor and G protein as well as of G protein and effector [86]. Based on shared sequence and structural features, GPCRs are classified into five major families: rhodopsin (class A), secretin (Class B), metabotropic glutamate (Class C), frizzled and adhesion [93]. The rhodopsin family (class A) is the largest of the five families of GPCRs, the endogenous ligands of these GPCRs include rhodopsins, catecholamines, acetylcholine, prostanoids, lipids, sugars and peptides [94]. The secretin family of GPCRs (Class B) includes 15 receptors for peptide hormones such as secretin, glucagon, and glucagon like peptide-1 and glucose-dependent insulinotropic peptide. These receptors are

important drug targets in many human diseases, including metabolic diseases and cancer [95]. The metabotropic glutamate GPCRs family, also known as class C family, is characterized by a large extracellular domain and constitutive dimers formation during activation. This family includes metabotropic glutamate receptors (mGluR), the gamma-amino-butyric acid type B ($GABA_B$) receptors, the calcium-sensing receptor (CaSR) as well as sweet and amino acid taste receptors [96]. The frizzled class GPCRs (FZDs) are activated by cysteine-rich lipo-glycoproteins and important progress has been made pointing to a direct activation of G proteins after WNT stimulation [97]. And finally, the adhesion GPCR family comprise 33 orphan receptors, identified by a very long N-termini with multiple functional domains known for the ability to facilitate cell and matrix interactions [98].

Upon ligand binding, GPCRs undergo conformational changes resulting in the recruitment/ activation of heterotrimeric G-proteins. GPCRs can be coupled to different types of G-proteins meaning that they can also modulate multiple cell responses via distinct signaling pathways [86]. Heterotrimeric G-proteins consist of an α-, a β- and a γ-subunit, the last two form a dimer complex. The Gα-subunit binds and hydrolyzes GTP, which leads to its dissociation from the dimeric Gβγ-subunits complex. Both Gα-GTP subunits and Gβγ subunit complexes can regulate a variety of downstream effectors [86, 99]. The G protein-mediated signaling system is functionally versatile due its modular architecture, and the numerous subtypes of G α-, β- and γ-subunits. The α-subunits, which define the basic properties of the heterotrimeric G protein, can be grouped into four families, $G\alpha_s$, $G\alpha_i/G\alpha_o$, $G\alpha_q/G\alpha_{11}$, and $G\alpha_{12}/G\alpha_{13}$. Most receptors are able to activate more than one G protein subtype. The expression pattern as well as the functional properties behind each family is very specific [99, 100].

Depending on what types of G-proteins are activated by a given receptor, different responses are triggered. GPCRs coupled to G_s and $G_{i/o}$ proteins activate or inhibit adenylyl cyclase, respectively. Adenylyl cyclase catalyzes the conversion of adenosine triphosphate (ATP) to 3',5'-cyclic adenosine monophosphate (cAMP), which is an important secondary messenger activating downstream effectors, such as protein kinase A (PKA) [101-103]. GPCRs

coupled to G_q/G_{11} and G_{12}/G_{13} activate phospholipase C-β (PLC-β) and Rho guanine nucleotide-exchange factors (GEFs), respectively [86, 104, 105]. Although these are the main and best-characterized downstream effectors, a variety of other effectors have also been described such as cadherins, A-kinase anchoring proteins, non-receptor tyrosine kinases and protein phosphatases [106]

2.1. GPCRs in the vascular system - contractility

The vascular system is rich in GPCRs, but the GPCR expression and functional responses differ depending on the vessel location and size. [107, 108]. They can modulate critical parameters such as vessel tone or smooth muscle differentiation and they can be activated by diverse chemical entities. These chemical messengers can function in blood vessels in different manners: directly acting vasoconstrictors (Figure 5), directly acting vasodilators or indirectly acting vasodilators (Figure 6) [39, 109].

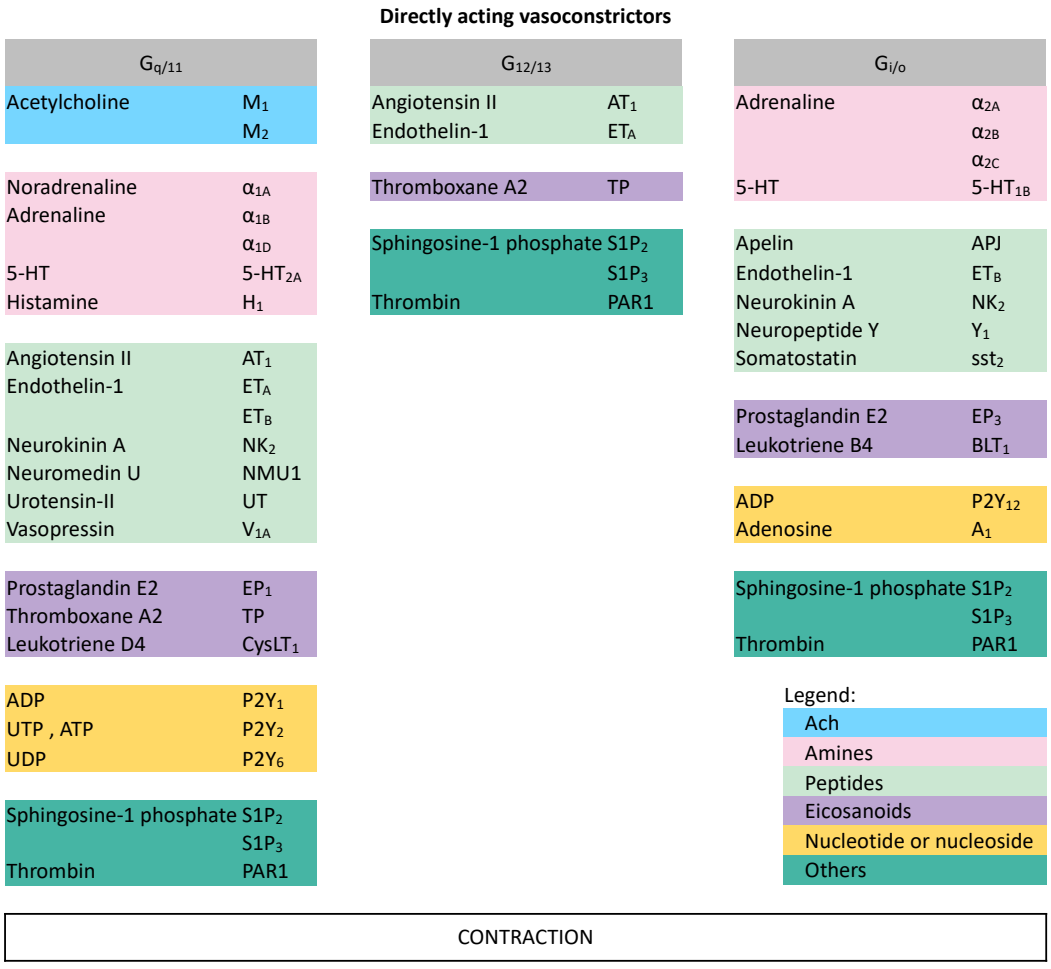

Figure 5 – Known and newer GPCRs that mediate vasoconstriction. Some receptors can be linked to more than one signaling cascade via different G-protein families, $G_{q/11}$, $G_{12/13}$ and/or $G_{i/o}$. The overall consequence is an increase in vascular tone. Ligands are grouped in colour-coded boxes based on their related chemical structure. (Adapted from [107]).

The indirect dilators, transduce their chemical message by GPCRs present on the surface of endothelial cells which induce production/release of dilatory factors such as NO or endothelium-derived hyperpolarising factor (EDHF) from the endothelium and dilatation of the underlying smooth muscle [110]. The search for new GPCRs regulating vascular tone is constant. In fact, over the past few years new ligands have been discovered, some with vasoconstrictor activity, including the apelin, motilin, neuromedin U, or sphingosine-1-phosphate, and some with vasodilation activity, such as ghrelin and nociceptin [107].

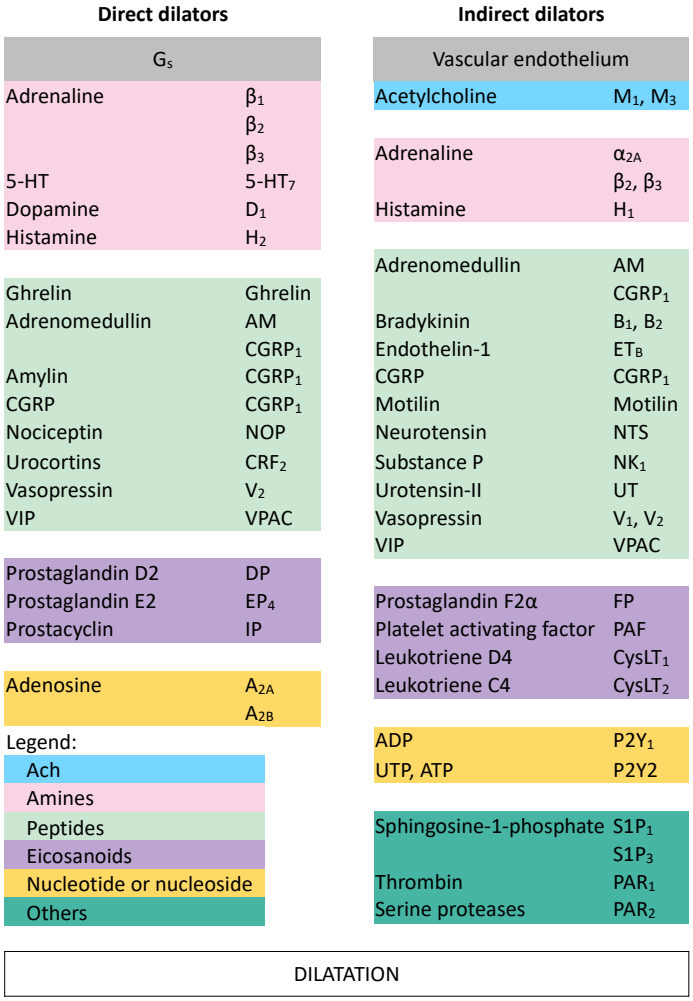

Figure 6 – GPCRs that mediate direct or indirect vasodilatation. Binding of ligands to receptors present on VSMC that are predominantly coupled via G_s results in subsequent vasodilatation (Direct vasodilatation). A large number of

GPCRs are localized on the vascular endothelium and their activation leads to vascular smooth muscle vasodilatation (indirect vasodilatation). The key indicates the colour-coded grouping of the endogenous ligands for vascular GPCRs by related chemical structure. (Adapted from [107]).

The intracellular signaling pathways induced by GPCRs critically mediate VSMC constriction or relaxation depending on the type of G-protein family activated. $G_{q/11}$, $G_{12/13}$ and/or $G_{i/o}$ are associated with vasoconstriction, while G_s is predominantly related to vasodilation [39, 107, 111]. A central process in the regulation of smooth muscle cell tone is the phosphorylation of Ser-19 of the regulatory light chain (MLC20) of myosin II [108, 112]. MLC20 is phosphorylated by the Ca^{2+}/Calmodulin (CaM)-dependent myosin light chain kinase (MLCK), this results in the interaction of MLC with αSMA filaments, initiating cross-bridge cycling and the generation of force which in turn produces contraction. Dephosphorylation of MLC20 is mediated by myosin phosphatase (MLCP), an enzyme that is negatively regulated by the Rho/Rho-kinase (ROCK) pathway. Thus increased contractility can be achieved through Ca^{2+}-mediated MLCK activation and through Rho-dependent inhibition of MLC20 dephosphorylation [86, 113, 114]. Vasoconstrictors such as angiotensin II, endothelin-1, sphingosine 1-phosphate, whose receptors AT_1R, ET_A, and $S1P_3$ are coupled to $G_{12/13}$ and $G_{q/11}$ proteins, facilitate the phosphorylation of the regulatory myosin light chain MLC20, thereby increasing actomyosin contractility. In detail, the activation of GPCRs and subsequent signaling via $G_{q/11}$ is responsible for the phosphorylation of myosin light chain (MLC20) by enhancing intracellular Ca^{2+} concentration, leading to MLCK activation. Signaling via $G_{12/13}$ inhibits dephosphorylation of MLC20 by phosphorylation of MLC phosphatase (MLCP) via Rho/ROCK-mediated signaling [114-116]. In addition, many $G_{q/11}$ coupled receptors have been shown to activate RhoA, thereby contributing to Ca^{2+}-independent smooth muscle contraction [114]. In contrast, G_s-coupled GPCRs such as prostacyclin receptor IP, adrenergic receptor β_2, or prostaglandin E_2 receptors EP2 and EP4 were shown to induce vascular smooth muscle relaxation [117-119]. Formation of cAMP, hyperpolarization of the membrane potential, or PKA-dependent interference with RhoA-mediated signaling were suggested as mechanisms underlying this G_s-dependent relaxation [39, 120]. Some GPCRs activated by vasoconstrictors also couple to G-proteins of the G_i family, which

may contribute to the procontractile activity of their ligands by activation of PLC-β or by inhibition of adenylyl cyclase, which decreases the intracellular levels of cAMP [86, 121-123] (Figure 7).

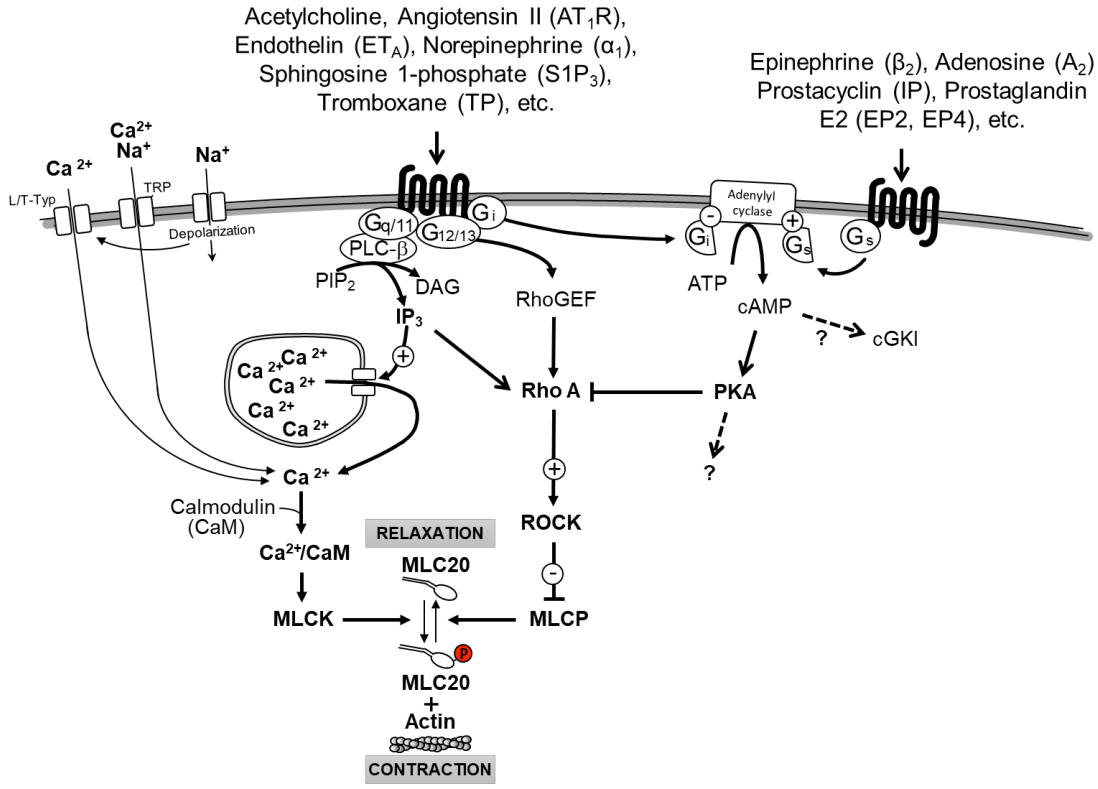

Figure 7 – Heterotrimeric G proteins involved in the regulation of smooth muscle tone. G_q/G_{11}-coupled receptors increase the intracellular Ca^{2+} concentration, leading to Ca^{2+}/calmodulin (CaM)-dependent MLCK activation and MLC20 phosphorylation. Especially G_{12}/G_{13}-coupled receptors mediate RhoA activation, thereby contributing to Ca^{2+}-independent smooth muscle contraction. Relaxation is induced by activation of G_s-coupled receptors, but the mechanisms underlying cAMP-mediated relaxation are not clear. G_i-mediated signaling might contribute to contraction by inhibiting G_s-mediated relaxation. cGMP-dependent protein kinase I (cGKI), diacylglycerol (DAG), inositol 1,4,5-trisphosphate (IP3), regulatory chain of myosin II (MLC20), myosin light-chain kinase (MLCK), myosin phosphatase (MLKP), phosphatidylinositol 4,5-bisphosphate (PIP2), cAMP-dependent kinase (PKA), phospholipase C-β (PLC-β), Rho specific guanine nucleotide exchange factor (RhoGEF), Rho-kinase (ROCK), transient receptor potential channel (TRP). (Adapted from [39]).

2.1.1. Vasocontractile ligands

a. Angiotensin II

Angiotensin II (AngII) is a vasoactive peptide that regulates blood pressure by directly controlling the VSMC tone, and indirectly by enhancing sympathetic tone, aldosterone secretion, and induction of cardiac hypertrophy. It is therefore a key player in hypertension [124].

There are two distinct AngII receptors: the angiotensin type 1 (AT_1R) and type 2 (AT_2R) receptors. Both are seven-transmembrane GPCRs which activate different signaling pathways with contrasting responses [125]. The AT_1R is abundantly expressed in numerous tissues, including vascular smooth muscle, endothelium, heart, brain, kidney, adrenal gland, and adipose tissue and facilitates most of the physiological functions induced by AngII, by mediating several signal transduction cascades causing hypertension, vascular remodeling, and organ damage. While still controversial, AT_2R has been suggested as a counterbalance to AT_1R-dependent signaling. General functions of the AT_2R include vasodilation through NO and cGMP stimulation, natriuresis, anti-angiogenesis, anti-proliferation, and decreased fibrosis. These effects are observed in different tissues including endothelium, vascular smooth muscle, heart, brain, and kidney [126, 127]. In VSMC, AngII-dependent mechanisms are dependent on the AT_1R interaction with heterotrimeric G proteins, including $G_{q/11}$, $G_{12/13}$, and possibly G_i. The subsequent activation of the effectors PLC-β and RhoA results in contraction mediated by the MLC phosphorylation, through increased MLCK and decreased MLCP activity, respectively [128].

b. Phenylephrine

Adrenergic receptors (ARs) mediate the diverse effects of the neurotransmitters of the sympathetic nervous system, epinephrine (commonly known as adrenaline) or norepinephrine (also known as noradrenaline). Phenylephrine is a synthetic sympathomimetic amine chemically related to epinephrine with potent vasoconstrictor activity. It is widely used for the treatment of hypotension [129].

There are two classes of ARs, alpha (α-AR) and beta (β-AR), with various subfamilies. The α_1AR subfamily consists of α_1A, α_1B, and α_1D-AR. The α_2AR

subfamily includes: α_2A-, α_2B-, and α_2C-AR. And in the βAR family there are three receptor subtypes β1, β2, and β3 [130, 131]. Phenylephrine is a selective pharmacological agonist of α_1AR with minimal β-receptor agonist activity. It induces constriction of vascular smooth muscle, resulting in increased arterial blood [130, 132]. The α_1AR subfamily couples to G-proteins of the $G_{q/11}$ family, the primary mode of signal transduction therefore involves activation of the phospholipase C/IP3/Ca^{2+} and calmodulin-sensitive pathways [89, 133]. In addition to acute SMC contraction, several studies have demonstrated that stimulation of α_1ARs induces dose-dependent proliferation, hypertrophy, and migration of VSMC [134-136].

c. U46619

U46619 is a stable synthetic analog of the endoperoxide prostaglandin H_2 (PGH2), it acts as a thromboxane receptor (TP) agonist and exhibits similar properties to thromboxane A2 (TXA_2) [137, 138]. TXA_2 is a lipid metabolite of the arachidonic acid metabolism, is produced via the consequent actions of cyclooxygenase and thromboxane synthase. TXA_2 plays an important role in VSMC vasoconstriction via activation of a G-protein coupled TP receptor, promotes platelet activation/aggregation [139] and seems also to contribute to vascular inflammation in atherosclerosis [140] and vascular injury [141-143].

The TP receptor is widely expressed in many cells and tissues including platelets, vasculature (smooth muscle and endothelial cells), lungs, kidneys, heart, thymus and spleen [144]. The surface TXA_2 receptor can couple with $G_{12/13}$ and $G_{q/11}$ to regulate several effectors and mediate its signaling, including PLC and guanine nucleotide exchange factor of the small G protein Rho (RhoGEF) [145].

2.1.2. Vasorelaxant ligands

a. Isoprenaline

Isoprenaline or isoproterenol is a synthetic sympathomimetic amine structurally related to adrenaline. Isoproterenol is a potent, nonselective β-adrenergic receptor (β-AR) agonist with minimal α-adrenergic-receptor (α-AR) affinity [132, 146]. The main actions of isoprenaline, through β-AR activation, are centered in the heart, where it promotes increased heart rate and contractility, and in the

skeletal, renal and mesenteric vascular beds, where it promotes vasodilation [130, 131].

The β-AR family is constituted by three G_s-coupled receptor subtypes β_1, β_2, and β_3 [130, 131]. β_1-adrenergic receptors are located commonly in the heart, β_2-adrenergic receptors are located mainly in vascular and skeletal smooth muscle, and β_3-adrenergic receptors are located in adipose tissue [147]. Isoprenaline has particularly high potency on β_1 and β_2 receptors, and at higher doses it also activates β_3 receptors [130, 148]. In VSMC, β_2-AR-dependent G_s activation causes smooth muscle relaxation by increased intracellular cAMP levels. In detail, G_s protein stimulates adenylyl cyclase, which catalyzes the conversion of ATP into cAMP with subsequent activation of PKA, and phosphorylation of various target proteins resulting in inhibition of MLCK that is responsible for the phosphorylation of smooth muscle myosin [149, 150].

b. Prostaglandin I_2

Prostaglandin I_2 (PGI_2) or prostacyclin is an endogenous prostanoid produced from the arachidonic acid metabolism. It is synthesized in endothelium and SMC of arteries, veins and microvessels [151, 152]. PGI_2 is well-known for its regulatory role within the cardiovascular system, where it promotes vasodilatation and inhibits platelet aggregation. Recently it was found that prostacyclin also stimulates differentiation and reduces proliferation in VSMC [153-155]. In different cardiovascular disorders such as atherosclerosis, myocardial infarction, thrombosis, and pulmonary hypertension, the activity of PGI_2 is reduced and therefore prostacyclin has been considered as an important endogenous factor for protection in cardiovascular diseases [154, 156].

PGI_2 binds and mediates signaling through a G_s coupled GPCR, the IP receptor, which triggers adenylyl cyclase activation and cAMP production [154]. Even though the correlation between IP receptor-mediated cAMP production and VSMC relaxation is well established, the precise the precise mechanisms by which cAMP relaxes VSMC are not fully understood [157-159]. While some studies propose a cAMP/PKA dependent inhibition of RhoA, other suggest a reduction of intracellular calcium levels or a cAMP-independent activation of hyperpolarizing MaxiK (BK) channels [113, 160, 161].

Analogs of PGI_2, including iloprost and beraprost, have been used clinically treat pulmonary arterial hypertension. These compounds are more stable with longer half-lives [153].

Two structurally distinct series of IP receptor antagonists have been developed, RO1138452 and RO3244794. Both display a high affinity for human and rodent IP receptors. Give the relatively high receptor affinity and selectivity, these compounds are providing useful insights into the physiology of PGI_2 and in the role of IP receptors in cardio-protection, blood flow regulation, pain and inflammation [162, 163].

2.2. GPCRs in the vascular system - differentiation

GPCRs are also known as potential modulators of SMC differentiation and inflammation [39]. Several procontractile GPCR ligands such as AngII, endothelin-1, or thromboxane A2 (TXA_2) have been shown to regulate SMC plasticity through GPCRs coupled to $G_{q/11}$, $G_{12/13,}$ and in some cases to G_i family [44, 164, 165]. VSMC deletion of G protein α-subunits $G_{12/13}$ decreases expression levels of SMC marker genes and exaggerates the response to dedifferentiation stimuli through RhoA-dependent nuclear translocation of transcription factors MRTF-A/B [39, 166, 167] (Figure 8). Contrarily, $G_{q/11}$ signaling is suggested to stimulate differentiation and proliferation of VSMCs. In vivo, SMC-specific deletion of $G_{q/11}$ was shown to increase and decrease, respectively, the expression levels of SMC differentiation markers and growth-related genes (egr-1, c-fos). This means that $G_{q/11}$-mediated activation of ERK1/2 and subsequent phosphorylation of its effector TCF is required for the control of these processes (Figure 8) [168]. Therefore, pro-contractile signaling pathways mediated by the G proteins $G_{12/13}$ and $G_{q/11}$ antagonistically regulate VSMC plasticity in a SRF-dependent manner (Figure 8) [168].

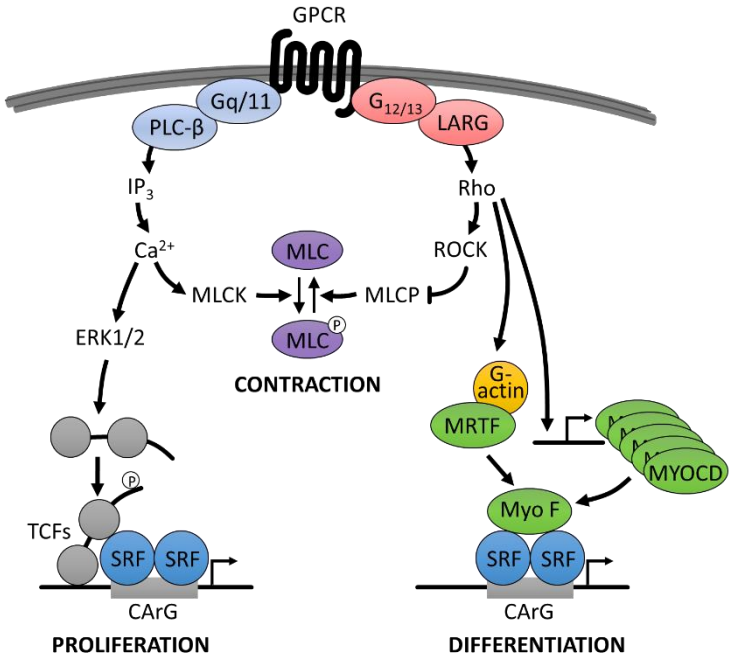

Figure 8 – $G_{q/11}$- and$G_{12/13}$-mediated signaling. Synergistic regulation of vascular tone and antagonistic regulation of VSMC plasticity. Phospholipase C (PLC), Rho-kinase (ROCK), inositol-1,4,5-trisphosphate (IP3), myosin light chain kinase (MLCK), myosin light chain phosphatase (MLCP), myocardin-related transcription factor A (MRTF), myocardin (MYOCD), myocardin family of transcriptional co-factors (Myo F). (Adapted from [39]).

Also G_s and G_i family G-proteins have been implicated in the regulation of VSMC differentiation: G_i signaling has been also implicated in increased VSMC proliferation, migration, and pathological vascular remodeling, for example through inhibition of cAMP production. The G_i-coupled receptors sphingosine 1-phosphate ($S1P_1$) or the apelin were shown to enhance transactivation of growth factor receptors and to induce of mitogen-activated protein kinase (MAPK) signaling [169, 170]. In contrast, activation of G_s-coupled receptors for example, prostaglandin I_2 and prostaglandin E_2, were shown to mediate inhibition of VSMC proliferation and migration, through cAMP-dependent signaling [171-173].

3. Novel GPCRs in SMC

GPCRs are very successful drug targets due to their substantial physiological relevance, and pharmacological manipulability. Several approaches have been used to find new GPCR-based therapies: 1) Identification of new biased or allosteric ligands at GPCRs with known function, 2) deorphanization of GPCRs for which ligands are not yet known and 3) identification of new pathophysiological

relevant functions for specific GPCRs, in particular for orphan receptors [174]. For the latter point, a detailed analysis of GPCR expression in functionally relevant cell subpopulations is helpful, for example, in subgroups of vascular cells. Regard et al. [175] quantified transcript levels of 353 non-odorant GPCRs in 41 adult mouse tissues. In this study, they found expression of GPCRs which have never been implicated in the regulation of a given specific tissue [175].The aorta, for example, did not only show expression of known regulators of cardiovascular functions such as angiotensin type 1a receptor (*Agtr1*) or sphingosine-1-phosphate receptor 1 (encoded by *S1pr1*), but also less well-known GPCR, such as Etl(*Eltd1*), *Fzd1*, *Fzd2*, *Fzd4*, *Kiaa0758* (*Gpr116*) and *Rdc1* (*Cxcr7*) [175]. However, this bulk cDNA approach has an enormous disadvantage, namely that the samples are a mixture of numerous cell types, in case of aorta not only SMC, but also endothelial cells, fibroblasts, immune cells, etc. This problem can be overcome by single-cell expression analysis, which allows for the first time to analyze the GPCR expression pattern of individual cells with known identity and functional state [175].

3.1. Single cell analysis expression – GPCR

To overcome the limitations of bulk RNA analysis, Kaur et al. [176] used a microfluidic-based system for single-cell reverse transcription polymerase chain reaction (RT-PCR) to determine GPCR expression in individual freshly isolated SMC (Figure 9). It was found that GPCR expression is highly heterogeneous in SMC, and that functionally relevant subgroups of SMC can be identified by their specific GPCR patterns. For example, the SMC GPCR repertoire differs depending on the vascular bed they originate from [176]: SMC from skeletal muscle (SMsk) vasculature, which is rich in resistance arteries, expressed significantly more GPCRs than aortic SMC, in particular more peptide hormone receptors with known vasoregulatory function, such as calcitonin receptor-like receptor (encoded by *Calcrl*), endothelin receptor type A (encoded by *Ednra*), Neuropeptide Y Receptor Y1 (encoded by *Npy1r*). In addition, SMsk showed high expression of orphan receptors, *Gpr19, Gpr21, Mrgprf, Gprc5b, Gprc5c, Gpr124, Gpr126*, or *Lphn1* (Figure 9) For these orphan GPCRs neither ligand nor function in SMC is known.

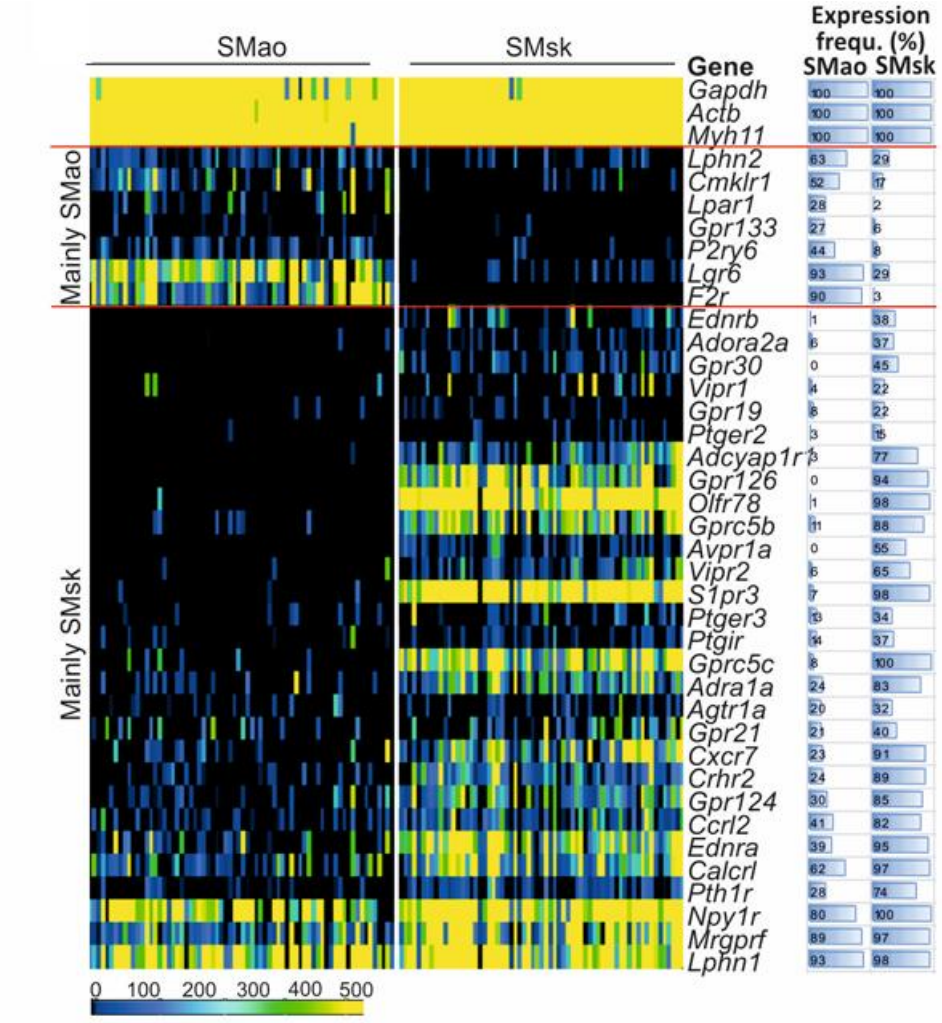

Figure 9 – Single-cell GPCR expression in different SMC types. Heat map of GPCR expression in SMao and SMsk (60 and 57 cells per SMC type, from seven to eight mice each); horizontal bars on the right side visualize expression frequency (in %). (Adapted from [176]).

More detailed analyses in aortic SMC showed that in healthy mice a small subpopulation showed signs of spontaneous dedifferentiation. These cells were characterized by a reduced expression of contractile proteins *Myh11* or *Acta2*, but increased expression of *Icam1, Vcam1, Col1a2* and *Col3a1*. Interestingly, this spontaneous dedifferentiated phenotype was also associated with increased expression of several orphan GCPRS, among them *Gprc5b*, a class C orphan GPCR [176] (Figure 10).

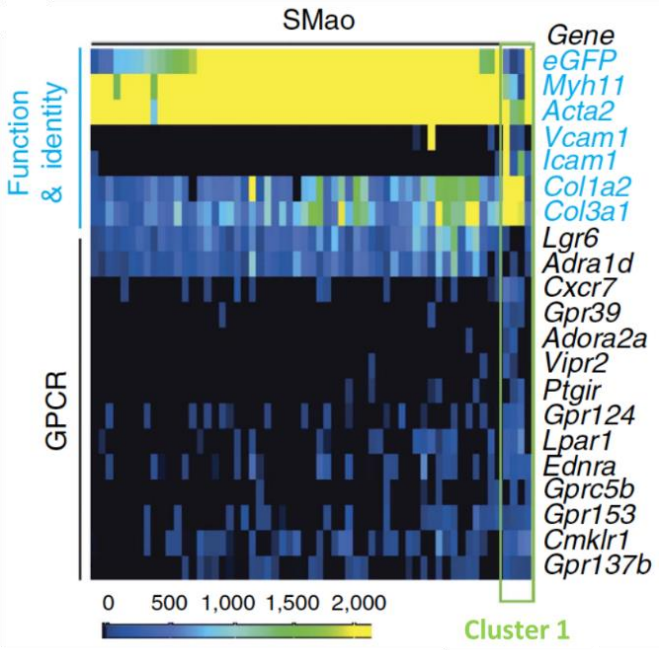

Figure 10 – Functional subgroups within SMao. Heat map indicating similarities and dissimilarities between 60 individual SMao. (Adapted from [176]).

Gprc5b is enriched in two interesting SMC subpopulations, namely SMC from resistance arteries on the one hand and in dedifferentiating aortal SMC on the other hand, which might indicate both functions in the regulation of SMC contractility and differentiation.

4. GPRC5B

4.1. Expression/localization

In human tissues, mRNA levels of GPRC5B are high in kidney, pancreas, and testis; medium in brain, heart, prostate, small intestine, and spleen; low in liver, placenta, skeletal muscle, colon, ovary, and thymus; and not detectable in lung and peripheral leukocyte [177]. Transient transfection experiments in HEK293T cells using epitope tags demonstrate that GPRC5B is expressed on the cell surface and perinuclear vesicles, which most likely represent the endoplasmic reticulum and Golgi apparatus. Treatment with retinoic acid induces GPRC5B expression in some human transformed cell lines [178].

4.2. Function

Global *Gprc5b*-deficient mice were viable, fertile and without apparent morphological abnormalities. However these mice display various neurological phenotypes such as behavioral abnormalities, altered cortical neurogenesis, and

disturbed cerebellar morphogenesis and long-term motor learning [179, 180]. Additionally, it was also described that mice lacking *Gprc5b* were protected from diet-induced obesity and obesity-associated inflammation [181]. The molecular mechanism suggested is that GPRC5B is phosphorylated by the tyrosine kinase Fyn and the subsequent interaction drives a local amplification of Fyn kinase activity to activate NF-κB signaling leading to cytokine production, inflammation in adipose tissue, and insulin resistance during the progression of diet-induced obesity [181]. Cell-based studies suggest that GPRC5B negatively regulates insulin secretion and β-cell viability in type-2 diabetes, and propose this GPCR as a novel target for the treatment and prevention of this chronic medical condition [182]. However further studies are needed to elucidate the precise mechanism. In fibroblasts, overexpression and siRNA-mediated knockdown of GPRC5B significantly increased and decreased, respectively, the transcription level of the pro-inflammatory and pro-fibrotic cytokines TNFα, IL-1β, IL-6 and MCP-1, and extracellular matrix-degrading MMP-9, suggesting that GPRC5B drives inflammation, fibrosis and cardiac remodeling [183]. The role of GPRC5B in SMC biology is unknown.

III. AIM OF THE THESIS

VSMCs play an important role in the pathogenesis of vascular diseases such as arterial hypertension and atherosclerosis. Elucidating the molecular mechanisms underlying the regulation of VSMC contractility and (de)differentiation is crucial for the development of new therapeutic agents to control these pathologies. GPCRs are important regulators of contractility and differentiation in VSMC. GPRC5B is enriched in both dedifferentiated and resistance SMC, and this suggests a role in dedifferentiation and contractility regulation, however the specific function of SMC-expressed GPRC5B is unclear. In this regard, the present thesis project was designed to study the role of GPRC5B in the regulation of contractility and dedifferentiation on two levels:

1. In vitro - in human and murine SMC,
2. In vivo - in tamoxifen-inducible, SMC-specific knockout mice (iSM-*Gprc5b*-KO) under conditions of arterial hypertension and atherosclerosis.

IV. MATHERIALS

Antibiotics	Supplier
Ampicillin	Sigma-Aldrich
Kanamycin	ROTH

Antibodies	Supplier
Anti-HA-tag mAb-Magentic Beads	MBL International
Anti-Sm α-actin	Abcam
c-Myc	Santa-Cruz
DAPI 4’,6-diamidin-2-phenylindol (DAPI)	Thermo Fisher Scientific
Donkey anti-Rabbit Alexa Fluor 488	Thermo Fisher Scientific
Donkey anti-Rabbit Alexa Fluor 594	Thermo Fisher Scientific
GAPDH	Cell Signaling Technology
GFP antibody	Rockland
GPRC5B	Abcam
HA-probe antibody AF594	Santa-Cruz
Monoclonal Anti-HA−Peroxidase antibody	Merk Millipore
p(Ser20)-Myosin light chain - MLC20	Thermo Fisher Scientific
PTGIR	Sigma-Aldrich
PTGIR (extracellular) antibody	Thermo Fisher Scientific

Cell lines	Supplier
Human Embryonic Kidney 293 cells HEK293T	DSMZ
Human Aortic Smooth Muscle Cells	Innoprot

Chemicals and reagents	Supplier
2-mercaptoethanol	Thermo Fisher Scientific
Acetic acid	ROTH
Acrylamid	SERVA Electrophoresis
Agarose	Sigma-Aldrich
Bovine Serum Albumin (BSA)	SERVA Electrophoresis
BSA fatty acid free	Sigma-Aldrich
Calcium chloride CaCl2.2H2O	ROTH
chemiluminescence reagent	Millipore
cOmplete Protease Inhibitor Cocktail	Roche
Dimethyl sulfoxide DMSO	SERVA Electrophoresis
Direct PCR Lysis Reagent	Viagen Biotech
Disodium hydrogen phosphate Na2HPO4	ROTH
Dithiothreitol DTT	New England Biolabs
DNA Ladder 50 bp	New England Biolabs

Chemicals and reagents	Supplier
DNA loading dye	Thermo Fisher Scientific
dNTPs	New England Biolabs
Dulbecco's modified eagle medium (DMEM)	Thermo Fisher Scientific
Dulbecco's phosphate buffered saline (PBS)	Thermo Fisher Scientific
Eosin	AppliChem
Ethanol	ROTH
Ethidium bromide	AppliChem
Ethylenediaminetetraacetic acid EDTA	ROTH
Fetal Bovine Serum (FBS)	Thermo Fisher Scientific
Fluoromount W	SERVA Electrophoresis
Glucose	ROTH
Glycerol	ROTH
Glycerol gelatin aqueous mounting media	Sigma-Aldrich
Glycine	ROTH
Hematoxylin	Sigma-Aldrich
High fat diet	Ssniff
Hydrochloric acid (HCl)	Thermo Fisher Scientific
Hydrogen peroxide (H_2O_2)	ROTH
IBMX 3-isobutyl-1-methylxanthine	Tocris Bioscience
Isopropanol (2-propanol)	ROTH
L-Gutamine	Thermo Fisher Scientific
LB agar	ROTH
LB medium	ROTH
Lipofectamine 2000	Thermo Fisher Scientific
Lipofectamine RNAiMAX	Invitrogen
Magnesium sulfate ($MgSO_4$-$7H_2O$)	ROTH
Methanol	ROTH
Miglyol	Caelo
Mineral oil	Sigma-Aldrich
Nonidet P-40	28324
Opti-MEM	Thermo Fisher Scientific
Optimal cutting temperature medium	Tissue-Tek
Paraformaldehyde (PFA)	ROTH
Penicillin and streptomycin	Thermo Fisher Scientific
Pertex Mounting medium	VWR
PhosSTOP	Roche
Potassium chloride (KCl)	ROTH
Potassium dihydrogenphosphate (KH_2PO_4)	ROTH
Protein Ladder PageRuler Prestained	Thermo Fisher Scientific
RNase inhibitor	New England Biolabs
SDS (sodium dodecyl sulphate)	ROTH
Sodium chloride (NaCl)	ROTH
Sodium hydroxide (NaOH)	Sigma-Aldrich
Sodium Pyruvate	Thermo Fisher Scientific
STOP Solution	Cell Signaling Technology

Chemicals and reagents	Supplier
Sucrose	Sigma-Aldrich
TMB Substrate	Cell Signaling Technology
Tris [Tris-(hydroxymethyl)-aminomethan]	ROTH
Tris Base	Fisher Scientific
Triton X-100	Merk Millipore
Trypsin-EDTA	Thermo Fisher Scientific
Tween 20	AppliChem
Xylene	ROTH

Consumables	Supplier
Cell Strainer 40µm	Corning
Cell Strainer 70µm	Corning
Nitrocellulose membrane	GE Healthcare
Osmotic minipumps	Alzet

Drugs	Supplier
Acetylcholine	Sigma-Aldrich
Angiotensin II	Cayman
Cay10441/ RO1138452	Cayman
Cicaprost	Cayman
DOCA pellet	Innovative Research of
Forskolin	Sigma-Aldrich
Iloprost	Tocris Bioscience
Isoflurane	Abbott
Isoprenaline	Sigma-Aldrich
Ketamine	Sigma-Aldrich
L-NAME	Sigma-Aldrich
Metamizole	Sanofi
Phenylephrine	Sigma-Aldrich
Sodium nitroprusside	FLUKA
Tamoxifen	Sigma-Aldrich
U-46619	Cayman
Xylazine	Bayer

Enzymes	Supplier
Collagenase II	Worthington
Dispase	Thermo Fisher Scientific
DNase1	New England Biolabs
Elastase-I	Sigma-Aldrich
Photoscript II reverse transcriptase	New England Biolabs
Proteinase-K	ROTH
T4 DNA ligase	New England Biolabs

Enzymes	Supplier
Taq polymerase	Thermo Fisher Scientific

Instruments/Equipments	Supplier
Agarose gel electrophoresis equipment	Bio Rad
Analytical balance	Sartorius
CCD camera	Danish Myo Technology A/S
ChemiDoc MP Imaging System	Bio-Rad
Cryotome	Leica
FACSCanto flow cytometer	BD Biosciences
Fluorescence microscope	Carl Zeiss
Gel casting platform	Bio Rad
Gel combs	Bio Rad
Gel documentation system	Intas ChemoCam Imager
JSAN cell sorter	Bay Biosciences
LabChip Gx Touch 24	Perkin Elmer
Leica DFC 280 camera	Leica
Leica DMLS2 microscope	Leica
Leica SP5 confocal microscope	Leica
Lightcycler 480 qPCR cycler	Roche
Microplate reader (Multiskan spectrum)	Thermo Fisher Scientific
Microtome	Leica
Mini Trans-Blot® Cell	Bio-Rad
Myograph setup (610-M)	Danish Myo Technology
MyoView software	XXXX
NanoDrop ND1000 Spectrophotometer	Thermo Fisher Scientific
Neubauer counting chamber	Karl Hecht
NextSeq500 instrument	Illumina
Pressure myograph chamber (114P)	Danish Myo Technology
Radiotelemetry system (PA-C10)	Data Sciences International
Thermo cycler	Analytik Jena
Thermomixer compact	Eppendorf Eppendorf
Zeiss Axio Observer.Z1	Zeiss

Kits	Supplier
Diaminobenzidine peroxidase substrate kit	Vector Laboratories
Direct cAMP ELISA kit	Enzo Life Sciences
DNase-Free DNase Set	Qiagen
LightCycler 480 Probes Master	Roche
Photoscript II cDNA synthesis kit	New England Biolabs
QIAGEN Plasmid Maxi Kit	QIAGEN
QIAGEN Plasmid Maxi Kit	QIAGEN
QIAGEN Plasmid Mini Kit	QIAGEN

Kits	Supplier
QIAGEN Plasmid Mini Kit	QIAGEN
RNA Microprep Kit	Zymo Research
RNA Microprep Kit	Zymo Research
RNeasy micro kit	Qiagen
SMART-Seq® v4 Ultra® Low Input RNA Kit	Takara Clontech
SMARTer® Stranded Total RNA-Seq Kit	Takara Clontech
SmGM-2 Supplements and Growth Factors	Lonza
Sso-Fast EvaGreen Supermix low ROX	BioRad
Universal probe library set, mouse	ROCHE
CellTiter 96® Cell Proliferation Assay (MTS)	Promega
Vectastain ABC Kit	Vector Laboratories

Plasmids	Supplier
CFP-β_2AR	Dorsch et al. 2009
HA-tagged EP2	cDNA.org
HA-tagged PTGIR	cDNA.org
Myc-tagged GPR156	Origene
Myc-tagged GPRC5B	Origene
Myc-tagged GPRC5C	Origene
PTGIR	cDNA.org

Medium	Composition	Receipe
DMEM culture medium	DMEM	500 ml
	FBS	10%
	penicillin and streptomycin	1%
	L-Gutamine	1%
	Sodium Pyruvate	1%
SMC growth medium	SmGMTM-2	500 ml
	FBS	5%
	Insulin	0.1%
	Human Fibroblast growth factor (hFGF-b)	0.2%
	Gentamicin GA-1000	0.1%
	Human epidermal growth factor (hEGF)	0.1%

Buffers	Composition	Recipe
TBS-T	Tris	25 mM
	NaCl	0,15 M
	Tween-20	0.05%
	NaCl	137 mM

Buffers	Composition	Recipe
Phosphate-buffered saline (PBS)	KCl	2.7 mM
	Na_2HPO_4	10 mM
	KH_2PO_4	2 mM
Krebs-Ringer buffer (KRB)	NaCl	119 mM
	KCl	4.7 mM
	$CaCl_22H_2O$	2.5 mM
	$MgSO_4$-$7H_2O$	1.17 mM
	$NaHCO_3$	20 mM
	KH_2PO_4	1.18 mM
	EDTA	0.027 mM
	Glucose	11 mM
	Carbogen (95% O_2 / 5% CO_2)	
Krebs High K+	KRB in which all NaCl is replaced by KCl	
Fixation solution	PFA	4%
	EDTA	20 mM
	Sucrose	5%
	PBS (10x)	15 ml
Pierce IP Lysis Buffer	Tris-HCl pH 7.4	25 mM
	NaCl	150 mM
	NP-40	1%
	EDTA	1 mM
	Glycerol	5%
RIPA Lysis and Extraction Buffer	Tris-HCl pH 7.6	25 mM
	NaCl	150 mM
	NP-40	1%
	Sodium deoxycholate	1%
	SDS	0.1%
TAE buffer	Tris Base	40 mM
	Acetic Acid	20 mM
	EDTA	1 mM
Tail-buffer	EDTA	100 mM
	SDS	0.5%
	Tris	50 mM
	Proteinase-K	0.5 mg/ml
PCR Buffer	Tris	200 mM
	KCl pH 8.4	500 mM
	dNTPs	25 µM

Buffers	Composition	Recipe
	$MgCl_2$	50 mM
SDS-PAGE stacking buffer	Tris/HCl pH 6.8	1 M
	SDS	0.8%
SDS-PAGE resolving gel buffer	Tris/HCl pH 8.8	1.5 M
	SDS	0.4%
SDS-PAGE running buffer	Tris	250 mM
	Glycine	1.92 M
	SDS	1%
Separating gel (10%)	H2O	0.9 ml
	30% Acrylamid	1.7 ml
	SDS-PAGE resolving gel buffer	2.5 ml
	TEMED 100%	4 µl
	APS 12,5%	40 µl
Stacking gel (6%)	H2O	0.75 ml
	30% Acrylamid	0.5 ml
	SDS-PAGE stacking buffer	1.25 ml
	TEMED 100%	3 µl
	APS 12,5%	30 µl
WB running buffer	Tris	20 mM
	Glycine	150 mM
	Methanol	20%
WB blocking buffer	PBS	1x
	Tween 20	0.5%
	Milk powder	5%
WB washing buffer	PBS	1x
	Tween 20	0.5%
Buffer 1	NaCl	137 mM
	KCl	5.4 mM
	$CaCl_2$	2 mM
	$MgCl_2$	1 mM
	HEPES	10 mM
4x Laemmli sample buffer	Tris-HCl, pH 6.8	277.8 mM
	Glycerol	44.4%
	Lithium dodecyl sulfate (LDS)	4.4%
	Bromophenol blue	0.02%

V. METHODS

1. Experimental animals

Gprc5b$^{fl/fl}$ mice were generated from clone EPD0534_1_A10 (EUCOMM) and intercrossed with Myh11-CreERT2 mice [25] to generate tamoxifen-inducible, smooth muscle specific knockouts of Gprc5b ("iSM-*Gprc5b*-KO"). Mice were maintained on a C57BL/6J background and genetically matched Cre-negative Gprc5b$^{fl/fl}$ mice were used as controls. Mice were housed under a 12 h light/dark cycle with free access to food and water and under pathogen free conditions. Animal experiments were approved by the Institutional Animal Care and Use Committee of the Regierungspräsidium Darmstadt and in accord with Directive 2010/63/EU of the European Parliament on the protection of animals used for scientific purposes. For atherosclerosis experiments, mice were crossed to the ApoE-deficient mouse line [184] and kept on high fat diet (21% butter fat, 1,5% cholesterol; Sniff, Soest, Germany) for 16 weeks. To allow flow cytometric isolation of vascular SMC, some mice carried in addition a Cre-dependent fluorescent reporter construct (Rosa26flox-mT-stop-flox-mG (Jackson Lab, Stock 007576) [185]). For induction of Cre-mediated recombination, mice were treated on 5 consecutive days with 1 mg tamoxifen intraperitoneally [25].

1.1. Genotyping PCR

Mice were genotyped by PCR performed on genomic DNA. Genomic DNA was extracted from tail biopsies using the Direct PCR Lysis Reagent. Tail samples were incubated overnight at 56°C on a thermomixer (900 rpm) in 300 µl of Tail-buffer. Next day, samples were vortexed and centrifuged 13000 rpm for 5 min at RT. 200 µl of the supernatant were transferred to fresh tube containing 700 µl of DNA precipitation buffer and centrifuged for 10 min -13000 rpm at 4°C, supernatant was discarded, and DNA washed with 1 ml of 70% ethanol. DNA pellet were dissolved 200 µl of PCR grade water, and concentration was measured by using Nano trop. For PCR, 1-2 µl of tail DNA was used as template in the PCR reaction containing 200 µM dNTPs, 10 pmol of each primer (forward and reverse), 1x PCR buffer and 0.5 µl of Taq polymerase. The PCR was carried out in a total volume of 50 µl. Agarose gel electrophoresis was used to separate PCR products. Genotyping for Gprc5b was done using primers

5’gctggaaggtttctccctct-3’ and 5’aagagacaaccaccagacagg-3’, resulting in band sizes of 361 for the wildtype allele and 478 bp for the floxed allele.

1.2. Agarose gel electrophoresis

A 2% agarose gel was prepared by microwave melting agarose in TAE buffer. After the agarose solution cooled down to ~45°C, ethidium bromide was added, and the solution was poured into a gel chamber. When the gel solidified, DNA mix was mixed with loading dye and then loaded onto the gel and run for 30-35 min at 180-200 V. DNA was visualized and photographed under UV light using a gel documentation system.

2. Pressure myography

Pressure myography experiments were performed as described previously [25]. In brief, 7 days after tamoxifen injection, first order and second order mesenteric arteries were removed from the mesentery and were mounted between 2 glass micropipettes seated in a pressure myograph chamber (Danish Myo Technology; 114P). The external diameter of the artery was visualized and recorded with a CCD camera using MyoView software. Arterial segments were pressurized stepwise from 20 mmHg to 140 mmHg. Myogenic tone was expressed as the percentage of passive diameter ((passive diameter - active diameter) / passive diameter x 100).

3. Wire myography

7 days after tamoxifen injection, first order mesenteric arteries (2mm) were removed from the mesentery and were mounted on a conventional myograph setup (610-M, Danish Myo Technology) and kept in Krebs solution. After a 30-min recovery period and normalization, we determined contractile responses by cumulative administration of the indicated agonists. All segments were exposed to 60 mM K^+ Krebs solution in order to elicit a reference contraction. Vessel relaxation in response to cumulative addition of cicaprost, iloprost, isoprenaline, SNP and acetylcholine was measured precontraction with phenylephrine (10 µM).

4. Telemetric blood pressure measurements

Measurements were performed in conscious, unrestrained mice with a radiotelemetry system (PAC10; Data Sciences International) as described previously [25]. In short, the pressure sensing catheter was implanted into the left carotid artery and the transducer unit was inserted into a subcutaneous pouch along the right flank. After a recovery period of 2 weeks the arterial pressure records were collected, stored and analyzed with Dataquest A.R.T. software 4.0. The blood pressure measurements were done with a 10-s scheduled sampling every 5 min and used the 24-h mean values for analysis. For the induction of arterial hypertension, osmotic minipumps releasing angiotensin II for 28 days (2000 ng/kg/min) were implanted subcutaneously on the back of 8- to 14-week-old male mice under anesthesia with isoflurane and intra/postoperative treatment with metamizole. In some cases, mice received on day 5 after tamoxifen injection intraperitoneal injections of IP antagonist Cay10441 (10 mg/kg, Cayman Chemicals) or vehicle control. In the DOCA salt model of arterial hypertension, mice were unilaterally nephrectomized and an aldosterone analogue deoxycorticosterone acetate (DOCA) pellet (50 mg DOCA, 21-d release time, Innovative Research of America, Sarasota, USA) was implanted subcutaneously. After recovery, mice received drinking water containing 1% (w/v) NaCl.

5. Histological and immunohistochemical analyses in murine tissues

Hematoxylin & Eosin staining of paraffin-embedded murine vessels was performed according to standard protocols. For histological analysis of atherosclerotic plaques, anesthetized mice were perfused with PBS followed by 4% PFA, 5% sucrose and 20mM EDTA in PBS, pH 7.4. Dissected aortae and hearts were fixed in the buffer used for perfusion at 4°C. After removal of the adventitia from the aortae, the vessels were opened longitudinally and stained with Oil-Red-O *en face* onto a glass plate coated with silicon. After rinsing with distillated water for 10 min and subsequently with 60% isopropanol, vessels were stained with oil-red-O for 60 min with gentle shaking, rinsed again in 60% isopropanol and finally in tap water for 10 min. Samples were mounted on the coverslips with the endothelial surface facing upwards with glycerol gelatin aqueous mounting media.

For immunostaining of the innominate artery, the dissected vessels were fixed in 4% PFA overnight (4% PFA, 20 mM EDTA, 5% sucrose in 15 ml PBS), embedded in optimal cutting temperature medium OCT and cyosectioned (10 µm). Frozen section specimens were air-dried and incubated in 3% H_2O_2 solution at (RT) for 10 min to block endogenous peroxidase activity. After incubating for 5 min in H_2O, the samples were washed three times for 5 minutes in PBS and blocked in PBS supplemented with 5% normal goat serum for 2h at RT followed by overnight incubation at 4°C with rabbit anti-Sm α-actin antibodies (1:100). Sections were washed three times in PBS for 5 minutes and antibody binding was detected using biotinylated anti-rabbit IgG secondary antibodies (1h at RT) and thereafter incubated with Avidin-Biotin complex reagent (Vectastain ABC Kit) according to the manufacturer's instructions. After washing with PBS three times in PBS for 5 minutes, staining was visualized using a diaminobenzidine (DAB) peroxidase substrate kit. Sections were counterstained with hematoxylin for 2 minutes, washed in tap water for 10 minutes and dehydrated 35 through a series of alcohol solutions in ascending concentration (70%, 85%, 95% and 100%, 5 min each). The samples were cleared in two changes of xylene for 5 minutes and mounted with Pertex Mounting medium.

For immunostaining of skeletal muscle vasculature, M. quadriceps femoris was dissected, fixed 1h at RT in 4% PFA, incubated in 30% sucrose overnight at 4 °C, embedded in optimal cutting temperature medium (OCT), and cyosectioned (10 µm). OCT. tissue freezing medium was removed by washing with PBS followed by a blocking step with 4% BSA for 60 min. Sections were immunostained overnight with anti-PTGIR antibody directed against the IP extracellular domain (IP(ec), PA5-77695, 1:100). After washing with PBS, antibody binding was detected using donkey anti-rabbit Alexa Fluor 594 (1:500). DAPI was used to label cell nuclei (1:1000, diluted in 0.1% Triton X-100). Samples were thoroughly washed with PBS, air dried and mounted with Fluoromount W. The intensity of IP(ec) immunostaining within the tunica media (identified by EGFP expression driven by a Cre-reporter mouse line) was determined using Fiji.

6. Plasmid transformation and isolation

Using the heat shock method, a tube of competent E.Coli cells (50 µl) was thawed on ice, gently mixed and pipetted into the transformation tubes on ice were 5 µl of the plasmid DNA was added. The competent cell/DNA mixture was incubated the on ice for 30 minutes followed by a heat shock at 42°C for 40 seconds, returning immediately to ice for 3 min. 500 µl of Luria-bertani medium (LB medium) (without antibiotic) was added to the bacteria and incubated at 37°C for 60 minutes on a shacking incubator. 50-100 µl of the transformation was spreader to a 10 cm LB agar selection plate containing the appropriate antibiotic and incubated overnight at 37°C.

7. Bacterial culture

Single colonies of transformed bacteria were picked from a LB agar selection plate or from a bacterial glycerol stock and inoculated into 5 ml of LB medium containing 100µg/ml of Ampicillin or 50µg/ml Kanamycin selective antibiotic. The bacteria culture was grown at 37°C with shaking 200 rpm overnight. On the next day 1 ml of bacterial culture was inoculated into 300 ml of LB medium (with antibiotic) and grown at 37°C with shaking 200 rpm overnight, the remaining bacterial culture was centrifuged at 6000xg, purified, quantified and sequenced. From each bacterial culture, a stock preparation was made by mixing 250 µl of the bacterial culture with 250 µl of 30% glycerol and stored at -80°C.

7.1. Plasmid DNA isolation

Plasmid DNA was purified from bacterial culture using the QIAGEN kit: small-scale (5 ml, mini preparation) (or large-scale (250 ml, maxi preparation) according to the manufacturer's protocol. Briefly, bacterial lysates were cleared by centrifugation at 6000xg, 15 minutes, 4°C and then loaded onto the anion-exchange tip where plasmid DNA selectively binds under appropriate low-salt and pH conditions. Contaminants and impurities were removed by a medium-salt wash, and pure plasmid DNA was eluted in high-salt buffer. The plasmid DNA was concentrated and desalted by isopropanol precipitation, collected by centrifugation and dissolved in ddH2O. DNA concentration was measured by using Nanodrop. All constructs were verified by sequencing (SeqLab GmbH, Göttingen, Germany).

8. Cell culture and transfection

Human aortic smooth muscle cells (hAoSMCs) were purchased from Innoprot (cat. No. P10456; Derio, Spain) and cultured in smooth muscle cell growth medium (SmGMTM-2, Lonza) supplemented with 5% FBS, 0.1% insulin, 0.2% basic human fibroblast growth factor (hFGF-b), 0.1% GA-100, and 0.1% human epidermal growth factor (hEGF).

Human embryonic kidney cells (HEK293T) cells were maintained in DMEM supplemented with 10% FBS, 1% penicillin and streptomycin, 1% L-glutamine and 1% sodium pyruvate. Cells were maintained at 37°C in a humidified atmosphere with 5% CO_2.

For knockdown experiments cells were transfected with two independent siRNA directed against human GPRC5B (cat. SASI_Hs01_00171699, Sigma-Aldrich, NM_016235, target sequence: 5'- CGUUUAGAAGCAACGUGUA-3' / cat. SI00114646, Qiagen, NM_016235; target sequence: 5'-TCCGTTTAGAAGCAACGTGTA-3') or respective negative control siRNA (MISSION® siRNA Universal Negative Control, cat. SIC001, Sigma-Aldrich / AllStars Negative Control siRNA, cat. SI03650318, Qiagen) using Opti-MEM (cat. 31985062, Thermo Fisher Scientific) and Lipofectamine RNAiMAX according to the manufacturer's instructions. Cells were used 48 h after transfection.

Transient transfections of HEK293T cells with expression vectors were carried out with Opti-MEM and Lipofectamine 2000 transfection reagent or for HEK293T cells measured in Figure 21 with Effectene according to the manufacturer's instructions. Expression plasmids encoding Myc-tagged GPRC5B, GPRC5C-Myc and GPR156-Myc were from Origene. The plasmids encoding PTGIR (cat. PTGIR00000), 3xHA-tagged PTGIR and HA-EP2 were from cDNA.org. cDNA encoding for CFP-β_2AR (Dorsch et al. 2009) has been described previously. To generate mTurquoise2-5 IP, mTurquoise2 preceded by the hemagglutinin signal sequence (Guan et al. 1992) was PCR-amplified and N-terminally inserted into IP receptor cDNA using restriction enzymes BamHI and EcoRI. GPRC5B-mCitrine was generated by inserting the PCR-amplified GPRC5B cDNA carrying BamHI and EcoRI restriction sites into a pcDNA3 backbone vector expressing a C-terminal mCitrine. The Myc-GPR133 plasmid was generated in house. The

complete mouse GPR133 cDNA, containing a double myc tag inserted after the signal peptide into the N-terminal domain of the receptor, was cloned into a pCDNA3.1 vector backbone for protein expression.

9. Cell proliferation Assay

Cell viability after transfection was determined using CellTiter 96® AQueous One Solution Cell Proliferation Assay (MTS) according to the manufacturer's instructions. Cells were seeded in multiple 96-well plates in 100 µl full growth medium. 4h before experiment, 20 µl/well CellTiter 96 AQueous One Solution was added to the plate and incubated for 4h at 37 °C in a humidified, 5% CO_2 incubator and thereafter the absorbance was recorded on a microplate reader at 490 nm.

10. cAMP assay

cAMP levels were measured using the Direct cAMP ELISA kit according to the manufacturer’s protocol. In detail, cells were preincubated with phosphodiesterase inhibitor IBMX 100 µM (1h) and stimulated as indicated, then washed in ice-cold PBS, lysed for 10 min with 20 HCl (0.1 M) + 0,1% Triton, and centrifuged at 600×g for 10 min. Supernatants were collected and cAMP levels in the supernatants were measured by using the Direct cAMP ELISA kit according to the manufacturer’s instructions for acetylation format. Protein concentration of the same samples was determined by Bradford protein quantification assay. Data were normalized to the protein amounts ((cAMP pmol/ml)/mg of protein).

11. Measurement of Surface HA-IP Expression (HA-Elisa)

Surface HA-IP expression was measured by ELISA as described [186]. Cells were seeded on 96-well dishes coated with poly-lysine (0.1 mg/ml) and 24 h later treated with iloprost at 37°C for 40 minutes. Reactions were stopped by aspiration and fixation with PFA 0.4% in PBS for 10 min at 4 °C. Cells were washed 3x with PBS, blocked for 30 min with 2% BSA in PBS at RT and incubated with monoclonal anti-HA-peroxidase antibody (1:4000 dilution, in PBS) for 90 min at RT. After 3 washes with PBS, cell surface horseradish peroxidase was revealed by incubation with TMB Substrate for 10 minutes and thereafter the reaction was stopped using STOP Solution. The absorption intensity was obtained with a microplate reader at 450 nm. A background control in which monoclonal anti

HA−Peroxidase antibody was not added was included in each plate and subtracted from the final absorbance measurements.

12. Immunoprecipitation

For immunoprecipitation of overexpressed proteins, cells were washed with cold PBS and lysed with IP Lysis Buffer supplemented with protease inhibitor cocktail for 30 min on ice. Samples were cleared by centrifugation at 14000 rpm, 15 minutes at 4°C and protein concentrations were determined by the Bradford procedure. 500 µg of clarified lysates were incubated with HA-tagged magnetic beads at 4°C with gentle rotation for 5h. After three washes with cold IP lysis buffer, proteins bound to the beads were eluted by boiling the beads in 1x LAEMMLI sample buffer at 95°C for 5 min and then resolved by SDS-PAGE, transferred to a membrane and immunoblotted with indicated antibodies. Equal amounts of proteins were used for the IP and 10 µg of total lysates were used for input controls.

13. Immunofluorescence staining in HEK cells and hAoSMC

For Immunofluorescence detection of HA-tagged IP receptor (HA-IP) and Myc-tagged GPRC5B (GPRC5B-Myc), growth medium was removed 48 hours after transfection and cells were washed twice with PBS. Cells were then fixed with 4% PFA for 10 min at RT followed by washing three times with PBS. Permeabilization was done by incubation of cells with and 0.1% Triton X-100 for 10 minutes at RT. Cells were blocked with 4% bovine serum albumin in PBS for 30 min at RT and secondary antibody was added 1:100 HA-probe antibody, 1:100 c-Myc and 1:1000 4’,6-diamidin-2-phenylindol (DAPI) diluted in 4% BSA. Plates were incubated at RT for 1 hour, after which cells were washed three times and stored at 4°C in PBS until ready for high content image analysis using a Leica TCS SP5 confocal microscope. The ratio of HA-IP intensity in plasma membrane vs cytosol was determined using Fiji. To evaluate the degree of overlay between GPRC5B-Myc and HA-IP, Manders’ coefficient 61 was determined using Fiji. For membrane staining of PTGIR, growth medium was removed 48 hours after kd and cells were washed twice with PBS. Cells were then fixed with 4% PFA for 10 min at RT, followed by washing three times with PBS. Cells were blocked with 4% bovine serum albumin (11930, SERVA Electrophoresis) in PBS for 30 min at

RT and then incubated for 1h at RT with anti-PTGIR Rb antibody directed against the IP extracellular domain (IP(ec), 1:100) diluted in 4% BSA, followed by three washes with 1X PBS. Cells were then incubated for 1h at RT with Alexa Fluor 488-conjugated donkey anti-rabbit secondary antibody (1:500) diluted in PBS followed by three washes with 1x PBS. Subsequently, cells were incubated 10 min at RT with DAPI (1:1000, diluted in 0,1% Triton X-100). Cells were washed three times and stored at 4°C in PBS until ready for high content image analysis using a Leica TCS SP5 confocal microscope.

14. Dual-color fluorescence recovery after photobleaching microscopy

HEK293T cells transiently transfected with either mTurquoise2-IP or CFP-β_2AR together with GPRC5B-mCitrine were grown on coverslips. Cells were washed twice with buffer 1 followed by immobilization of the N-terminally labeled receptors for 30 mins at 37°C via crosslinking with a polyclonal GFP antibody diluted 1:100 in buffer 1 supplemented with 2.5 % fatty acid free BSA. Antibody treatment was omitted for non-immobilized controls. Subsequently, cells were washed three times with buffer 1 and fluorescence recovery after photobleaching (FRAP) microscopy was performed as described [187] using a Leica TCS SP5 confocal microscope with a Lambda Blue 63x/1.4 NA oil-immersion objective. CFP and mTurquoise2 were excited at 405 nm using a diode laser and emission was collected at 470 ± 20 nm. mCitrine was excited at 514 nm with an argon ion laser and emission was collected at 560 ± 35 nm. The scan speed was set to 1000 Hz, image format was 256 x 256 pixels, zoom factor was set to 6.0 and the pinhole was set to airy 1 (95.52 µm). For bleaching the laser intensity was increased to 80% resulting in 80 – 90 % loss of fluorescence in the 3 µm x 1 µm rectangular bleached region in the equatorial plane of the cell membrane. Fluorescence recovery into the bleached region was monitored for 110 s at low laser intensity. Fluorescence intensities were corrected for photobleaching and the resulting values normalized by setting the initial fluorescence intensities (pre-bleach) to 100 % and the lowest intensity directly after bleaching to 0 %. The resulting FRAP curves were averaged and plotted as mean ± SEM. For statistical analysis of recovery, FRAP of GPRC5B-citrine was averaged between 100 and 120 s for all conditions and recovery after immobilization of IP or β_2AR was

normalized to the average value under conditions of non-immobilized IP or β_2AR receptors.

15. Western blotting

Samples were lysed in RIPA buffer supplemented with protease inhibitor cocktail and phosphatase inhibitor cocktail. Proteins were separated by SDS-PAGE (Tris-glycine gels with Tris/glycine/SDS buffer) and transferred onto nitrocellulose membranes using the Mini Trans-Blot® Cell. Membranes were probed over night with specific primary antibodies as indicated and then with peroxidase-conjugated secondary antibodies (1:3000) for 2h. The following primary antibodies were used: p(Ser20)-Myosin light chain (1:500), GAPDH (1:1000), PTGIR (1:500), GPRC5B (1:500). Secondary antibodies are horseradish peroxidase-conjugated Rabbit or Mouse IgG (1:3000) purchased from Cell Signaling Technology Europe. The target proteins were visualized by enhanced chemiluminescence reagent and a ChemiDoc MP Imaging System. Quantification of band intensities were analyzed by ImageJ software (NIH). Equal loading was assessed using antibodies to GAPDH.

16. Tissue digestion and cell sorting

Animals were killed, perfused with PBS and different tissues (skeletal muscle or whole aorta including common carotid arteries) were dissected, minced and enzymatically digested for 60 min while shaking at 37 °C in a digestion mix containing collagenase II (2 mg ml^{-1}), elastase-I (0.04 mg/ml), Dispase (1.2 U/ml) and DNase1 (5 U/ml). Cell suspensions were serially filtered through 70µm and 40 µm cell strainers followed by washing twice with PBS. Cells were sorted on a JSAN cell sorter based on EGFP expression.

17. Expression analysis

RNA from was isolated and purified using the RNA Microprep Kit according to the manufacturer's instructions. Quality control of samples was carried out using a Nanodrop ND-100 Spectrophotometer. RNA was reverse transcribed using the Photoscript II cDNA synthesis kit according to the manufacturer's instructions. Shortly, 0.5-1 µg of purified RNA was incubated with random hexamer primer for 10 min at 65°C on a thermocycler, the mix was then transferred onto ice, and a premixed solution containing RNase inhibitor, DTT, dNTPs, reaction buffer and

Photoscript II reverse transcriptase was added. The reaction mix was then incubated at 29°C for 10 min and at 48°C for 60 min. The reverse transcriptase was eventually inactivated by incubation at 85°C for 5 min. The synthesized cDNAs were subjected to a Quantitative real-time PCR (RT-qPCR) performed in a 20-µl reaction containing 5µl of cDNA using the LightCycler 480 Probe Master System. Primers were designed with the online tool provided by Roche. PCR was performed by initial denaturation at 95 °C for 5 min, followed by 40 cycles of 10s at 95 °C, 30s at 60 °C and 1s at 72 °C. Gene expression was normalized to the endogenous control (GAPDH) and calculated using the ΔΔCt method and calculated using the ΔΔCt method.The following primers were used to analyze mRNA expression: GAPDH (probe #82) Fwd: 5' GCATCCTGGGCTACACTGA 3' / Rev 5' CCAGCGTCAAAGGTGGAG 3'; Gprc5b (probe #78) Fwd: 5' CCGCAGAGATGTGACTCG 3' / Rev 5' TCTCTGATGCCACGAACATT 3'; Acta2 (probe #20) Fwd: 5' CATGCCATCATGCGTCTG 3' / Rev 5' CGGACAATCTCACGCTCAG 3'; Tagln (probe #2) Fwd: 5' GGCCAAGGCTCTACTGTCTG 3' / Rev 5' GCCATAGGAAGGACCCTTGT 3'; VCAM1 (probe #15) Fwd: 5' GCAGAGTACGCAAACACTTTATG 3' / Rev 5' GCCTGCTCCACAGGATTTT 3'; Mki67 (probe #2) Fwd: 5' CAGAGAATTTGCTTGGAAAACA 3' / Rev 5' GAGGTGGGGAGCAGAGGT 3'; PCNA (probe #4) Fwd: 5' CCTAAAGATTCTGAAAAAGAGAATCAG 3' / Rev 5' CAGGTTGCAAAGGACATGC 3'; CCNA (probe #67) Fwd: 5' CCATACCTCAAGTATTTGCCATC 3' / Rev 5' TCCAGTCTTTCGTATTAATGATTCAG 3'.

For RNA sequencing, RNA was isolated from FAC-sorted EGFP-expressing SMC from skeletal muscle vasculature or atherosclerotic aortae using RNeasy micro kit combined with on-column DNase digestion to avoid contamination by genomic DNA. RNA and library preparation integrity were verified with LabChip Gx Touch 24 (Perkin Elmer). Depending on the available RNA amount the SMARTer® Stranded Total RNA-Seq Kit - Pico Input Mammalian (Takara Clontech) or the SMART-Seq® v4 Ultra® Low Input RNA Kit (Takara Clontech) were used for cDNA library preparation. Sequencing was performed on the NextSeq500 instrument (Illumina) using v2 chemistry, resulting in 10 - 23M reads per library with 1x75 bp single end setup. The resulting raw reads were assessed

for quality, adapter content and duplication rates with FastQC (Andrews S. 2010, FastQC: a quality control tool for high throughput sequence data. Available online at: http://www.bioinformatics.babraham.ac.uk/projects/fastqc). Reaper version 13-100 was employed to trim reads after a quality drop below a mean of Q20 in a window of 10 nucleotides (Davis et al., Kraken: A set of tools for quality control and analysis of high-throughput sequence data). Only reads between 30 and 150 nucleotides were cleared for further analyses. Trimmed and filtered reads were aligned versus the Ensembl mouse genome version mm10 (GRCm38) using STAR 2.4.0a with the parameter "--outFilterMismatchNoverLmax 0.1" to increase the maximum ratio of mismatches to mapped length to 10% (Dobin et al., STAR: ultrafast universal RNA-seq aligner). The number of reads aligning to genes was counted with featureCounts 1.4.5-p1 tool from the Subread package (Liao et al., featureCounts: an efficient general-purpose program for assigning sequence reads to genomic features). Only reads mapping at least partially inside exons were admitted and aggregated per gene. Reads overlapping multiple genes or aligning to multiple regions were excluded. The Ensemble annotation was enriched with UniProt data (release 06.06.2014) based on Ensembl gene identifiers (Activities at the Universal Protein Resource (UniProt)). Gene Ontology (GO term analysis was performed using the GOrilla tool (http://cbl-gorilla.cs.technion.ac.il), heat maps were generated using Perseus software (https://www.biochem.mpg.de/5111810/perseus).

18. Statistical analyses

Data are presented as means ± standard errors of the means (SEM). Comparisons between two groups were performed with unpaired or paired student's t-test, comparisons between two groups over time were done using repeated measures ANOVA with Bonferroni post hoc test. "n" refers to the number of independent experiments or mice per group. P-values are indicated as follows: *, $P<0.05$; **, $P<0.01$; ***, $P<0.001$.

VI. RESULTS

1. Vascular tone regulation in iSM-*Gprc5b*-KO mice

1.1. Generation and characterization of SMC-specific *Gprc5b* KO mice

Gprc5b$^{fl/fl}$ mice, where exon 2 of the *Gprc5b* gene was flanked with loxP sites, were intercrossed with Myh11-CreERT2 mice [25], which express the tamoxifen-inducible Cre/ERT2 fusion protein under control of the SMC-specific *Myh11* promoter, to generate tamoxifen-inducible SMC specific Gprc5b knockouts (iSM-*Gprc5b*-KO). Furthermore iSM-*Gprc5b*-KO and control mice were also bred to the Cre reporter line *Gt(ROSA)26Sor*$^{tm4(ACTB-tdTomato,-EGFP)Luo}$ [185], which allows isolation of smooth muscle cells by fluorescence activated cell sorting (FACS). To investigate Cre-mediated recombination after tamoxifen induction in iSM-*Gprc5b*-KO mice, we performed western blotting of lysates prepared from the smooth muscle layer of mesenteric arteries and mRNA sequencing in isolated EGFP-expressing smooth muscle cells from skeletal muscle vasculature. We found a clear reduction of GPRC5B mRNA expression and immunoreactivity in iSM-*Gprc5b*-KO compared with the control (Figure 11A, B). Morphological analysis of vessels from iSM-*Gprc5b*-KO did not show major differences (Figure 11C).

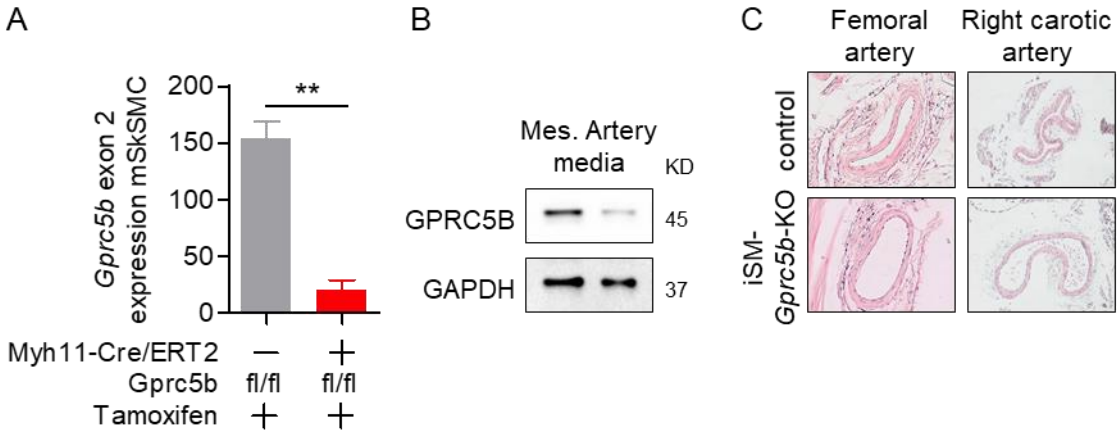

Figure 11 – Knockout efficiency in smooth muscle-specific *Gprc5b* knockout mice (iSM-*Gprc5b*-KO). A, Library size-normalized counts detected by mRNA sequencing in EGFP-expressing SMC sorted from skeletal muscles of tamoxifen-treated control mice and iSM-*Gprc5b*-KOs bred to a Cre-dependent EGFP reporter line. **B**, GPRC5B immunoreactivity in the media of mesenteric arteries obtained 7-14 days after the end of tamoxifen induction from control mice (*Gprc5b*$^{fl/fl}$) and iSM-*Gprc5b*-KOs (Myh11-CreERT2;*Gprc5b*$^{fl/fl}$). GAPDH as

loading control. **C,** Exemplary histological sections of femoral and carotid arteries from control mice and iSM-*Gprc5b*-KOs 21 days after tamoxifen induction. Data are means ± SEM; differences between genotypes were analyzed using unpaired Student's *t*-test. *, $P < 0.05$; **, $P < 0.01$.

1.2. Vascular contractility in iSM-*Gprc5b*-KO mice

Vascular contractility studies were performed by pressure and wire myography in mesenteric arteries 7-14 days after induction with tamoxifen. SMC-specific deletion of *Gprc5b* did not affect myogenic tone in pressure myography (Figure 12 A). No differences were also found in the contractile responses to the α_1 adrenergic agonist phenylephrine (Figure 12 B) and the TXA_2 analogue U46619, acting on the TP receptor (Figure 12 C).

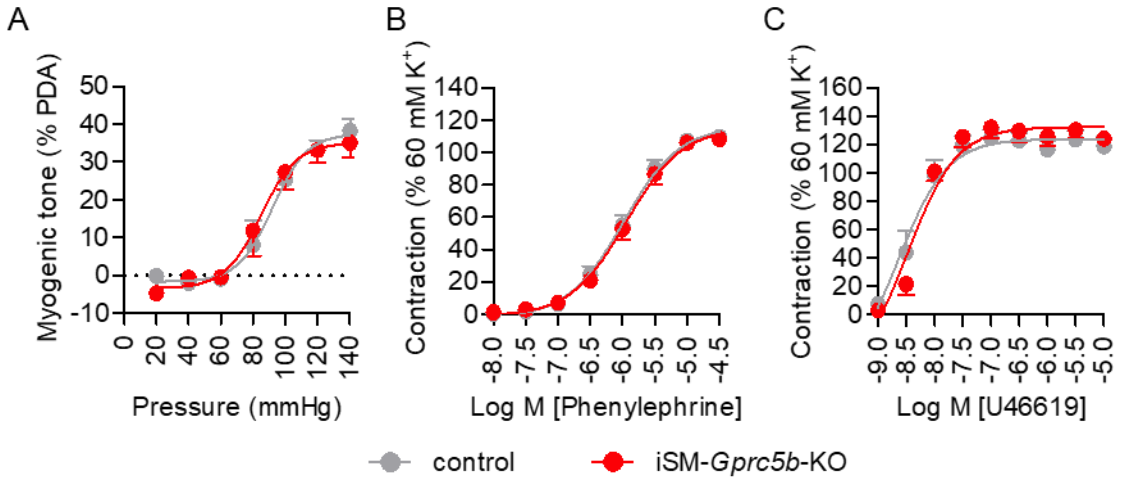

Figure 12 – Vascular reactivity in tamoxifen-inducible, smooth muscle-specific *Gprc5b* knockout mice (iSM-*Gprc5b*-KO). A, Myogenic contraction in response to increased pressure in first order mesenteric arteries from control mice and iSM-*Gprc5b*-KOs (n=4). **B-C,** Dose-response curves of different vasoconstrictors were determined by wire myography in first and second order mesenteric arteries from control mice and iSM-*Gprc5b*-KOs. Numbers of mice tested were n=7 (B), n=6 (C). All values are expressed as percentages of reference contraction induced by 60 mM K^+ or 10 µM phenylephrine. Data are means ± SEM; differences between genotypes were analyzed using 2-way repeated measures ANOVA and Bonferroni's post-hoc test. *, $P < 0.05$; **, $P < 0.01$; ***, $P < 0.001$, ****, $P < 0.0001$.

However, vessel relaxation responses were significantly enhanced for the two prostacyclin analogues cicaprost and iloprost, both acting on the prostacyclin receptor IP (Figure 13 A, B). Of note, neither relaxant responses to the β_2 adrenergic agonist isoprenaline nor the nitric oxide-donor sodium nitroprusside

(SNP) were altered (Figure 13 C, D), and also endothelium-dependent relaxation induced by acetylcholine was normal (Figure 13 E). These data suggest that SMC-deletion of GPRC5B selectively enhances IP-mediated relaxation.

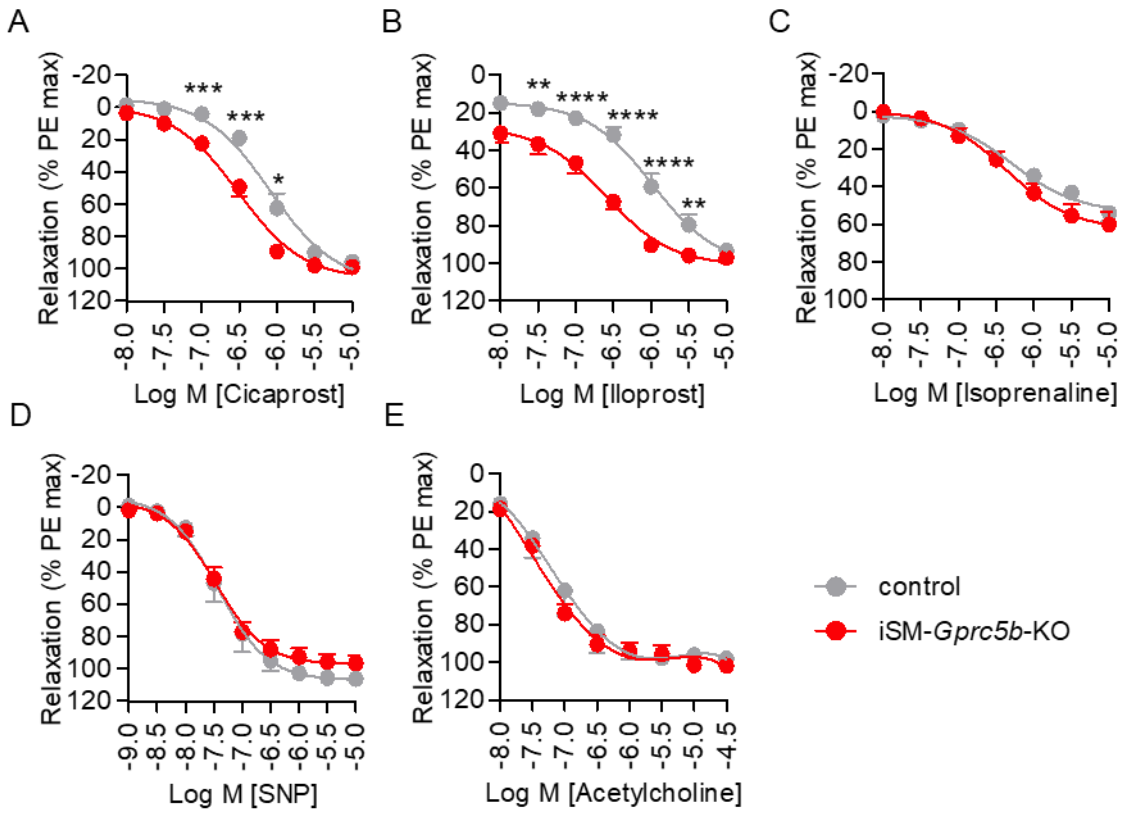

Figure 13 – Vascular reactivity in tamoxifen-inducible, smooth muscle-specific *Gprc5b* knockout mice (iSM-*Gprc5b*-KO). A-D, Dose-response curves of different or vasodilators were determined by wire myography in first and second order mesenteric arteries from control mice and iSM-*Gprc5b*-KOs. Numbers of mice tested were n=4 (A), n=7 (B), n=4 (C), n=3 (D) (1-5 vessels per mouse). **E,** Endothelium-dependent relaxation induced by acetylcholine (n=4). All values are expressed as percentages of reference contraction induced by 60 mM K^+ or 10 µM phenylephrine. Data are means ± SEM; differences between genotypes were analyzed using 2-way repeated measures ANOVA and Bonferroni's post-hoc test. *, $P < 0.05$; **, $P < 0.01$; ***, $P < 0.001$, ****, $P < 0.0001$.

2. Prostacyclin receptor signaling in GPRC5B-deficient SMC

2.1. cAMP production in GPRC5B-deficient human aortic SMC

Activation of GPCRs coupled to G_s family proteins, such as the IP, promote cAMP/PKA-dependent reduction of intracellular Ca^{2+} levels, cellular hyperpolarization, and suppression of RhoA/ROCK-mediated inhibition of myosin phosphatase by G_s-mediated activation of adenylyl cyclase isoforms [188]. This

results in decreased MLC20 phosphorylation and consequent actomyosin contractility, which in turn promotes SMC relaxation. Therefore, to further determine whether IP receptor-mediated cAMP production was affected by GPRC5B deletion in SMC, we performed siRNA-mediated knockdown in human aortic SMC (hAoSMC) (Figure 14 A). While knockdown of GPRC5B did not affect basal and isoprenaline-induced cAMP production, iloprost-induced cAMP production was much greater when compared with control cells (Figure 14 B).

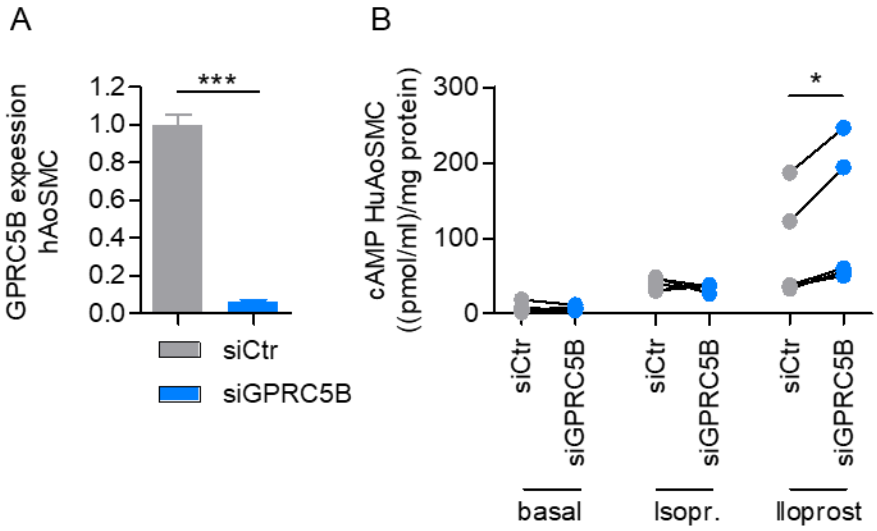

Figure 14 – IP receptor-mediated cAMP production in GPRC5B-deficient SMC. A, Efficiency of siRNA-mediated GPRC5B knockdown (kd) in hAoSMC was evaluated by qRT-PCR (all data normalized to respective control, n = 3). **B,** cAMP production in control and GPRC5B-kd hAoSMC under basal conditions and after stimulation with isoprenaline (Isopr., 1 µM) or iloprost (1 µM) (n = 4).Data are means ± SEM; comparisons between genotypes were performed using unpaired (A) or paired (B) Student's t-test. siCtr, sample treated with scrambled control siRNA; *, $P < 0.05$.

2.2. IP-mediation of MLC phosphorylation in GPRC5B deficient hAoSMC

We then tested whether MLC20 phosphorylation was affected by the enhanced IP receptor-mediated cAMP production in hAoSMC (Figure 15 A, B). We found that in both control and GPRC5B knockdown cells stimulation with TXA_2 receptor agonist U46619 increased MLC20 phosphorylation (Figure 15 A). However further concomitant iloprost application significantly reduced MLC20 phosphorylation in knockdown cells when compared with the mild reduction observed in the control cells (Figure 15 A, B). This effect was not dependent on the expression of the IP receptor neither on mRNA nor protein level (Figure 15

C-E). Taken together, these and the previous results suggest that deletion of GPRC5B promotes a selective improvement of IP receptor signaling in murine and human SMC.

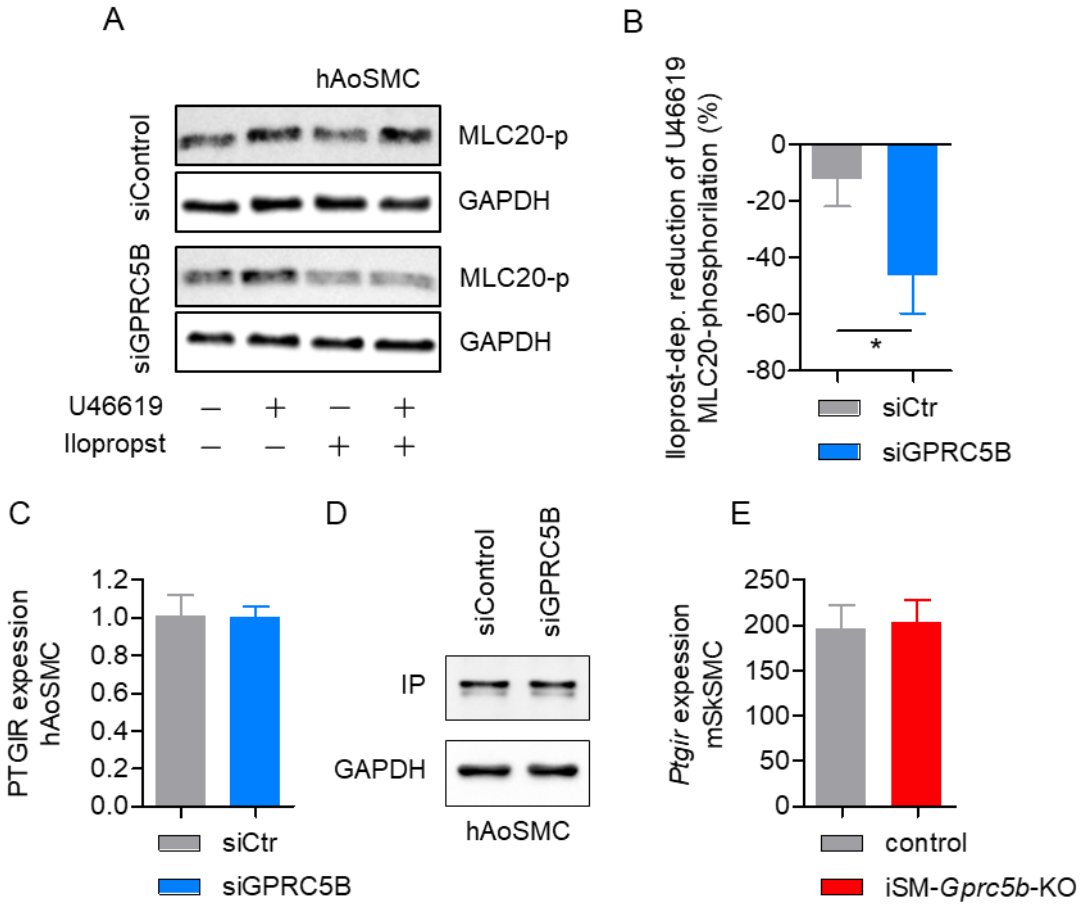

Figure 15 – Enhanced IP receptor-mediated intracellular signaling in GPRC5B-deficient SMC. A, B, Exemplary Western blot (C) and statistical evaluation (D) of MLC20 phosphorylation in control and GPRC5B-kd hAoSMC after addition of thromboxane A2 analogue U46619 (1 µM) for 1 minute and consecutive treatment with Iloprost (1 µM) for 3 minutes; GAPDH as loading control (n=5-7). **C, D,** mRNA (C) and protein (D) levels of prostacyclin receptor IP in control and GPRC5B-kd hAoSMC (n = 2-3). **E,** mRNA levels of *Ptgir* (encoding IP) in primary smooth muscle cells from skeletal muscle (mSkSMC) of control mice and iSM-*Gprc5b*-KO (n = 2). Data are means ± SEM; comparisons between genotypes were performed using unpaired Student's *t*-test. *, $P < 0.05$.

3. Effect of GPRC5B on IP receptor localization

3.1. IP receptor localization in GPRC5B-deficient HEK cells

Since the preceding results showed no differences on the IP receptor levels, we investigated whether GPRC5B modulates intracellular IP receptor trafficking. To do so, we transfected HEK293 cells with plasmids encoding HA-tagged IP receptor (HA-IP). Membrane expression of HA-IP was detected by ELISA in non-permeabilized cells after knockdown or overexpression of GPRC5B. Interestingly, while knockdown of GPRC5B enhanced HA-IP membrane abundance, overexpression of GPRC5B decreased it (Figure 16 A). This result was not due to decreased cell viability after GPRC5B overexpression (Figure 16 B). Moreover, overexpression of other GPCRs randomly selected, such as HCA2 or P2Y10, did not affect IP surface expression (Figure 16 C).

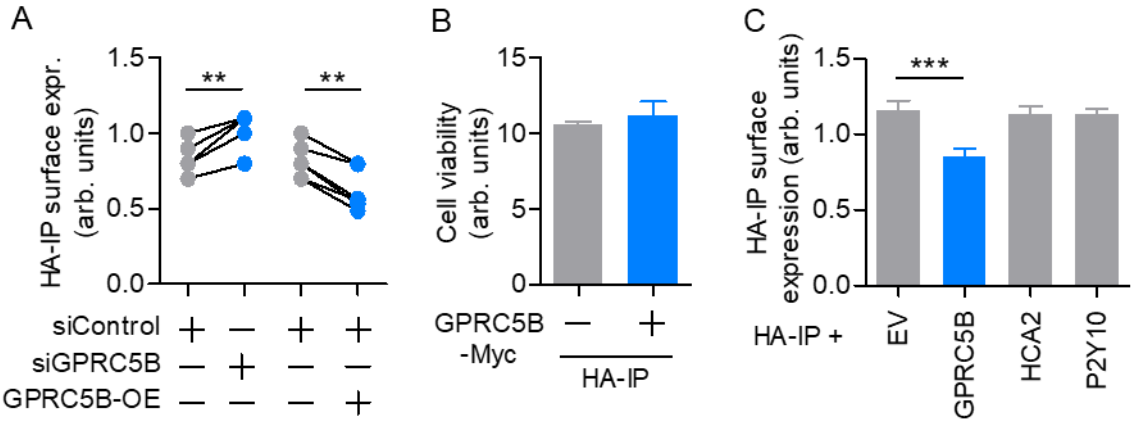

Figure 16 – Modulation of intracellular IP receptor trafficking by GPRC5B. **A, B**, ELISA-based detection of HA-tagged IP receptor in the plasma membrane of HEK293 cells after siRNA-mediated knockdown (siGPRC5B) or overexpression (OE) of GPRC5B (**A**) or after OE of other GPCRs such as HCA2 or P2Ry10 (**B**) (n = 6-12). **C,** Viability of GPRC5B-overexpressing cells (n=3). Data are means ± SEM; comparisons between genotypes were performed using paired (A), unpaired (B) Student's t-test and one way ANOVA (C). siControl, sample treated with scrambled control siRNA; *, P < 0.05; **, P < 0.01; ***, P < 0.001.

Furthermore, immunofluorescence staining done in permeabilized cells overexpressing either HA-IP alone or in combination with Myc-tagged GPRC5B (GPRC5B-Myc) showed that in cells lacking GPRC5B-overexpression the IP signal was mainly found in or close to the membrane, whereas in cells co-expressing GPRC5B the HA-IP signal was shifted to intracellular regions (Figure

17 A, B). The IP protein level in HEK cells was not affected by this altered cellular trafficking (Figure 17 C), and also the kinetic of iloprost-induced internalization of the HA-IP receptor was unchanged (Figure 17 D).

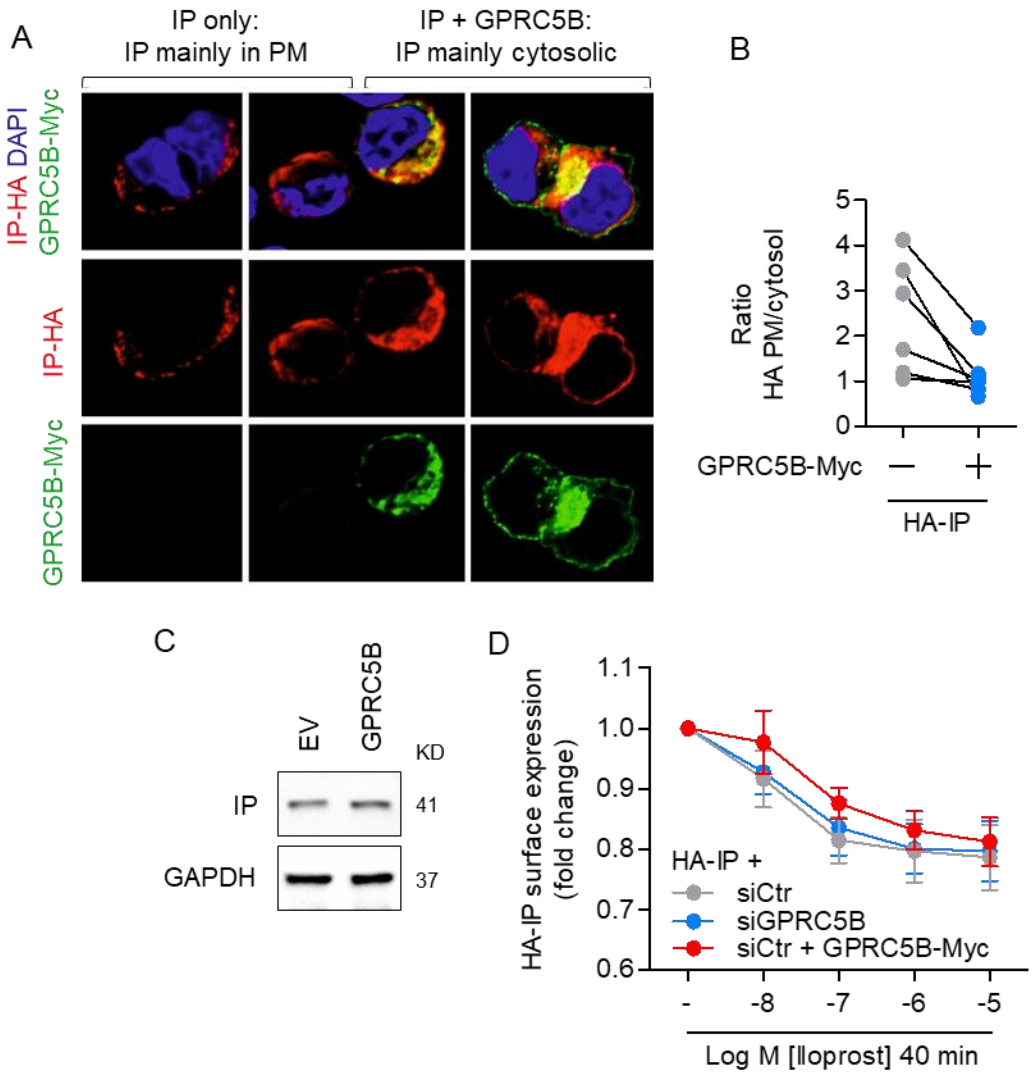

Figure 17 – Modulation of IP receptor localization by GPRC5B. **A, B**, Immunofluorescent staining of HA-IP/Myc-GPRC5B transfected HEK293 cells with anti-Myc and anti-HA antibodies: **A**, exemplary photomicrographs showing the intracellular localization of HA-IP in cells expressing HA-IP alone or in combination with GPRC5B-Myc; **B**, statistical evaluation of the IP-HA plasma membrane (PM)- to-intracellular (IC) ratio in GPRC5B-neg. and -pos. cells (n = 6, paired cells come from the same view field). **C**, Levels of endogenous IP receptor in HEK293 cells overexpressing GPRC5B. **D**, Internalization of surface HA-IP 40 minutes after addition of different concentrations of iloprost in control HEK293 cells or after knockdown/overexpression of GPRC5B (n = 8). Data are means ± SEM; comparisons between genotypes were performed using paired D Student's t-test. siCtr, sample treated with scrambled control siRNA; *, $P < 0.05$; **, $P < 0.01$; ***, $P < 0.001$.

3.2. IP receptor localization in GPRC5B-deficient SMC

To test whether our findings in HEK cells were also observed in GPRC5B-deficient SMC, we determined surface IP expression using an antibody directed against extracellular loop 3 of the IP receptor (IP(ec)) in non-permeabilized hAoSMC, after siRNA mediated knockdown. In agreement with our HEK data, we found that GPRC5B-deficient hAoSMC showed increased IP membrane staining when compared to control cells (Figure 18 A, B). We also performed immunohistochemical analysis in non-permeabilized small arteries from skeletal muscle of iSM-Gprc5b KO reporter mice. We found that in the media layer, identified by Cre-reporter-mediated EGFP expression, IP(ec) immunoreactivity was strongly increased (Figure 18 C, D). Therefore, SMC-specific deletion of GPRC5B increased membrane IP expression in hAoSMC as well as in mouse resistance vessels.

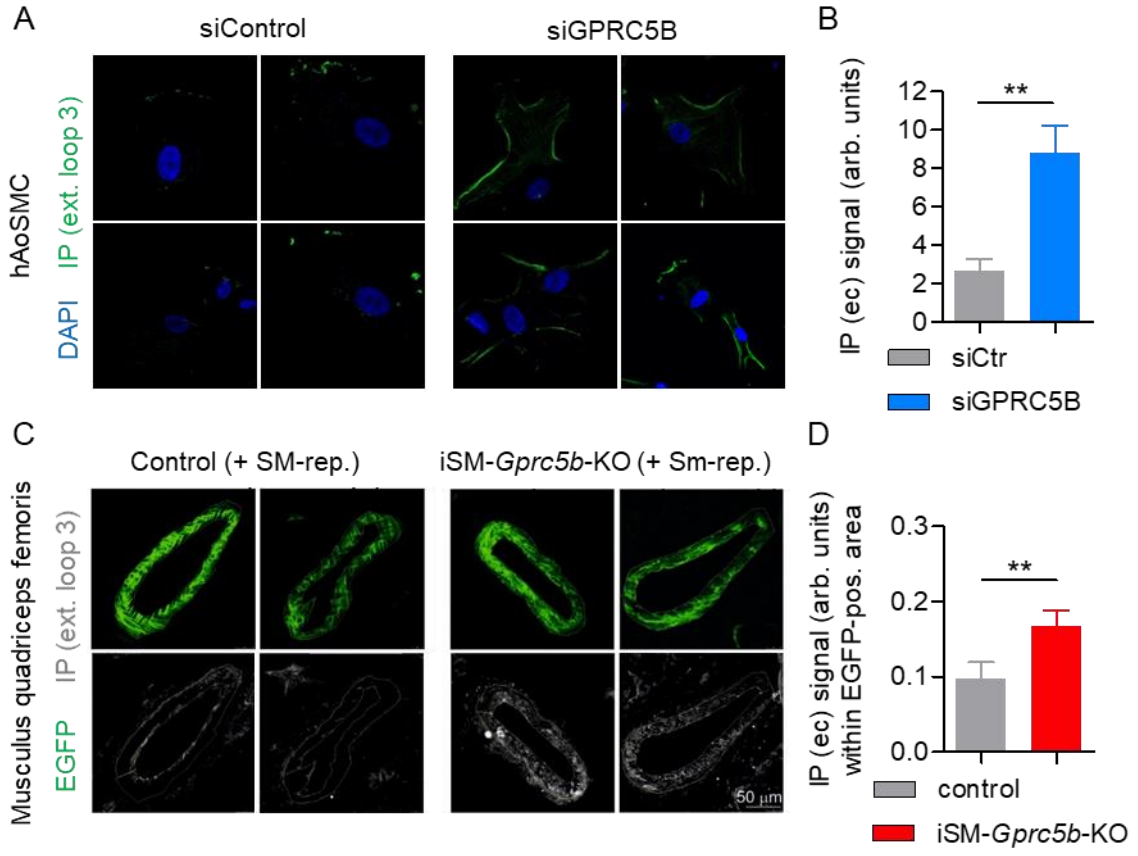

Figure 18 – IP membrane localization in GPRC5B-deficient SMC and iSM-*Gprc5b*-KO mice. **A, B**, Antibody-mediated detection of the extracellular domain of the endogenous IP receptor (IP(ec)) in non-permeabilized hAoSMC treated with control siRNA or GPRC5B-specific siRNA (A, exemplary photomicrographs; B, statistical evaluation) (n = 6). **C, D,** Antibody-mediated detection of IP(ec) in

non-permeabilized sections of murine skeletal muscle from control mice and iSM-*Gprc5b*-KOs bred to a Cre-dependent EGFP reporter line: **C**, exemplary photomicrographs; **D**, statistical evaluation of IP(ec) immunoreactivity within EGFP-positive areas (n = 12 vessels from 3 mice each). Data are means ± SEM; comparisons between genotypes were performed using unpaired Student's t-test. siCtr, sample treated with scrambled control siRNA; *, P < 0.05; **, P < 0.01; ***, P < 0.001.

3.3. Physical interaction between IP and GPRC5B

We next tested whether IP receptor trafficking was modulated by a physical interaction with GPRC5B. To do so, HEK293 cells were transfected with GPRC5B-Myc and HA-IP plasmids. We observed that GPRC5B-Myc and HA-IP signals were localized to the same compartments of the cells, and they had a high Manders' overlap coefficient (Figure 19).

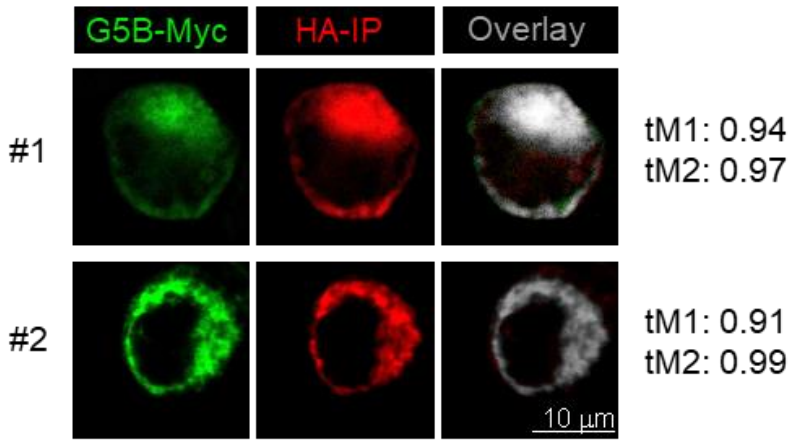

Figure 19 – Interaction between IP and GPRC5B. Colocalization of GPRC5B-Myc (green) and HA-IP (red) is displayed in white; Manders' colocalization coefficients tM1 and tM2 are shown next to each panel (1.0 indicates complete overlay).

Given our previous results, we next investigated the interaction of GPRC5B and IP by co-immunoprecipitation (CoIP). Western blotting of proteins precipitated by anti HA beads ("HA pulldown" in Figure 20 A - bottom) showed in cells co-expressing HA-IP and GPRC5B-Myc a Myc signal of the same expected molecular size observed for lysates ("Input" in Figure 20 A - top). However, no Myc signal was detected after HA pulldown in cells co-expressing the Myc tagged adhesion GPR133, a randomly chosen orphan GPCR (Figure 20 A). To further investigate the potential interactions between prostanoid receptors and class C

orphan GPCRs, we attempted a more structured analysis. We found that HA-IP pulldown not only resulted also in co-immunoprecipitation of GPRC5B, but also of GPRC5C, a closely related smooth muscle-expressed member of the GPRC5 subfamily (Figure 20 B, left side). In contrast, GPR156, another class C orphan GPCR with lower homology to GPRC5B, was not detected (Figure 20 B, left side). Besides the IP receptor, we also studied the interaction of these class C orphan GPCRs with other prostanoid receptors expressed in smooth muscle, for example the PGE_2 receptor subtype EP2 (Figure 20 B, right side). We observed that the GPRC5B Myc signal was evidently reduced and GPRC5C signal was not detected, though HA pulldown was equally efficient in EP2-HA expressing cells (Figure 20 B, right side). These data suggest that GPRC5B physically interacts with the prostacyclin IP receptor and, with lower efficiency, also with other prostanoid receptors in the HEK293 overexpression system.

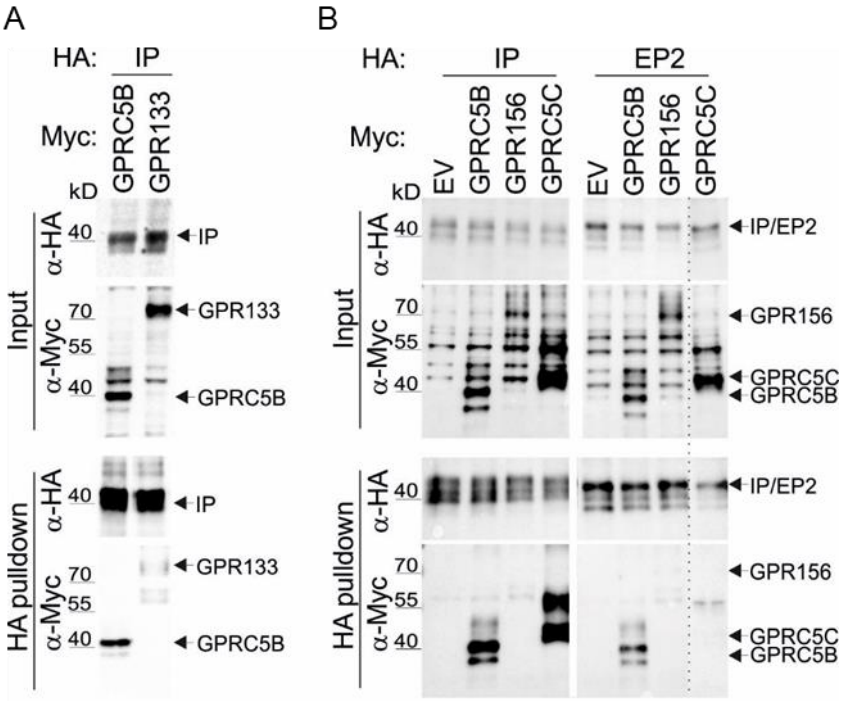

Figure 20 – Co-immunoprecipitation of the IP receptor. **A**, Western blot detection of HA and Myc signals in lysates of HEK293 cells expressing HA-IP (40 kDa) in combination with GPRC5B-Myc (44 kDa) or Myc-GPR133 (96 kDa) without ("input") and after immunoprecipitation of HA-IP ("HA pulldown"). **B**, Western blot detection of HA and Myc signals in lysates of HEK293 cells expressing HA-IP (left) or EP2-HA (right) in combination with empty vector, GPRC5B-Myc (44 kD), GPR156 (89 kD), or GPRC5C-Myc (53 kD) without ("input") and after immunoprecipitation of HA-IP ("HA pulldown"). Dotted line indicates border between membranes.

The physical interaction data observed previously was validated by dual color fluorescence recovery after photobleaching (FRAP) experiments using laser scanning microscopes to follow the in vivo dynamics of proteins tagged to fluorescent markers [189]. We tested whether immobilization of the IP receptor, but not of other GPCRs such as the β_2 adrenergic receptor (β_2AR), affected lateral mobility of GPRC5B. HEK293 cells were transfected with GPRC5B-mCitrine and either 1) mTurq2-IP or 2) CFP-β_2AR, and a large fraction of N-terminally mTurq2- and CFP-tagged receptors were specifically immobilized using polyclonal antibodies recognizing these GFP variants. After photobleaching of a defined membrane area, lateral mobility of immobilized and non-immobilized receptors was measured as the recovery of mTurq2/CFP and YFP fluorescence. As first tentative control, we observed a strongly reduced recovery of mTurq2-IP or CFP-β_2AR after antibody-mediated immobilization (Figure 21 A). We then investigated the mobility of GPRC5B-mCitrine. We found that while immobilization of CFP-β_2AR had only little effect on GPRC5B-mCitrine lateral mobility, mTurq2-IP immobilization markedly reduced GPRC5B-mCitrine recovery (Figure 21 B). These data further support the notion that GPRC5B physically interacts with the IP receptor.

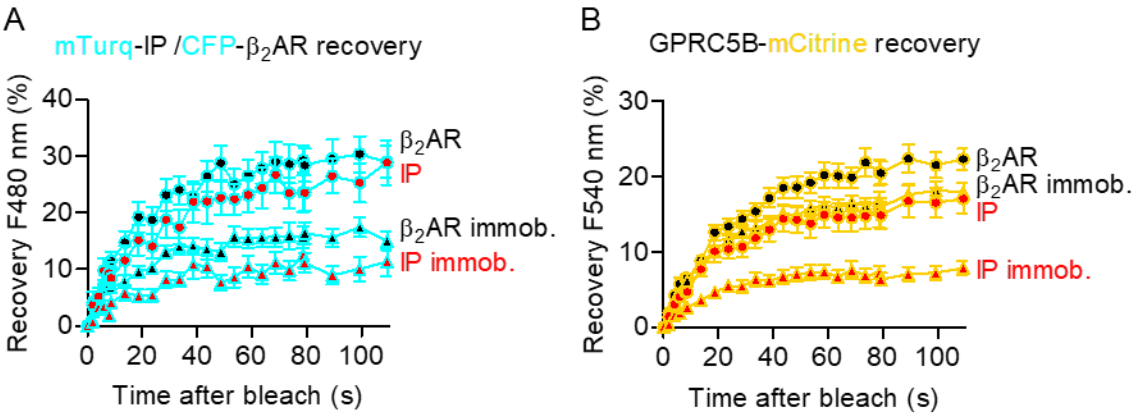

Figure 21 – Effect of immobilization of IP on GPRC5B lateral mobility. **A, B**, Co-immobilization experiments using dual color FRAP were performed in HEK cells expressing GPRC5B-mCitrine and either mTurquoise (mTurq2)-IP (red symbols) or CFP- β_2AR (black symbols) as indicated. Fluorescence recovery after photobleaching was determined for mTurq2-IP / CFP- β_2AR (**A**) and for GBRC5B-mCitrine (**B**) in the presence (triangles) or absence (circles) of antibodies mediating immobilization of IP or β_2AR (n=22-29 cells per group). Data are means ± SEM. (The experiment was performed by Prof. Dr. Moritz Bünemann Group at the Marburg University - Department of Pharmacology and Clinical Pharmacy).

4. Relevance of SMC GPRC5B in arterial hypertension

4.1. Effect of SMC-GPRC5B in systolic blood pressure

To study the in vivo effects of increased IP-mediated relaxation in vascular tone in iSM-*Gprc5b*-KO mice, we used an implantable radio telemetry device for blood pressure measurement. Basal blood pressure was measured for 3 days in non-induced control and KO mice and then SMC-*Gprc5b* deletion was induced by administration of tamoxifen (TX) on five consecutive days. During the tamoxifen treatment period, there was a transient increase in the blood pressure in mice of both genotypes (Figure 22), and after this initial phase we observed a mild hypotension in iSM-*Gprc5b*-KOs compared to tamoxifen-treated controls. This difference, however, was not statistically significant and was compensated after 3 weeks (Figure 22).

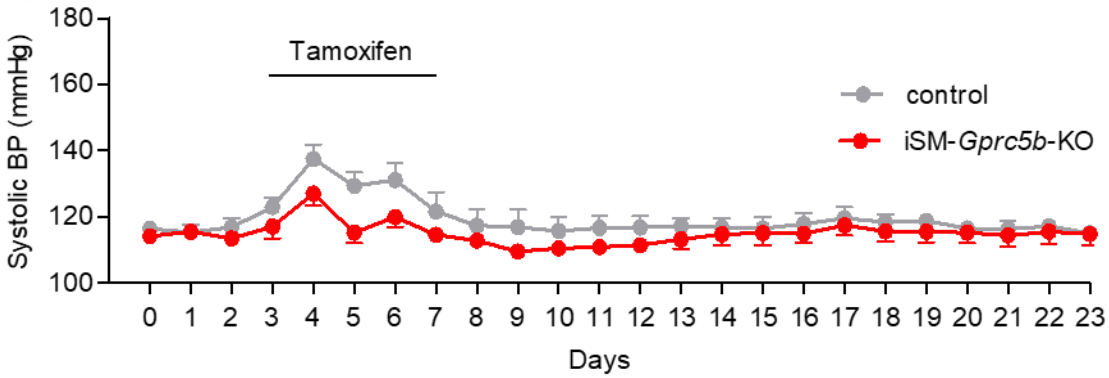

Figure 22 – Telemetric blood pressure measurement in iSM-*Grpc5b*-KOs. A-C, Telemetric recording of blood pressure in control and iSM-*Gprc5b*–KO mice before and after knockout induction with tamoxifen under basal conditions (**A**, n=12 controls, 10 KOs). Data are means ± SEM; differences between genotypes were analyzed using 2-way repeated measures ANOVA and Bonferroni's post-hoc test.

We next investigated whether loss of GPRC5B in SMC was able to ameliorate hypertensive disease. To test this, we used two models, 1) implantation of AngII-releasing miniosmotic pumps (Figure 23 A) and 2) subcutaneous implantation of a DOCA pellet in combination with unilateral nephrectomy and salt load via drinking water (Figure 23 B). In both models AngII and DOCA-salt treatment produced similar increases in the blood pressure of control mice and not yet induced knockout mice (Figure 23 A, B). However, induction of SMC-specific GPRC5B deficiency resulted, in both models, in a significant reduction of blood

pressure compared with control. Therefore, these data suggest that GPRC5B deficiency facilitates relaxation in hypertensive disease.

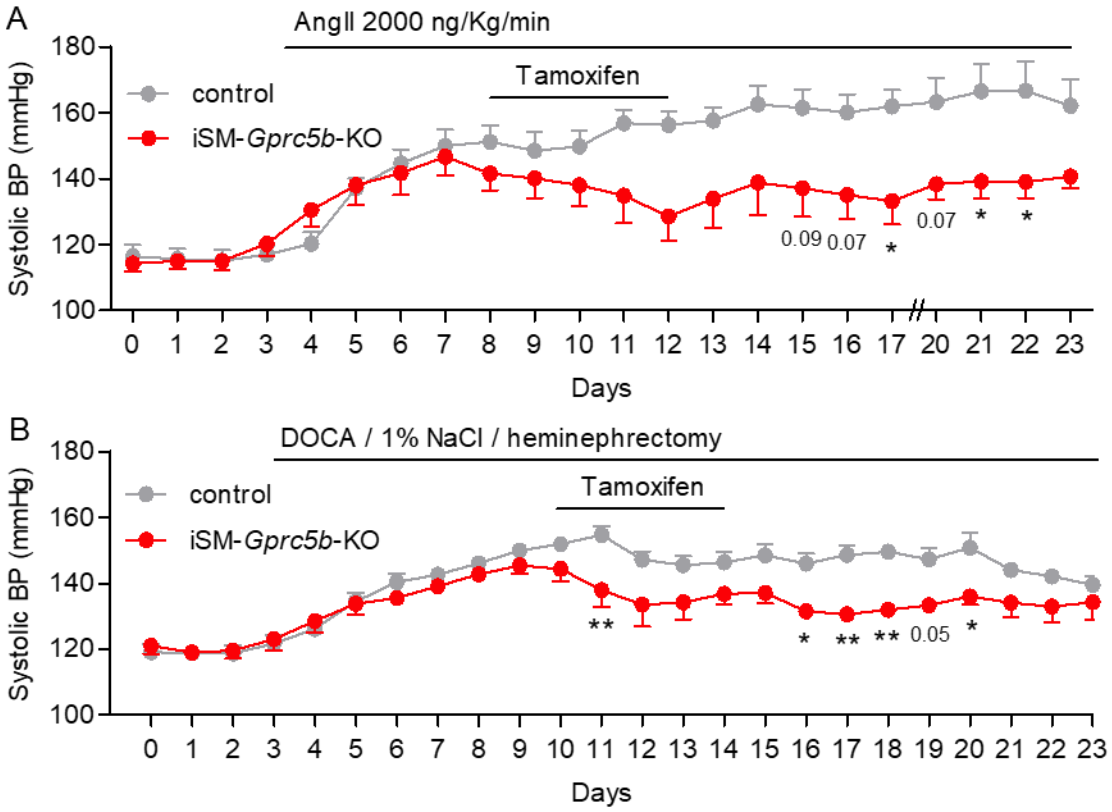

Figure 23 – Telemetric blood pressure measurement in iSM-*Grpc5b*-KOs. A-C, Telemetric recording of blood pressure in control and iSM-*Gprc5b*–KO mice before and after knockout induction with tamoxifen after implantation of an AngII-releasing miniosmotic pumps (**A**, n=11 controls, 6 KOs; data for days 18/19 are missing due to system failure), or after implantation of a DOCA-releasing pellet in combination with unilateral nephrectomy and exposure to 1 % NaCl in drinking water (**B**, n=8 controls, 10 KOs). Data are means ± SEM; differences between genotypes were analyzed using 2-way repeated measures ANOVA and Bonferroni's post-hoc test.

4.2. Effect of IP receptor in systolic blood pressure

Following the previous results, we investigated to what degree enhanced IP signaling contributed to the amelioration of the hypertensive disease. To test this, we studied the blood pressure effect of the IP antagonist Cay10441 in control and iSM-*Gprc5b*-KOs after induction of AngII-dependent hypertension (Figure 24 A). We observed that intraperitoneal injection of 10 mg/kg Cay10441, but not vehicle, produced increased blood pressure in iSM-*Gprc5b*-KOs, with no effect on control mice (Figure 24 B). This finding indicates that enhanced IP signaling is a prime

contributor to the observed amelioration of hypertensive disease in iSM-*Gprc5b*-KO mice.

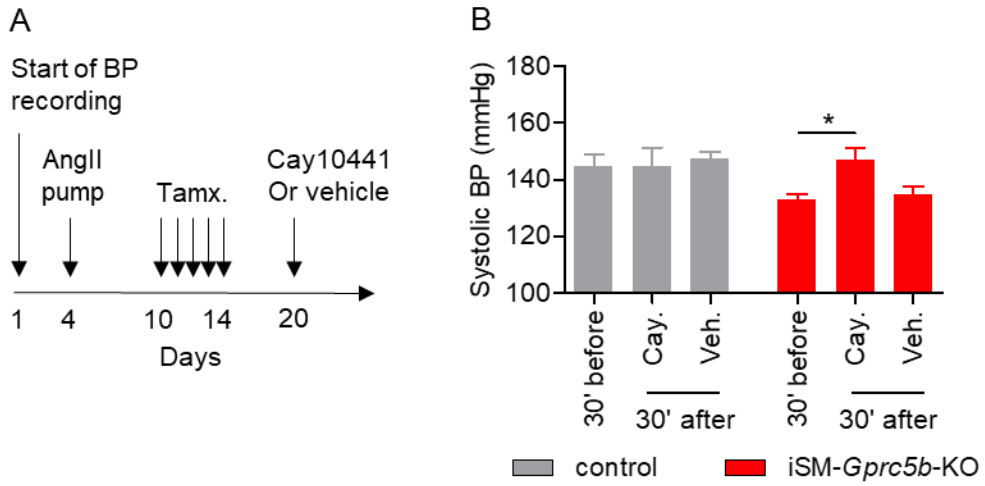

Figure 24 – Effect of IP antagonist Cay10441 (10 mg/kg i.p.) on systolic blood pressure in control mice and iSM-*Gprc5b*-KOs after induction of AngII hypertension. **A, B,** Experimental design (**A**) and statistical evaluation (**B**) of blood pressure 30 min before and 30 min after application of Cay10441 or vehicle. Data are shown as average values of 2 control mice and 5 iSM-Gpr5b-KO mice in 4 rounds of Cay10441 application and 2 vehicle applications; treatment-induced changes were analyzed using 2-way repeated measures ANOVA and Bonferroni's post-hoc test. *, $P < 0.05$.

5. Relevance of GPRC5B in smooth muscle differentiation

5.1. SMC gene expression in SMC-GPRC5B deficient hAoSMC

VSMCs have significant cellular plasticity. They can undergo profound changes between two phenotypes: a quiescent, contractile phenotype with differentiated SMCs, and a synthetic, proliferative one with dedifferentiated SMCs [190]. To investigate whether loss of GPRC5B was able to change proliferative and contractile gene expression we performed RT-qPCR analysis in hAoSMC. We found that cells lacking GPRC5B showed enhanced expression of contractile genes such as *ACTA2* (encoding αSMA) and *TAGLN* (encoding SM22α), and reduced expression of proliferative markers such as *MKi67*, *PCNA*, and *CCNA2* (Figure 25 A). Since it is known that the IP receptor, in addition to its vasoregulatory functions in mediation of relaxation, also promotes differentiation of SMC [155], we tested whether the expression profile observed after siRNA mediated knockdown of GPRC5B could be due to an increased IP receptor signaling. To do so, hAoSMC were treated with IP receptor antagonist Cay10441.

We found that inhibition of IP receptor did not changed the proliferation markers, *MKI67* and *PCNA*, however it largely normalized expression of contractile markers such as *ACTA2* and *TAGLN* (Figure 25 B). This suggests that increased IP signaling contributed, at least partially, to the increased SMC differentiation in GPRC5B-deficient hAoSMC.

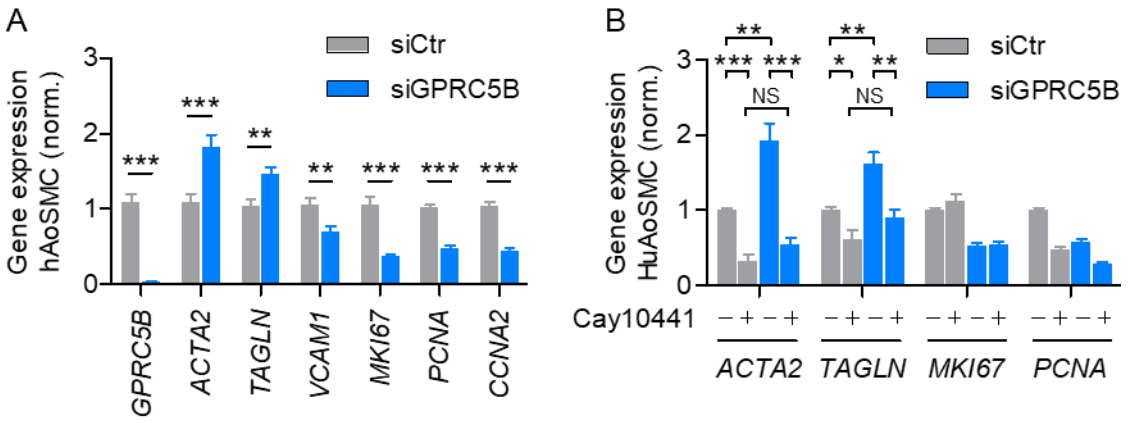

Figure 25 – Enhanced differentiation and reduced proliferation in GPRC5B-deficient hAoSMC A, B, qRT-PCR gene expression analysis in control and GPRC5B knockdown hAoSMC under basal conditions (**A**, n = 15) or after addition of IP receptor antagonist Cay10441 (**B**, n = 6) (all data normalized to respective control). Data are means ± SEM; comparisons between genotypes were performed using unpaired Student's *t*-test. *, $P < 0.05$; **, $P < 0.01$; ***, $P < 0.001$.

5.2. SMC gene expression in iSM-*Gprc5b*-KO mice

Published work in single cell expression analysis show that *Gprc5b* expression frequency is low in murine aortal SMC (mAoSMC), but high in resistance arteries from skeletal (mSkSMC) and mesenteric SMC (mMesSMC) [176] (Figure 26 A). To determine whether deletion of GPRC5B increased SMC differentiation in vivo, we performed mRNA sequencing in FACS-sorted mSkSMC from control and iSM-*Gprc5b*-KO reporter mice with SMC-specific EGFP expression. Gene ontology term analysis showed that expression of contraction-related genes was clearly changed in GPRC5B deficient mSkSMC (Figure 26 B). We found that specific inactivation of GPRC5B increased markers of SMC differentiation such as *Acta2* or *Tagln*, as well as myosin heavy and light chain isoforms and molecules involved in fiber organization such as *Actn1, Flna, Des, Tpm1/2, Dstn* (Figure 26 C). In contrast, we observed decreased expression of genes indicative of inflammatory activation, such as *Icam1, Ptgs1/2* (encoding COX1/2), *Nfkb1*, or

proteoglycans such as lumican (*Lum*) or decorin (*Dcn*) (Figure 26 C). The proliferation markers such as *Mki67, Pcna* and *Ccna2* were not reliably detected in freshly isolated SMC. To further corroborate the notion that reduced Gprc5b expression is associated with increased SMC differentiation, we re-analyzed previously generated single cell expression data from the murine aorta [176]. These data showed that aortal SMC that express Gprc5b ("*Gprc5b*-positive" in Figure 26 D) had reduced expression of *Myh11* and *Acta2* compared to cells that did not express Gprc5b ("*Gprc5b*-negative" in Figure 26 D). These data in human and murine SMC supports the notion that GPRC5B is a regulator of SMC differentiation.

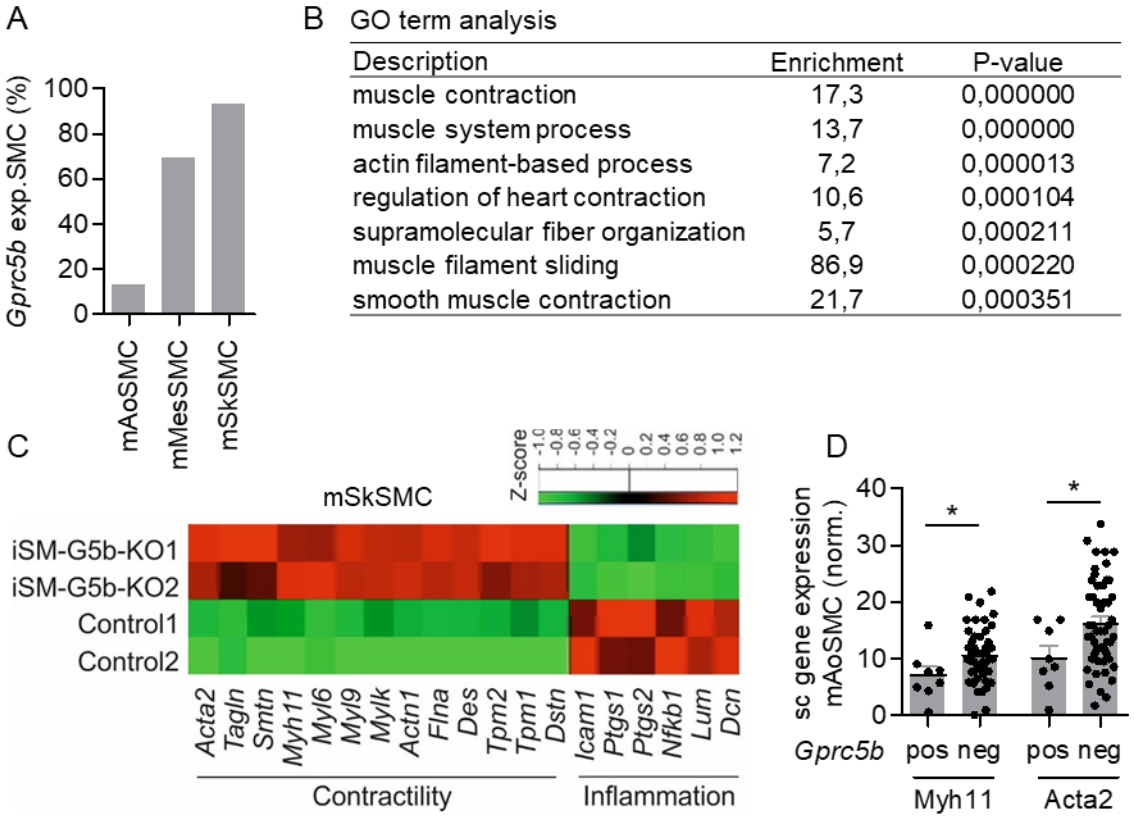

Figure 26 – Enhanced differentiation and reduced proliferation in iSM-*Gprc5b*-KO mice. A, Frequency of *Gprc5b*-expressing cells in murine aortic SMC (mSMao) and smooth muscle cells from the murine skeletal (mSMsk) or mesenteric (mSMmes) vasculature as judged by single cell RT-PCR (n= 29, 57, 60 cells). **B-C,** Heat map of library size-normalized counts detected by mRNA sequencing in EGFP-expressing SMC sorted from skeletal muscle of tamoxifen-treated control mice and iSM-*Gprc5b*-KOs bred to a Cre-dependent EGFP reporter line (n=2 per group, data are normalized to respective control): **B**, Top 7 changes according to GOrilla GO term analysis; **C**, Heat map showing Z-score (column)-normalized gene expression of selected contractility- and inflammation-

related genes. **D,** Expression of differentiation markers *Myh11* and *Acta2* in *Gprc5b*-positive and -negative murine aortic SMC (mAoSMC) as judged by single-cell (sc) RT-PCR (n=60 cells; data normalized to geometric mean of reference genes). Data are means ± SEM; comparisons between genotypes were performed using unpaired Student's *t*-test. *, $P < 0.05$; n, number of individual cells (D).

6. Relevance of SMC GPRC5B in arterial atherosclerosis

6.1. Atherosclerotic plaque development in iSM-*Gprc5b*-KO mice

In atherosclerosis, VSMCs dedifferentiate, proliferate and migrate, thus contributing to plaque formation. However, they may also display a beneficial role by stabilization of the fibrous cap [52]. Atherosclerotic lesions occur predominantly in the large vessels such aorta [191], and our single-cell expression data show that the expression frequency of *Gprc5b* increases in mAoSMC with aging and in response to atherosclerosis development in ApoE-deficient mice (Figure 27 A). Considering the suggested role of GPRC5B in the regulation of SMC differentiation, we investigated atherosclerosis development in iSM-*Gprc5b*-KOs. To do so we crossed in iSM-*Gprc5b*-KO mouse with ApoE-deficient mouse. After 16 weeks of high fat diet (HFD), atherosclerosis development was analyzed by oil red O-staining. We found that the plaque area was in trend reduced for total aorta and significantly reduced in the aortic arch after SMC specific deletion of *Gprc5b* (Figure 27 B-D).

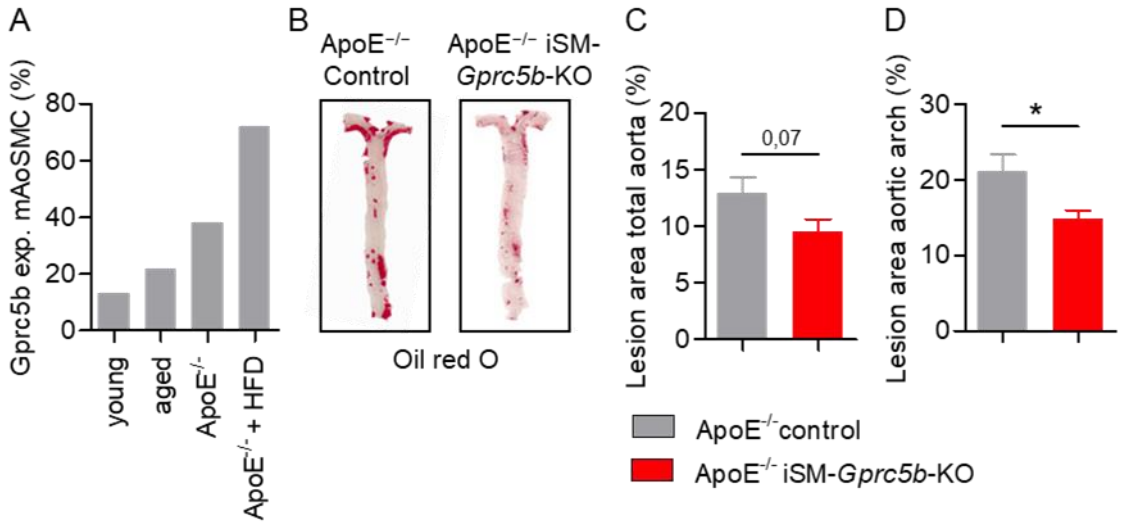

Figure 27 – Atherosclerosis development in iSM-*Gprc5b*-KO mice. A, The frequency of *Gprc5b* expression in murine aortic SMC (mAoSMC) from young mice (3 mo.), aged mice (16 mo.), young ApoE-deficient mice, and ApoE$^{-/-}$ mice

kept for 16 weeks on high fat diet (HFD) was determined by single-cell RT-PCR (data reanalyzed from 16). **B-D**, Oil red O-staining of aortae from ApoE$^{-/-}$ control mice and ApoE$^{-/-}$ iSM-*Gprc5b*-KO mice after 16 weeks of Western-type diet (3 independent experiments with n=14-16 in total): Exemplary photomicrograph (**B**) and statistical evaluation of plaque area in total aorta (**C**) and aortic arch only (**D**). Data in C, D are means ± SEM; comparisons between genotypes were performed using unpaired Student's t-test. *P<0.05.

6.2. Atherosclerotic plaque characterization in iSM-*Gprc5b*-KO mice

In addition, iSM-*Gprc5b*-KOs showed significantly smaller plaques in the innominate artery (Figure 28 A, B) and increased immunoreactivity for smooth muscle differentiation marker αSMA compared with control mice (Figure 28 C). These data suggest that SMC-deletion of *Gprc5b* reduces atherosclerosis development.

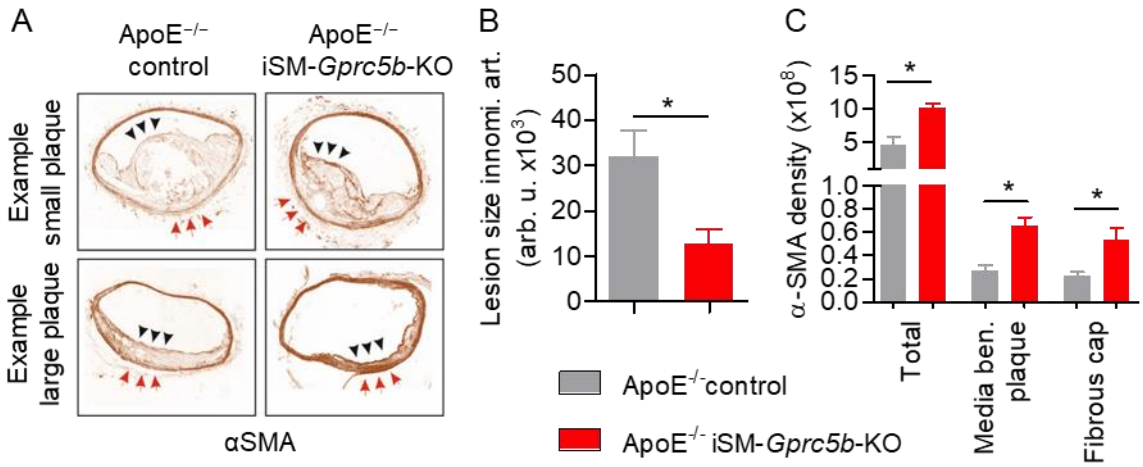

Figure 28 – Characterization of the Atherosclerotic plaques in iSM-*Gprc5b*-KO mice. A-C, αSMA staining in innominate arteries of ApoE$^{-/-}$ control mice and ApoE$^{-/-}$ iSM-*Gprc5b*-KO mice after 16 weeks of Western-type diet (samples from experiment #3 in B-D): **A**, Exemplary photomicrographs; **B**, evaluation of plaque size; **C**, statistical evaluation of αSMA staining in total vessel, media underlying plaque, and fibrous cap (n = 4-5) Data in B and C are means ± SEM; comparisons between genotypes were performed using unpaired Student's t-test. *P<0.05, **P<0.01, and ***P<0.001.

6.3. SMC gene expression in atherosclerotic iSM-*Gprc5b*-KO mice

To further corroborate the previous data, we performed mRNA sequencing of FACS-isolated mAoSMC from aortae of early atherosclerotic mice. We observed that GPRC5B-deficient SMC expressed higher levels of contractile markers such as *Acta2*, *Tagln* or *Smtn* (Figure 29).

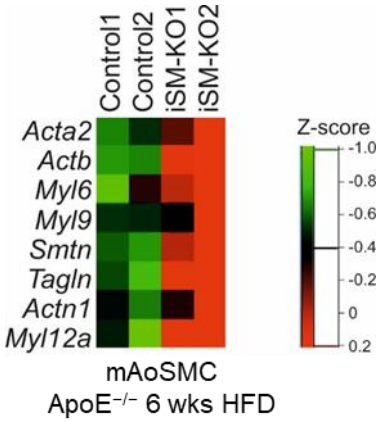

Figure 29 – SMC expression of contractile markers in early atherosclerotic iSM-*Gprc5b*-KO mice. Heat map showing Z-score (column)-normalized gene expression of selected contractility-related genes as detected by mRNA sequencing in EGFP-expressing SMC sorted from aortae of tamoxifen-treated control mice and iSM-*Gprc5b*-KOs bred to the ApoE$^{-/-}$ line and a Cre-dependent EGFP reporter line after 6 weeks on Western type diet.

VII. DISCUSSION

Taken together, the work of this thesis shows that GPRC5B, a class C orphan GPCR, modulates SMC contractility and differentiation by negatively regulating IP receptor trafficking, probably by physical interaction and cytosolic retention.

GPCR dimerization

Our data show not only that GPRC5B colocalizes with the IP receptor, but also that both receptors can be coimmunoprecipitated and that immobilization of the IP receptor affects lateral mobility of GPRC5B in FRAP microscopy. Together, these data indicate that in fact GPRC5B physically interacts with the IP receptor. It is has been suggested previously that GPCRs, besides acting as monomeric entities, can form homo- and heterodimers [192, 193]. In general, GPCR dimerization might affect ligand recognition, receptor activation [194], trafficking [195] and signaling [195, 196]. Although the functional significance of dimerization is uncertain for most class A receptors, it is clear that class C receptors can exist and operate as stable dimers.

Most class C GPCRs are structurally defined by three features: 1) a conserved common seven-helix transmembrane domains (7TM), containing the allosteric sites, 2) an exceptionally large N-terminal extracellular domain (ECD) that consists of a Venus flytrap domain (VFT) and a cysteine rich domain (CRD) (except in the $GABA_B$ receptor), and 3) an intracellular carboxyl-terminal (C-terminal) domain with high variability, which plays a role in scaffolding and signaling protein coupling [197]. It is established that all domains participate in the dimerization process, and the proper folding arrangement is critical for the process [198]. The homodimers are stabilized by an inter-promoter disulfide bond, polar contacts between VFT domains and interactions between 7TM domains [199]. The CRD has been also shown to play a critical role in the process of dimerization allowing the formation of disulfide bonds within the homodimer [200]. Metabotropic glutamate receptor (mGluR) and the calcium-sensing receptor (CaSR) form homodimers by cross-link the ECD via an intermolecular disulfide bond, whereas $GABA_B$ and taste receptors (TAS) are obligatory heterodimers without being covalently linked. $GABA_B$ receptors, since they don’t contain a CRD, they heterodimerize through their C-terminus coiled-

coil domains (CCD). It is known that the translocation of $GABA_{B1}$ from the endoplasmic reticulum (ER) to the cell surface as an active heterodimer with $GABA_{B2}$ requires an interaction between $GABA_{B1}$ and $GABA_{B2}$ receptor subunits. The molecular determinant of this interaction is a C-terminal retention motif (RXR) downstream of the putative CCD of $GABA_{B1}$ receptor that seems to be crucial for ER retention. The CCD of the $GABA_{B2}$ subunit binds and masks this RXR motif, allowing the trafficking of the $GABA_{B1}$-$GABA_{B2}$ heterodimer from the ER to the cell surface [201, 202]. Furthermore, several studies demonstrate that dimerization of C-Class GPCRs is not only required for trafficking but also for the mechanism of activation and signaling [200, 203]. For example, the $GABA_B$ receptors require heterodimerization of the two homologous subunits, $GABA_{B1}$ and $GABA_{B2}$. While $GABA_{B1}$ is capable of ligand binding, the $GABA_{B2}$ subunit promotes signal transduction [204].

GPRC5B, was first identified by Bräuner-Osborne during a screening for new mGluR subtypes [177]. It belongs to a family of four receptors that can be divided in two clusters based on the sequence identity in the TM region: GPRC5B and GPRC5C with 50% homology, and GPRC5A and GPRC5D with 52% [205]. Since GPRC5B did not display homology with the class A or B receptors, and had a 20-25% homology to metabotropic glutamate receptors of class C, it was first classified as a glutamate-like (class C) receptor [177]. However, in contrast to prototypical class C GPCRs, orphan GPRC5 family members have a very short N-terminus and lack both VTF and full CRD [205]. Other motifs are similar, GPRC5B contains for example in its N-terminus two cysteine residues analogues to the two cysteines closest to the membrane in the CRD found in glutamate receptors, calcium-sensing receptor and taste receptors [205]. Taken together, the classification as a class C GPCR is not compulsory, and a more recent study classified GPRC5B as “Other 7TM Receptors” because it could not be included in any classical families of GPCRs [78]. Besides the disputable GPRC5B classification as C-class receptor, our data suggest that GPRC5B indeed is able to undergo dimerization with certain receptors, in particular the IP receptor. Yet the mechanism underlying this finding remains to be elucidated.

The IP receptor is a class A GPCR. It has a molecular weight of 41 to 83 KDa and is located in the plasma membrane. Structurally it has seven transmembrane domains with a short extracellular N-terminal region and an extended intracellular C-terminal region [206]. In the IP receptor, transmembrane domains VI and VII bind with PGI_2 side chains. Transmembrane domains I and II confer broader binding functions, including recognition and interaction with the cyclopentane ring of prostacyclin [207], the transmembrane domain I also contains a dimerization motif [206]. Despite lack of information about GPRC5B dimerization, several studies suggest that the prostacyclin receptor can form dimers [208, 209]. Detailed experiments done by co-immunoprecipitation of differentially tagged IP in COS-7 cells demonstrate that the IP receptor can homodimerize and this depends on disulfide bonds between cysteines in different locations [210]. Furthermore, co-expression of a dysfunctional IP that is retained in the endoplasmic reticulum (ER) (IP(R212C) [211] exerted a dominant action on the wild type IP, leading to ER retention of the wild type receptor [212]. All these findings suggest homodimerization as a prerequisite for proper IP receptor trafficking. In line with this notion we found that the presence of GPRC5B decreases the ability of the IP receptor (as monomer or dimer) to traffic to the plasma membrane possible by GPRC5B/IP heterodimerization which restricts IP homodimerization. In support, we found that both receptors are expressed and colocalize in the plasma membrane and cytosol. In contrast to class C, A-class GPCRs are believed to dimerize through their transmembrane domain, however the structural motifs and specific sites mediating dimerization, are not clear [208, 209]. Likewise, it is still unknown if GPRC5B/IP interaction is ligand-dependent or -independent. In fact, our current findings show that GPRC5B and IP interact without exogenous ligand. Such result opens the possibility that SMC-autonomous ligands play a role, either SMC-produced prostacyclin [119, 152] or a yet unknown autocrine activator of GPRC5B.

Role of prostacyclin signaling in arterial hypertension

PGI_2 is the major arachidonic acid metabolite produced in endothelium and VSMC [151, 152]. Subsequent to its binding to the G_s-coupled IP receptor, it stimulates adenylyl cyclase-dependent cAMP formation which, among other effects, causes vascular relaxation [157-159]. Although several mechanisms

have been proposed, none of them completely clarifies the mode of regulation of VSMC contractile responses. [113, 160, 213]**.** The relevance of PGI_2-IP signaling for the regulation of systemic blood pressure is complex. On the one hand, mice lacking IP receptor are normotensive when compared with control animals [156], and the administration of the IP antagonist Cay10441/RO3244794 does not change mean arterial blood pressure in healthy rats [214, 215]. On the other hand, iloprost, a synthetic agonist of the IP receptor, caused hypotension in healthy mice [214] and lowered blood pressure in hypertensive mongrel dogs [216]. Furthermore, patients with pregnancy-induced hypertension and some patients with essential hypertension have reduced endogenous synthesis of PGI_2 [119, 217]. Also, in patients with pulmonary arterial hypertension (PAH) the production of prostacyclin synthase, a key enzyme in formation of PGI_2, was shown to be decreased [218]. In agreement with this, mice lacking the same enzyme displayed hypertension and chronic kidney disease [217]. This accumulation body of evidence suggests that while loss of the IP receptor can be compensated by other receptors, for example EP4, PGI_2 has important anti-hypertensive effects [219-221]. Our in vivo results shown that VSMC-specific deletion of GPRC5B results in an antihypertensive effect. This might be explained by the facilitation of IP receptor-mediated responses to PGI_2. Additional mechanisms by which GPRC5B regulates vascular function may exist even so, but the significant reduction of the beneficial effects of GPRC5B deficiency promoted by the IP antagonist Cay10441 strongly suggest that enhanced IP receptor signaling is a major contributing factor.

Role of prostacyclin signaling in VSMC differentiation

We investigated whether enhanced IP signaling in GPRC5B-deficient SMC would affect VSMC functions such as proliferation and differentiation. Our in vivo analyses show that SMC-specific deletion of GPRC5B resulted in reduced atherosclerosis development concomitant with a preservation of the differentiated SMC phenotype. Furthermore, on the same mice we found a significant greater expression of αSMA in the media underlying plaque as well as the fibrous cap. The fibrous cap has a critical role in preservation of the integrity of the plaque and the number of SMCs in fibrous cap is directly correlated with plaque stability [222]. SMCs of the fibrous cap have been shown to strongly express differentiated SMC

markers including αSMA [52, 54]. Therefore, SMC-specific deletion of GPRC5B by reducing SMC dedifferentiation, prevented plaque growth and plaque rupture. The IP receptor plays a role in facilitation of SMC differentiation and reduced proliferation. It has been shown that IP agonists can inhibit vascular SMC migration and proliferation [172, 173] and induce SMC differentiation via the G_s/PKA/CREB pathway [155, 223]. In vivo studies have been showing the role of IP receptor in cardiovascular homeostasis. IP-deficient mice display increased propensities toward thrombotic events [156], restenosis and atherosclerosis [224], and in both atherogenic apolipoprotein E (apo-E)- and low-density lipoprotein receptor (LDL-R)-deficient mice backgrounds, deletion of IP receptor increased atherosclerotic lesion size [225, 226]. This indicates that reduction of PGI_2 facilitates the phenotypic switch from contractile SMC to the more proliferative, migratory and synthetic dedifferentiated phenotype that contributes to vascular remodeling [171, 227].

Our previous studies showed that in healthy aortas a small population of cells exist that differs from the other SMC [176]. This small group of cells shows signs of dedifferentiation as judged by reduced expression of contractile proteins *Myh11* or *Acta2*, but increased expression of *Icam1, Vcam1, Col1a2* and *Col3a1*. In addition, they are characterized by expression of specific orphan GPCRs, including *Gprc5b*, *Ptgir, Vipr2, Gpr39, Lpar1, Gpr124, Cxcr7, Gpr137b, Ednra* and others. Interestingly, SMC from atherosclerotic mice show similar features, including clear signs of inflammatory activation and dedifferentiation: *Icam1*, *Vcam1* and *Il6* were upregulated, whereas contractile proteins such as *Acta2* and *Myh11* were reduced [176].

Our data suggest that upregulation of GPRC5B in SMC enhances the process of SMC dedifferentiation by inhibiting IP-mediated protective effects. Therefore, pharmacological inhibition of GPRC5B or its interaction with IP is likely to be an effective therapy targeting chronic vascular diseases such as atherosclerosis. Of note, our data suggest that pharmacological inhibition of the GPRC5B/IP interaction would also have beneficial effects in arterial hypertension, one of the leading risk factors of atherosclerosis.

GPRC5B-mediated modulation of IP signaling - putative functions in other cell types

A. Fibroblasts

Our data show that after deletion of GPRC5B the expression of proliferative and inflammatory markers is reduced due to increased activation of IP signaling in hAoSMC. Therefore, it would be of interest to investigate if this correlation is also applicable in other cell types. From our single-cell analysis (data not shown) we know that GPRC5B and IP are coexpressed in fibroblasts, and upon injury the expression of both receptors is significantly increased. Fibroblasts are the most prevalent non-cardiomyocyte cell type in the heart. They are mainly responsible for the deposition of the extra cellular matrix (ECM) [228, 229]. These cells play a role in the regulation of heart development, but also in myocardial remodeling during hypertrophy, scar formation, myocardial infarction and heart failure. [230, 231]. PGI_2, has been shown to negatively modulate fibrotic activation in the heart [232]. In detail, stimulation of cardiac fibroblasts with analogues of PGI_2 markedly reduced cardiac fibroblast growth, collagen deposition, and prevented up-regulation of collagen I and other extracellular matrix related genes which suggests a potential role for prostacyclin receptor in cardiac fibroblasts [233]. Given our findings in VSMC, it would be interesting to test whether inactivation of GPRC5B enhances IP signaling in cardiac fibroblasts, thereby dampening adverse remodeling. In line with this notion, recently a new role for GPRC5B in fibroblast-driven myocardial inflammation and cardiac remodeling was suggested [183]. The authors of this study found that GPRC5B modulates the inflammatory response of cardiac fibroblasts and the degradation of extracellular matrix-proteins in the mice heart. In detail, the overexpression of GPRC5B significantly increased the transcription levels of the pro-inflammatory and pro-fibrotic cytokines TNFα, IL-1β, IL-6 and MCP-1, and extracellular matrix-degrading MMP-9. Contrariwise, siRNA-mediated knockdown of GPRC5B resulted in a decrease expression of these markers in cardiac fibroblasts [183].

B. β-cells

Cell-based studies also suggest that GPRC5B negatively regulates insulin secretion, potentially by reducing β-cell viability. Deletion of GPRC5B is in constitutive knockout mice associated with increased glucose- and glutamate-

induced insulin secretion, and in type-2 diabetes the expression level of GPRC5B is increased [182]. These findings raised the possibility that GPRC5B negatively regulates insulin secretion, but the molecular mechanisms underlying this remain unclear. It is suggested that an antagonist of GPRC5B might be effective in means of restoring normal insulin secretory function in diabetic patients. In contrast, it is known that IP signaling through PGI_2, play a positive role in β-cells by enhancing glucose-stimulated insulin secretion. The IP agonist iloprost was shown to increase glucose-stimulated insulin secretion, whereas the PGI_2 antagonist Cay10441 decreased insulin release β-cells [234]. Moreover, beraprost, another PGI_2 analog, improved islet viability during isolation, which suggests that PGI_2 may regulate β-cell mass by enhancing β-cell survival. In addition, it has also described that IP signaling plays a positive role in protecting against β-cell death [235]. Given the opposite roles of GPRC5B and IP receptor in β-cells it would be interesting to know if GPRC5B is also modulating negatively IP glucose-stimulated insulin secretion signaling and β-cell survival.

GPRC5B-mediated modulation of other prostaglandin receptors

Our study provided new evidence that GPRC5B not only interacts with IP, but also with other prostanoid receptors expressed in VSMC, for example with the PGE_2 receptor subtype EP2. EP2 is one of the four G-protein coupled EP receptors, EP1, EP2, EP3 and EP4. EP1 and EP3 are known to couple to G_q to activate Ca^{2+} signaling and G_i to inhibit adenylyl cyclase, respectively, whereas EP2 and EP4 couple to G_s to stimulate adenylyl cyclase. The EP2 receptor is expressed in the human small intestine, lung, kidney, thymus, uterus, leukocytes, smooth muscle, central nervous system (CNS), reproductive system and bones [236]. Global EP2-deficient mice exhibit impaired ovulation and reduced fertilization. When fed with a high-salt diet, these mice develop significant hypertension with concomitant increase in urinary excretion of PGE_2 [154, 237]. Furthermore, treatment with the EP2 agonist butaprost induced a transient hypotension in wildtype mice, but not in $EP2^{-/-}$ mice [237]. This means that similar to the IP receptor, activation of the EP2 receptor mediates anti-hypertensive effects. However, whether EP2 signaling is indeed altered in the absence of GPRC5B has not yet been studied.

It should in this contexto be noted that the amount of GPRC5B precipitated with EP2 is lower than that precipitated with IP, suggesting that the interaction between GPRC5B and EP2 is weaker. In general, little is known about the dimerization ability of EP receptors. The only study about EP2 dimerization is in line with our results and shows that indeed EP2 can form dimers with other GPCRs [238]. Furthermore they also suggest that EP2 when in a heterodimer affects the active conformation of the partner GPCR as an endogenous allosteric modulator, altering subsequent signaling [238]. Therefore, there is a possibility that GPRC5B also regulates SMC contractility by allosteric modulation of EP2 or by trafficking as observed for the IP receptor. Further continuation of these studies should highlight the significance of this potential interaction as well as the signaling and mechanisms involved. Additionally, it will be also interesting to study the possible interaction of GPRC5B with other prostanoid receptors. Might be that GPRC5B only interacts with the relaxant receptors (IP, DP, EP2, and EP4) negatively regulating their signaling, as we demonstrate in our study for IP receptor. Or can be that GPRC5B also interacts with the contractile prostanoid receptors (EP1, EP3, FP, and TP) potentiating its vasoconstrictor effects, having in this case a dual role for positively or negatively regulation of prostanoid receptors.

GPRC5C-mediated modulation of GPCR trafficking

GPRC5C, another member of the retinoic acid-induced GPRC5 family, shows 50% sequence homology with the most closely related GPCR, but expression studies and studies in global KO suggest many differences: GPRC5B and GPRC5C are differentially expressed and distributed in the brain, GPRC5C deficient mice do not manifest defects in their cognitive and behavioral capabilities, while GPRC5B-deficient mice exhibited altered spontaneous activity pattern and decreased response to a new environment [179]. However, in SMC, GPRC5B and GPRC5C show similar expression patterns, both are enriched in SMC of resistance arteries and in dedifferentiating aortal SMC. Furthermore, both could be co-immunoprecipitated with IP receptor. However, whether GPRC5C influences IP signaling has not yet been studied. Therefore, might be interesting to know if in VSMCs they have complementary functions, if the deletion of one can be compensated by the other receptor or if they act independently. Studies

in VSMC specific double KO mice for GPRC5B and GPRC5C might lead to further insights concerning the role of these proteins in the regulation of proliferation and dedifferentiation.

Clinical relevance

Our data show that GPRC5B regulates VSMC tone and differentiation by negatively regulating IP signaling. From a therapeutic point of view, this suggests GPRC5B as potential drug target, since inhibition of GPRC5B function might be clinically beneficial in vascular diseases such as arterial hypertension or atherosclerosis. A major obstacle in the development of GPRC5B inhibitors or inhibitors of GPRC5B/IP interaction is the fact that neither the ligand nor the downstream second messenger have been identified, and the crystal structure has not been analyzed. However, from a theoretical viewpoint candidate-compounds should act in at least one of these ways:

1) To promote conformational changes affecting ability to GPRC5B to form dimers;
2) To bind to GPRC5B promoting internalization and degradation of the receptor;
3) To bind to GPRC5B when it is localized in the intracellular regions and exist as a monomer preventing its trafficking to the membrane;
4) To bind to GPRC5B preventing its activation and internalization, and therefore IP internalization as well.

However, there are certainly some important points which need to be considered when using GPRC5B as potential drug target. For instance, GPRC5B is also expressed in other tissues and cells such as the central nervous and EC. Whether antagonists of GPRC5B cause considerable side effect in these cells and tissues remains also to be elucidated.

VIII. BIBLIOGRAPHY

1. Owens, G.K., M.S. Kumar, and B.R. Wamhoff, *Molecular regulation of vascular smooth muscle cell differentiation in development and disease.* Physiol Rev, 2004. **84**(3): p. 767-801.
2. Beamish, J.A., et al., *Molecular regulation of contractile smooth muscle cell phenotype: implications for vascular tissue engineering.* Tissue Eng Part B Rev, 2010. **16**(5): p. 467-91.
3. Brozovich, F.V., et al., *Mechanisms of Vascular Smooth Muscle Contraction and the Basis for Pharmacologic Treatment of Smooth Muscle Disorders.* Pharmacol Rev, 2016. **68**(2): p. 476-532.
4. Patton, K.T. and G.A. Thibodeau, *The human body in health & disease*. 2018.
5. Atluri, P., *The surgical review : an integrated basic and clinical science study guide*. 2006, Philadelphia, Pa.; London: Lippincott Williams & Wilkins.
6. Chiu, J.J. and S. Chien, *Effects of disturbed flow on vascular endothelium: pathophysiological basis and clinical perspectives.* Physiol Rev, 2011. **91**(1): p. 327-87.
7. Carroll, R.G., *Vascular System*, in *Elsevier's Integrated Physiology*, R.G. Carroll, Editor. 2007, Mosby: Philadelphia. p. 77-89.
8. Mozafari, H., C. Zhou, and L. Gu, *Mechanical contribution of vascular smooth muscle cells in the tunica media of artery*, in *Nanotechnology Reviews*. 2019. p. 50.
9. Klabunde, R.E., *Cardiovascular physiology concepts*. 2012: Second edition. Philadelphia, PA : Lippincott Williams & Wilkins/Wolters Kluwer, [2012] ©2012.
10. dela Paz, N.G. and P.A. D'Amore, *Arterial versus venous endothelial cells.* Cell and Tissue Research, 2009. **335**(1): p. 5-16.
11. Cleaver, O. and P.A. Krieg, *Molecular Mechanisms of Vascular Development*, in *Heart Development*, R.P. Harvey and N. Rosenthal, Editors. 1999, Academic Press: San Diego. p. 221-252.
12. Carroll, R.G., *Elsevier's integrated physiology.* 2007.
13. Barral, J.-P. and A. Croibier, *Circulatory physiology*, in *Visceral Vascular Manipulations*, J.-P. Barral and A. Croibier, Editors. 2011, Churchill Livingstone: Oxford. p. 27-45.
14. Sicard, G.A., *Rutherford's Vascular Surgery and Endovascular Therapy.* Journal of Vascular Surgery, 2018. **68**(5): p. 1611-1612.
15. Tykocki, N.R., E.M. Boerman, and W.F. Jackson, *Smooth Muscle Ion Channels and Regulation of Vascular Tone in Resistance Arteries and Arterioles.* Compr Physiol, 2017. **7**(2): p. 485-581.
16. Davis, M.J. and M.A. Hill, *Signaling mechanisms underlying the vascular myogenic response.* Physiol Rev, 1999. **79**(2): p. 387-423.
17. Jackson, W.F., *Ion channels and vascular tone.* Hypertension (Dallas, Tex. : 1979), 2000. **35**(1 Pt 2): p. 173-178.
18. Hall, J.E., *Guyton and Hall textbook of medical physiology*. 2016.
19. Kanagy, N.L. and S.W. Watts, *Components of the Vascular System*, in *xPharm: The Comprehensive Pharmacology Reference*, S.J. Enna and D.B. Bylund, Editors. 2007, Elsevier: New York. p. 1-3.

20. Levy, M.N., A.J. Pappano, and R.M. Berne, *Cardiovascular physiology*. 2007, Philadelphia: Mosby Elsevier.
21. Lv, P., et al., *SM22alpha inhibits lamellipodium formation and migration via Ras-Arp2/3 signaling in synthetic VSMCs.* Am J Physiol Cell Physiol, 2016. **311**(5): p. C758-c767.
22. Webb, R.C., *Smooth muscle contraction and relaxation.* Adv Physiol Educ, 2003. **27**(1-4): p. 201-6.
23. Campbell, J.H. and G.R. Campbell, *Smooth muscle phenotypic modulation--a personal experience.* Arterioscler Thromb Vasc Biol, 2012. **32**(8): p. 1784-9.
24. Rensen, S.S., P.A. Doevendans, and G.J. van Eys, *Regulation and characteristics of vascular smooth muscle cell phenotypic diversity.* Neth Heart J, 2007. **15**(3): p. 100-8.
25. Wirth, A., et al., *G12-G13-LARG-mediated signaling in vascular smooth muscle is required for salt-induced hypertension.* Nat Med, 2008. **14**(1): p. 64-8.
26. van der Loop, F.T., et al., *Smoothelin, a novel cytoskeletal protein specific for smooth muscle cells.* J Cell Biol, 1996. **134**(2): p. 401-11.
27. Zhang, J., et al., *Generation of an adult smooth muscle cell-targeted Cre recombinase mouse model.* Arterioscler Thromb Vasc Biol, 2006. **26**(3): p. e23-4.
28. Kuhbandner, S., et al., *Temporally controlled somatic mutagenesis in smooth muscle.* Genesis, 2000. **28**(1): p. 15-22.
29. Miano, J.M. and E.N. Olson, *Expression of the smooth muscle cell calponin gene marks the early cardiac and smooth muscle cell lineages during mouse embryogenesis.* J Biol Chem, 1996. **271**(12): p. 7095-103.
30. Huang, J. and C.D. Kontos, *Inhibition of vascular smooth muscle cell proliferation, migration, and survival by the tumor suppressor protein PTEN.* Arterioscler Thromb Vasc Biol, 2002. **22**(5): p. 745-51.
31. Shanahan, C.M. and P.L. Weissberg, *Smooth muscle cell heterogeneity: patterns of gene expression in vascular smooth muscle cells in vitro and in vivo.* Arterioscler Thromb Vasc Biol, 1998. **18**(3): p. 333-8.
32. Clarke, M.C., et al., *Vascular smooth muscle cell apoptosis induces interleukin-1-directed inflammation: effects of hyperlipidemia-mediated inhibition of phagocytosis.* Circ Res, 2010. **106**(2): p. 363-72.
33. Pan, D., et al., *Platelet-derived growth factor BB modulates PCNA protein synthesis partially through the transforming growth factor beta signalling pathway in vascular smooth muscle cells.* Biochem Cell Biol, 2007. **85**(5): p. 606-15.
34. Zhao, Y., et al., *Rho-associated protein kinase isoforms stimulate proliferation of vascular smooth muscle cells through ERK and induction of cyclin D1 and PCNA.* Biochem Biophys Res Commun, 2013. **432**(3): p. 488-93.
35. Li, Y., et al., *Enhanced Rb/E2F and TSC/mTOR Pathways Induce Synergistic Inhibition in PDGF-Induced Proliferation in Vascular Smooth Muscle Cells.* PLoS One, 2017. **12**(1): p. e0170036.
36. Blau, H.M., et al., *Plasticity of the differentiated state.* Science, 1985. **230**(4727): p. 758-66.

37. Shankman, L.S., et al., *KLF4-dependent phenotypic modulation of smooth muscle cells has a key role in atherosclerotic plaque pathogenesis.* Nat Med, 2015. **21**(6): p. 628-37.
38. Clarke, M.C., et al., *Chronic apoptosis of vascular smooth muscle cells accelerates atherosclerosis and promotes calcification and medial degeneration.* Circ Res, 2008. **102**(12): p. 1529-38.
39. Althoff, T.F. and S. Offermanns, *G-protein-mediated signaling in vascular smooth muscle cells - implications for vascular disease.* J Mol Med (Berl), 2015. **93**(9): p. 973-81.
40. Pipes, G.C., E.E. Creemers, and E.N. Olson, *The myocardin family of transcriptional coactivators: versatile regulators of cell growth, migration, and myogenesis.* Genes Dev, 2006. **20**(12): p. 1545-56.
41. Werth, D., et al., *Proliferation of human primary vascular smooth muscle cells depends on serum response factor.* Eur J Cell Biol, 2010. **89**(2-3): p. 216-24.
42. Zhou, J. and B.P. Herring, *Mechanisms responsible for the promoter-specific effects of myocardin.* J Biol Chem, 2005. **280**(11): p. 10861-9.
43. Kimura, T.E., et al., *Inhibition of Egr1 expression underlies the anti-mitogenic effects of cAMP in vascular smooth muscle cells.* Journal of molecular and cellular cardiology, 2014. **72**(100): p. 9-19.
44. Alexander, M.R. and G.K. Owens, *Epigenetic control of smooth muscle cell differentiation and phenotypic switching in vascular development and disease.* Annu Rev Physiol, 2012. **74**: p. 13-40.
45. Yoshida, T., et al., *Smooth muscle-selective inhibition of nuclear factor-kappaB attenuates smooth muscle phenotypic switching and neointima formation following vascular injury.* J Am Heart Assoc, 2013. **2**(3): p. e000230.
46. Parmacek, M.S., *Myocardin: dominant driver of the smooth muscle cell contractile phenotype.* Arterioscler Thromb Vasc Biol, 2008. **28**(8): p. 1416-7.
47. Basatemur, G.L., et al., *Vascular smooth muscle cells in atherosclerosis.* Nature Reviews Cardiology, 2019.
48. Takahashi, K., et al., *Induction of pluripotent stem cells from adult human fibroblasts by defined factors.* Cell, 2007. **131**(5): p. 861-72.
49. Liu, Y., et al., *Kruppel-like factor 4 abrogates myocardin-induced activation of smooth muscle gene expression.* J Biol Chem, 2005. **280**(10): p. 9719-27.
50. Owens, G.K., *Regulation of differentiation of vascular smooth muscle cells.* Physiol Rev, 1995. **75**(3): p. 487-517.
51. Bentzon, J.F., et al., *Smooth muscle cells healing atherosclerotic plaque disruptions are of local, not blood, origin in apolipoprotein E knockout mice.* Circulation, 2007. **116**(18): p. 2053-61.
52. Bennett, M.R., S. Sinha, and G.K. Owens, *Vascular Smooth Muscle Cells in Atherosclerosis.* Circ Res, 2016. **118**(4): p. 692-702.
53. Wang, Y., et al., *Smooth Muscle Cells Contribute the Majority of Foam Cells in ApoE (Apolipoprotein E)-Deficient Mouse Atherosclerosis.* Arteriosclerosis, Thrombosis, and Vascular Biology, 2019. **39**(5): p. 876-887.
54. Albarran-Juarez, J., et al., *Lineage tracing of cells involved in atherosclerosis.* Atherosclerosis, 2016. **251**: p. 445-53.

55. Gomez, D., et al., *Detection of histone modifications at specific gene loci in single cells in histological sections.* Nat Methods, 2013. **10**(2): p. 171-7.
56. Misra, A., et al., *Integrin beta3 regulates clonality and fate of smooth muscle-derived atherosclerotic plaque cells.* Nature Communications, 2018. **9**(1): p. 2073.
57. Feil, S., et al., *Transdifferentiation of Vascular Smooth Muscle Cells to Macrophage-Like Cells During Atherogenesis.* Circulation Research, 2014. **115**(7): p. 662-667.
58. Chappell, J., et al., *Extensive Proliferation of a Subset of Differentiated, yet Plastic, Medial Vascular Smooth Muscle Cells Contributes to Neointimal Formation in Mouse Injury and Atherosclerosis Models.* Circ Res, 2016. **119**(12): p. 1313-1323.
59. Allahverdian, S., et al., *Contribution of intimal smooth muscle cells to cholesterol accumulation and macrophage-like cells in human atherosclerosis.* Circulation, 2014. **129**(15): p. 1551-9.
60. Gomez, D. and G.K. Owens, *Smooth muscle cell phenotypic switching in atherosclerosis.* Cardiovascular Research, 2012. **95**(2): p. 156-164.
61. Yu, H., et al., *Bone marrow-derived smooth muscle-like cells are infrequent in advanced primary atherosclerotic plaques but promote atherosclerosis.* Arterioscler Thromb Vasc Biol, 2011. **31**(6): p. 1291-9.
62. Oparil, S., et al., *Hypertension.* Nature Reviews Disease Primers, 2018. **4**: p. 18014.
63. Bakris, G.L. and M.J. Sorrentino, *Hypertension : a companion to Braunwald's heart disease.* 2018.
64. Yaribeygi, H., et al., *The impact of stress on body function: A review.* EXCLI journal, 2017. **16**: p. 1057-1072.
65. Brown, I.A.M., et al., *Vascular Smooth Muscle Remodeling in Conductive and Resistance Arteries in Hypertension.* Arteriosclerosis, Thrombosis, and Vascular Biology, 2018. **38**(9): p. 1969-1985.
66. Rizzoni, D., et al., *Prognostic Significance of Small-Artery Structure in Hypertension.* Circulation, 2003. **108**(18): p. 2230-2235.
67. Hamet, P., et al., *Vascular smooth muscle cell hyper-responsiveness to growth factors in hypertension.* J Hypertens Suppl, 1988. **6**(4): p. S36-9.
68. Hayashi, K. and T. Naiki, *Adaptation and remodeling of vascular wall; biomechanical response to hypertension.* J Mech Behav Biomed Mater, 2009. **2**(1): p. 3-19.
69. Lemarie, C.A., P.L. Tharaux, and S. Lehoux, *Extracellular matrix alterations in hypertensive vascular remodeling.* J Mol Cell Cardiol, 2010. **48**(3): p. 433-9.
70. Wynne, B.M., C.-W. Chiao, and R.C. Webb, *Vascular smooth muscle cell signaling mechanisms for contraction to angiotensin II and endothelin-1.* Journal of the American Society of Hypertension, 2009. **3**(2): p. 84-95.
71. Touyz, R.M., et al., *Mitogen-activated protein/extracellular signal-regulated kinase inhibition attenuates angiotensin II-mediated signaling and contraction in spontaneously hypertensive rat vascular smooth muscle cells.* Circ Res, 1999. **84**(5): p. 505-15.
72. Montezano, A.C., et al., *Vascular smooth muscle cell differentiation to an osteogenic phenotype involves TRPM7 modulation by magnesium.* Hypertension, 2010. **56**(3): p. 453-62.

73. Zhou, N., et al., *Inhibition of SRF/myocardin reduces aortic stiffness by targeting vascular smooth muscle cell stiffening in hypertension.* Cardiovasc Res, 2017. **113**(2): p. 171-182.
74. Zhou, N., et al., *Rho Kinase Regulates Aortic Vascular Smooth Muscle Cell Stiffness Via Actin/SRF/Myocardin in Hypertension.* Cell Physiol Biochem, 2017. **44**(2): p. 701-715.
75. Zhang, Y. and S. Wu, *Effects of fasudil on pulmonary hypertension in clinical practice.* Pulm Pharmacol Ther, 2017. **46**: p. 54-63.
76. Touyz, R.M., et al., *Vascular smooth muscle contraction in hypertension.* Cardiovasc Res, 2018. **114**(4): p. 529-539.
77. Pierce, K.L., R.T. Premont, and R.J. Lefkowitz, *Seven-transmembrane receptors.* Nat Rev Mol Cell Biol, 2002. **3**(9): p. 639-50.
78. Fredriksson, R., et al., *The G-Protein-Coupled Receptors in the Human Genome Form Five Main Families. Phylogenetic Analysis, Paralogon Groups, and Fingerprints.* Molecular Pharmacology, 2003. **63**(6): p. 1256-1272.
79. Tang, X.L., et al., *Orphan G protein-coupled receptors (GPCRs): biological functions and potential drug targets.* Acta Pharmacol Sin, 2012. **33**(3): p. 363-71.
80. Rask-Andersen, M., M.S. Almen, and H.B. Schioth, *Trends in the exploitation of novel drug targets.* Nat Rev Drug Discov, 2011. **10**(8): p. 579-90.
81. Ngo, T., et al., *Identifying ligands at orphan GPCRs: current status using structure-based approaches.* Br J Pharmacol, 2016.
82. Wise, A., S.C. Jupe, and S. Rees, *The identification of ligands at orphan G-protein coupled receptors.* Annu Rev Pharmacol Toxicol, 2004. **44**: p. 43-66.
83. Sriram, K. and P.A. Insel, *G Protein-Coupled Receptors as Targets for Approved Drugs: How Many Targets and How Many Drugs?* Mol Pharmacol, 2018. **93**(4): p. 251-258.
84. Rosenbaum, D.M., S.G. Rasmussen, and B.K. Kobilka, *The structure and function of G-protein-coupled receptors.* Nature, 2009. **459**(7245): p. 356-63.
85. Dorsam, R.T. and J.S. Gutkind, *G-protein-coupled receptors and cancer.* Nat Rev Cancer, 2007. **7**(2): p. 79-94.
86. Wettschureck, N. and S. Offermanns, *Mammalian G proteins and their cell type specific functions.* Physiol Rev, 2005. **85**(4): p. 1159-204.
87. Lappano, R. and M. Maggiolini, *G protein-coupled receptors: novel targets for drug discovery in cancer.* Nat Rev Drug Discov, 2011. **10**(1): p. 47-60.
88. Insel, P.A., et al., *Impact of GPCRs in clinical medicine: monogenic diseases, genetic variants and drug targets.* Biochim Biophys Acta, 2007. **1768**(4): p. 994-1005.
89. Salazar, N.C., J. Chen, and H.A. Rockman, *Cardiac GPCRs: GPCR signaling in healthy and failing hearts.* Biochim Biophys Acta, 2007. **1768**(4): p. 1006-18.
90. Heng, B.C., D. Aubel, and M. Fussenegger, *An overview of the diverse roles of G-protein coupled receptors (GPCRs) in the pathophysiology of various human diseases.* Biotechnol Adv, 2013. **31**(8): p. 1676-94.

91. O'Hayre, M., M.S. Degese, and J.S. Gutkind, *Novel insights into G protein and G protein-coupled receptor signaling in cancer.* Curr Opin Cell Biol, 2014. **27**: p. 126-35.
92. Montaner, S., et al., *Molecular mechanisms deployed by virally encoded G protein-coupled receptors in human diseases.* Annu Rev Pharmacol Toxicol, 2013. **53**: p. 331-54.
93. Fredriksson, R., et al., *The G-protein-coupled receptors in the human genome form five main families. Phylogenetic analysis, paralogon groups, and fingerprints.* Mol Pharmacol, 2003. **63**(6): p. 1256-72.
94. Kakarala, K.K. and K. Jamil, *Sequence-structure based phylogeny of GPCR Class A Rhodopsin receptors.* Mol Phylogenet Evol, 2014. **74**: p. 66-96.
95. Hollenstein, K., et al., *Insights into the structure of class B GPCRs.* Trends Pharmacol Sci, 2014. **35**(1): p. 12-22.
96. Chun, L., W.H. Zhang, and J.F. Liu, *Structure and ligand recognition of class C GPCRs.* Acta Pharmacol Sin, 2012. **33**(3): p. 312-23.
97. Dijksterhuis, J.P., J. Petersen, and G. Schulte, *WNT/Frizzled signalling: receptor-ligand selectivity with focus on FZD-G protein signalling and its physiological relevance: IUPHAR Review 3.* Br J Pharmacol, 2014. **171**(5): p. 1195-209.
98. Bjarnadottir, T.K., R. Fredriksson, and H.B. Schioth, *The adhesion GPCRs: a unique family of G protein-coupled receptors with important roles in both central and peripheral tissues.* Cell Mol Life Sci, 2007. **64**(16): p. 2104-19.
99. Birnbaumer, L., *Signal Transduction by G Proteins: Basic Principles, Molecular Diversity, and Structural Basis of Their Actions*, in *Handbook of Cell Signaling (Second Edition)*, R.A. Bradshaw and E.A. Dennis, Editors. 2010, Academic Press: San Diego. p. 1597-1614.
100. Lambright, D.G., *Heterotrimeric G-Protein Signaling at Atomic Resolution*, in *Handbook of Cell Signaling (Second Edition)*, R.A. Bradshaw and E.A. Dennis, Editors. 2010, Academic Press: San Diego. p. 1615-1619.
101. Sunahara, R.K., C.W. Dessauer, and A.G. Gilman, *Complexity and diversity of mammalian adenylyl cyclases.* Annu Rev Pharmacol Toxicol, 1996. **36**: p. 461-80.
102. Turan, S. and M. Bastepe, *The GNAS complex locus and human diseases associated with loss-of-function mutations or epimutations within this imprinted gene.* Horm Res Paediatr, 2013. **80**(4): p. 229-41.
103. Plagge, A., G. Kelsey, and E.L. Germain-Lee, *Physiological functions of the imprinted Gnas locus and its protein variants Galpha(s) and XLalpha(s) in human and mouse.* J Endocrinol, 2008. **196**(2): p. 193-214.
104. Lefkowitz, R.J., *Seven transmembrane receptors: something old, something new.* Acta Physiol (Oxf), 2007. **190**(1): p. 9-19.
105. Rhee, S.G., *Regulation of phosphoinositide-specific phospholipase C.* Annu Rev Biochem, 2001. **70**: p. 281-312.
106. Kurose, H., *Galpha12 and Galpha13 as key regulatory mediator in signal transduction.* Life Sci, 2003. **74**(2-3): p. 155-61.
107. Maguire, J.J. and A.P. Davenport, *Regulation of vascular reactivity by established and emerging GPCRs.* Trends in Pharmacological Sciences, 2005. **26**(9): p. 448-454.

108. Somlyo, A.P. and A.V. Somlyo, *Signal transduction and regulation in smooth muscle.* Nature, 1994. **372**(6503): p. 231-6.
109. Kauffenstein, G., et al., *Emerging role of G protein-coupled receptors in microvascular myogenic tone.* Cardiovascular Research, 2012. **95**(2): p. 223-232.
110. Triggle, C.R., et al., *The endothelium in health and disease--a target for therapeutic intervention.* J Smooth Muscle Res, 2003. **39**(6): p. 249-67.
111. Chun, J., et al., *International Union of Basic and Clinical Pharmacology. LXXVIII. Lysophospholipid Receptor Nomenclature.* Pharmacological Reviews, 2010. **62**(4): p. 579-587.
112. Walsh, M.P., *Vascular smooth muscle myosin light chain diphosphorylation: mechanism, function, and pathological implications.* IUBMB Life, 2011. **63**(11): p. 987-1000.
113. Offermanns, S. and W. Rosenthal, *Encyclopedia of molecular pharmacology.* 2008.
114. Somlyo, A.P. and A.V. Somlyo, *Ca2+ sensitivity of smooth muscle and nonmuscle myosin II: modulated by G proteins, kinases, and myosin phosphatase.* Physiol Rev, 2003. **83**(4): p. 1325-58.
115. Gohla, A., G. Schultz, and S. Offermanns, *Role for G(12)/G(13) in agonist-induced vascular smooth muscle cell contraction.* Circ Res, 2000. **87**(3): p. 221-7.
116. Siehler, S., *Regulation of RhoGEF proteins by G12/13-coupled receptors.* Br J Pharmacol, 2009. **158**(1): p. 41-9.
117. Wirth, A. and S. Offermanns, *G-Protein-Coupled Receptors in Smooth Muscle*, in *Muscle - Fundamental Biology and Mechanisms of Disease*. 2012, Elsevier. p. 1145-1153.
118. Wilson, R.J. and H. Giles, *Piglet saphenous vein contains multiple relaxatory prostanoid receptors: evidence for EP4, EP2, DP and IP receptor subtypes.* Br J Pharmacol, 2005. **144**(3): p. 405-15.
119. Frolich, J.C., *Prostacyclin in hypertension.* J Hypertens Suppl, 1990. **8**(4): p. S73-8.
120. Tanaka, Y., K. Koike, and L. Toro, *MaxiK channel roles in blood vessel relaxations induced by endothelium-derived relaxing factors and their molecular mechanisms.* J Smooth Muscle Res, 2004. **40**(4-5): p. 125-53.
121. Gurevich, V.V. and E.V. Gurevich, *Molecular Mechanisms of GPCR Signaling: A Structural Perspective.* Int J Mol Sci, 2017. **18**(12).
122. Pavlos, N.J. and P.A. Friedman, *GPCR Signaling and Trafficking: The Long and Short of It.* Trends Endocrinol Metab, 2017. **28**(3): p. 213-226.
123. Jong, Y.I., S.K. Harmon, and K.L. O'Malley, *Intracellular GPCRs Play Key Roles in Synaptic Plasticity.* ACS Chem Neurosci, 2018. **9**(9): p. 2162-2172.
124. Griendling, K.K., et al., *Angiotensin II Signaling in Vascular Smooth Muscle.* Hypertension, 1997. **29**(1): p. 366-370.
125. Dinh, D.T., et al., *Angiotensin receptors: distribution, signalling and function.* Clin Sci (Lond), 2001. **100**(5): p. 481-92.
126. Matavelli, L.C. and H.M. Siragy, *AT2 receptor activities and pathophysiological implications.* J Cardiovasc Pharmacol, 2015. **65**(3): p. 226-32.

127. Padia, S.H. and R.M. Carey, *AT2 receptors: beneficial counter-regulatory role in cardiovascular and renal function.* Pflugers Arch, 2013. **465**(1): p. 99-110.
128. Higuchi, S., et al., *Angiotensin II signal transduction through the AT1 receptor: novel insights into mechanisms and pathophysiology.* Clin Sci (Lond), 2007. **112**(8): p. 417-28.
129. D'Ocon, P., *Phenylephrine*, in *Reference Module in Biomedical Sciences*. 2017, Elsevier.
130. Mei, Y., et al., *The Regulatory Role of the Adrenergic Agonists Phenylephrine and Isoproterenol on Fetal Hemoglobin Expression and Erythroid Differentiation.* Endocrinology, 2013. **154**(12): p. 4640-4649.
131. Kamal, F.A., J.G. Travers, and B.C. Blaxall, *G Protein–Coupled Receptor Kinases in Cardiovascular Disease: Why "Where" Matters.* Trends in Cardiovascular Medicine, 2012. **22**(8): p. 213-219.
132. Haskins, S.C., *Catecholamines*, in *Small Animal Critical Care Medicine (Second Edition)*, D.C. Silverstein and K. Hopper, Editors. 2015, W.B. Saunders: St. Louis. p. 829-835.
133. Exton, J.H., *Mechanisms involved in alpha-adrenergic phenomena.* Am J Physiol, 1985. **248**(6 Pt 1): p. E633-47.
134. Faber, J.E., N. Yang, and X. Xin, *Expression of alpha-adrenoceptor subtypes by smooth muscle cells and adventitial fibroblasts in rat aorta and in cell culture.* J Pharmacol Exp Ther, 2001. **298**(2): p. 441-52.
135. Zhang, H. and J.E. Faber, *Trophic effect of norepinephrine on arterial intima-media and adventitia is augmented by injury and mediated by different alpha1-adrenoceptor subtypes.* Circ Res, 2001. **89**(9): p. 815-22.
136. Teeters, J.C., et al., *Systemic alpha 1A-adrenoceptor antagonist inhibits neointimal growth after balloon injury of rat carotid artery.* Am J Physiol Heart Circ Physiol, 2003. **284**(1): p. H385-92.
137. Abramovitz, M., et al., *The utilization of recombinant prostanoid receptors to determine the affinities and selectivities of prostaglandins and related analogs.* Biochim Biophys Acta, 2000. **1483**(2): p. 285-93.
138. Sachinidis, A., et al., *Thromboxane A2 and Vascular Smooth Muscle Cell Proliferation.* Hypertension, 1995. **26**(5): p. 771-780.
139. Nakahata, N., *Thromboxane A2: physiology/pathophysiology, cellular signal transduction and pharmacology.* Pharmacol Ther, 2008. **118**(1): p. 18-35.
140. Gabrielsen, A., et al., *Thromboxane synthase expression and thromboxane A2 production in the atherosclerotic lesion.* J Mol Med (Berl), 2010. **88**(8): p. 795-806.
141. Ting, H.J., et al., *Thromboxane A2 receptor: biology and function of a peculiar receptor that remains resistant for therapeutic targeting.* J Cardiovasc Pharmacol Ther, 2012. **17**(3): p. 248-59.
142. McAdam, B.F., et al., *Effect of regulated expression of human cyclooxygenase isoforms on eicosanoid and isoeicosanoid production in inflammation.* J Clin Invest, 2000. **105**(10): p. 1473-82.
143. Fitzgerald, D.J., et al., *Thromboxane A2 synthesis in pregnancy-induced hypertension.* Lancet, 1990. **335**(8692): p. 751-4.
144. Norel, X., *Prostanoid receptors in the human vascular wall.* ScientificWorldJournal, 2007. **7**: p. 1359-74.

145. Offermanns, S., *Activation of Platelet Function Through G Protein–Coupled Receptors.* Circulation Research, 2006. **99**(12): p. 1293-1304.
146. Procaccini, D.E., J.E. Sawyer, and K.M. Watt, *Pharmacology of Cardiovascular Drugs*, in *Critical Heart Disease in Infants and Children (Third Edition)*, R.M. Ungerleider, et al., Editors. 2019, Elsevier: Philadelphia. p. 192-212.e6.
147. Johnson, M., *Molecular mechanisms of β2-adrenergic receptor function, response, and regulation.* Journal of Allergy and Clinical Immunology, 2006. **117**(1): p. 18-24.
148. Pelat, M., et al., *High Isoproterenol Doses Are Required to Activate β3-Adrenoceptor-Mediated Functions in Dogs.* Journal of Pharmacology and Experimental Therapeutics, 2003. **304**(1): p. 246-253.
149. Werstiuk, E.S. and R.M. Lee, *Vascular beta-adrenoceptor function in hypertension and in ageing.* Can J Physiol Pharmacol, 2000. **78**(6): p. 433-52.
150. McGraw, D.W. and S.B. Liggett, *Molecular mechanisms of beta2-adrenergic receptor function and regulation.* Proceedings of the American Thoracic Society, 2005. **2**(4): p. 292-312.
151. Meyer-Kirchrath, J., et al., *Gene expression profile of the Gs-coupled prostacyclin receptor in human vascular smooth muscle cells.* Biochemical Pharmacology, 2004. **67**(4): p. 757-765.
152. Smith, W.L., *Prostaglandin biosynthesis and its compartmentation in vascular smooth muscle and endothelial cells.* Annu Rev Physiol, 1986. **48**: p. 251-62.
153. Stitham, J., et al., *Prostacyclin: an inflammatory paradox.* Front Pharmacol, 2011. **2**: p. 24.
154. Narumiya, S., Y. Sugimoto, and F. Ushikubi, *Prostanoid receptors: structures, properties, and functions.* Physiol Rev, 1999. **79**(4): p. 1193-226.
155. Fetalvero, K.M., et al., *The prostacyclin receptor induces human vascular smooth muscle cell differentiation via the protein kinase A pathway.* Am J Physiol Heart Circ Physiol, 2006. **290**(4): p. H1337-46.
156. Murata, T., et al., *Altered pain perception and inflammatory response in mice lacking prostacyclin receptor.* Nature, 1997. **388**(6643): p. 678-82.
157. Jones, R.L., et al., *Relaxant Actions of Nonprostanoid Prostacyclin Mimetics on Human Pulmonary Artery.* Journal of Cardiovascular Pharmacology, 1997. **29**(4): p. 525-535.
158. Baxter, G.S., et al., *Characterization of the prostanoid receptors mediating constriction and relaxation of human isolated uterine artery.* British Journal of Pharmacology, 1995. **116**(1): p. 1692-1696.
159. Walch, L., et al., *Prostanoid receptors involved in the relaxation of human pulmonary vessels.* British Journal of Pharmacology, 1999. **126**(4): p. 859-866.
160. Tanaka, Y., et al., *New insights into the intracellular mechanisms by which PGI2 analogues elicit vascular relaxation: cyclic AMP-independent, Gs-protein mediated-activation of MaxiK channel.* Curr Med Chem Cardiovasc Hematol Agents, 2004. **2**(3): p. 257-65.
161. Wikström, K., et al., *Differential regulation of RhoA-mediated signaling by the TPα and TPβ isoforms of the human thromboxane A2 receptor:*

Independent modulation of TPα signaling by prostacyclin and nitric oxide. Cellular Signalling, 2008. **20**(8): p. 1497-1512.
162. Bley, K.R., et al., *RO1138452 and RO3244794: characterization of structurally distinct, potent and selective IP (prostacyclin) receptor antagonists.* British Journal of Pharmacology, 2006. **147**(3): p. 335-345.
163. Jones, R.L., et al., *Investigation of the prostacyclin (IP) receptor antagonist RO1138452 on isolated blood vessel and platelet preparations.* Br J Pharmacol, 2006. **149**(1): p. 110-20.
164. Hahn, A.W., et al., *Effects of endothelin-1 on vascular smooth muscle cell phenotypic differentiation.* J Cardiovasc Pharmacol, 1992. **20 Suppl 12**: p. S33-6.
165. Kim, M.R., et al., *Thromboxane a(2) induces differentiation of human mesenchymal stem cells to smooth muscle-like cells.* Stem Cells, 2009. **27**(1): p. 191-9.
166. Wamhoff, B.R., et al., *L-type voltage-gated Ca2+ channels modulate expression of smooth muscle differentiation marker genes via a rho kinase/myocardin/SRF-dependent mechanism.* Circ Res, 2004. **95**(4): p. 406-14.
167. Olson, E.N. and A. Nordheim, *Linking actin dynamics and gene transcription to drive cellular motile functions.* Nat Rev Mol Cell Biol, 2010. **11**(5): p. 353-65.
168. Althoff, T.F., et al., *Procontractile G protein-mediated signaling pathways antagonistically regulate smooth muscle differentiation in vascular remodeling.* J Exp Med, 2012. **209**(12): p. 2277-90.
169. Lockman, K., et al., *Sphingosine 1-phosphate stimulates smooth muscle cell differentiation and proliferation by activating separate serum response factor co-factors.* J Biol Chem, 2004. **279**(41): p. 42422-30.
170. Kojima, Y., et al., *Upregulation of the apelin-APJ pathway promotes neointima formation in the carotid ligation model in mouse.* Cardiovasc Res, 2010. **87**(1): p. 156-65.
171. Klemm, D.J., et al., *cAMP response element-binding protein content is a molecular determinant of smooth muscle cell proliferation and migration.* J Biol Chem, 2001. **276**(49): p. 46132-41.
172. Zucker, T.P., et al., *Tolerance development to antimitogenic actions of prostacyclin but not of prostaglandin E1 in coronary artery smooth muscle cells.* Eur J Pharmacol, 1998. **345**(2): p. 213-20.
173. Blindt, R., et al., *Activation of IP and EP(3) receptors alters cAMP-dependent cell migration.* Eur J Pharmacol, 2002. **444**(1-2): p. 31-7.
174. Wootten, D., A. Christopoulos, and P.M. Sexton, *Emerging paradigms in GPCR allostery: implications for drug discovery.* Nat Rev Drug Discov, 2013. **12**(8): p. 630-44.
175. Regard, J.B., I.T. Sato, and S.R. Coughlin, *Anatomical profiling of G protein-coupled receptor expression.* Cell, 2008. **135**(3): p. 561-71.
176. Kaur, H., et al., *Single-cell profiling reveals heterogeneity and functional patterning of GPCR expression in the vascular system.* Nat Commun, 2017. **8**: p. 15700.
177. Brauner-Osborne, H. and P. Krogsgaard-Larsen, *Sequence and expression pattern of a novel human orphan G-protein-coupled receptor, GPRC5B, a family C receptor with a short amino-terminal domain.* Genomics, 2000. **65**(2): p. 121-8.

178. Robbins, M.J., et al., *Molecular cloning and characterization of two novel retinoic acid-inducible orphan G-protein-coupled receptors (GPRC5B and GPRC5C).* Genomics, 2000. **67**(1): p. 8-18.
179. Sano, T., et al., *Comparative characterization of GPRC5B and GPRC5C LacZ knockin mice; behavioral abnormalities in GPRC5B-deficient mice.* Biochemical and Biophysical Research Communications, 2011. **412**(3): p. 460-465.
180. Kurabayashi, N., M.D. Nguyen, and K. Sanada, *The G protein-coupled receptor GPRC5B contributes to neurogenesis in the developing mouse neocortex.* Development, 2013. **140**(21): p. 4335-4346.
181. Kim, Y.-J., et al., *GPRC5B Activates Obesity-Associated Inflammatory Signaling in Adipocytes.* Science Signaling, 2012. **5**(251): p. ra85-ra85.
182. Soni, A., et al., *GPRC5B a putative glutamate-receptor candidate is negative modulator of insulin secretion.* Biochemical and Biophysical Research Communications, 2013. **441**(3): p. 643-648.
183. von Samson-Himmelstjerna, F.A., et al., *The orphan receptor GPRC5B modulates inflammatory and fibrotic pathways in cardiac fibroblasts and mice hearts.* Biochemical and Biophysical Research Communications, 2019. **514**(4): p. 1198-1203.
184. Piedrahita, J.A., et al., *Generation of mice carrying a mutant apolipoprotein E gene inactivated by gene targeting in embryonic stem cells.* Proceedings of the National Academy of Sciences of the United States of America, 1992. **89**(10): p. 4471-4475.
185. Muzumdar, M.D., et al., *A global double-fluorescent Cre reporter mouse.* Genesis, 2007. **45**(9): p. 593-605.
186. Smyth, E.M., et al., *Internalization and sequestration of the human prostacyclin receptor.* J Biol Chem, 2000. **275**(41): p. 32037-45.
187. Zindel, D., et al., *Engineered hyperphosphorylation of the β2-adrenoceptor prolongs arrestin-3 binding and induces arrestin internalization.* Molecular pharmacology, 2015. **87**(2): p. 349-362.
188. Morgado, M., et al., *Cyclic nucleotide-dependent relaxation pathways in vascular smooth muscle.* Cell Mol Life Sci, 2012. **69**(2): p. 247-66.
189. Dorsch, S., et al., *Analysis of receptor oligomerization by FRAP microscopy.* Nat Methods, 2009. **6**(3): p. 225-30.
190. Salmon, M., et al., *Cooperative binding of KLF4, pELK-1, and HDAC2 to a G/C repressor element in the SM22alpha promoter mediates transcriptional silencing during SMC phenotypic switching in vivo.* Circ Res, 2012. **111**(6): p. 685-96.
191. Aboyans, V., P. Lacroix, and M.H. Criqui, *Large and Small Vessels Atherosclerosis: Similarities and Differences.* Progress in Cardiovascular Diseases, 2007. **50**(2): p. 112-125.
192. George, S.R., B.F. O'Dowd, and S.P. Lee, *G-protein-coupled receptor oligomerization and its potential for drug discovery.* Nat Rev Drug Discov, 2002. **1**(10): p. 808-20.
193. Angers, S., A. Salahpour, and M. Bouvier, *Dimerization: an emerging concept for G protein-coupled receptor ontogeny and function.* Annu Rev Pharmacol Toxicol, 2002. **42**: p. 409-35.
194. Milligan, G., *G protein-coupled receptor dimerization: function and ligand pharmacology.* Mol Pharmacol, 2004. **66**(1): p. 1-7.

195. Milligan, G., *G protein-coupled receptor hetero-dimerization: contribution to pharmacology and function.* Br J Pharmacol, 2009. **158**(1): p. 5-14.
196. Lohse, M.J., *Dimerization in GPCR mobility and signaling.* Curr Opin Pharmacol, 2010. **10**(1): p. 53-8.
197. Pin, J.P., T. Galvez, and L. Prezeau, *Evolution, structure, and activation mechanism of family 3/C G-protein-coupled receptors.* Pharmacol Ther, 2003. **98**(3): p. 325-54.
198. Park, J., et al., *Structural architecture of a dimeric class C GPCR based on co-trafficking of sweet taste receptor subunits.* J Biol Chem, 2019. **294**(13): p. 4759-4774.
199. Møller, T.C., et al., *Class C G protein-coupled receptors: reviving old couples with new partners.* Biophysics Reports, 2017. **3**(4): p. 57-63.
200. Gurevich, V.V. and E.V. Gurevich, *How and why do GPCRs dimerize?* Trends Pharmacol Sci, 2008. **29**(5): p. 234-40.
201. Margeta-Mitrovic, M., Y.N. Jan, and L.Y. Jan, *A trafficking checkpoint controls GABA(B) receptor heterodimerization.* Neuron, 2000. **27**(1): p. 97-106.
202. Calver, A.R., C.H. Davies, and M. Pangalos, *GABA(B) receptors: from monogamy to promiscuity.* Neurosignals, 2002. **11**(6): p. 299-314.
203. Milligan, G., *G protein-coupled receptor hetero-dimerization: contribution to pharmacology and function.* British Journal of Pharmacology, 2009. **158**(1): p. 5-14.
204. Robbins, M.J., et al., *GABA(B2) is essential for g-protein coupling of the GABA(B) receptor heterodimer.* J Neurosci, 2001. **21**(20): p. 8043-52.
205. Lagerström, M.C. and H.B. Schiöth, *Structural diversity of G protein-coupled receptors and significance for drug discovery.* Nature Reviews Drug Discovery, 2008. **7**: p. 339.
206. Smyth, E.M. and G.A. FitzGerald, *Human prostacyclin receptor.* Vitam Horm, 2002. **65**: p. 149-65.
207. Kobayashi, T., F. Ushikubi, and S. Narumiya, *Amino acid residues conferring ligand binding properties of prostaglandin I and prostaglandin D receptors. Identification by site-directed mutagenesis.* J Biol Chem, 2000. **275**(32): p. 24294-303.
208. Carrillo, J.J., J.F. López-Giménez, and G. Milligan, *Multiple Interactions between Transmembrane Helices Generate the Oligomeric α_{1b}-Adrenoceptor.* Molecular Pharmacology, 2004. **66**(5): p. 1123-1137.
209. Lee, S.P., et al., *D2 dopamine receptor homodimerization is mediated by multiple sites of interaction, including an intermolecular interaction involving transmembrane domain 4.* Biochemistry, 2003. **42**(37): p. 11023-31.
210. Giguere, V., et al., *Role of extracellular cysteine residues in dimerization/oligomerization of the human prostacyclin receptor.* Eur J Pharmacol, 2004. **494**(1): p. 11-22.
211. Arehart, E., et al., *Acceleration of cardiovascular disease by a dysfunctional prostacyclin receptor mutation: potential implications for cyclooxygenase-2 inhibition.* Circ Res, 2008. **102**(8): p. 986-93.
212. Ibrahim, S., et al., *Dominant negative actions of human prostacyclin receptor variant through dimerization: implications for cardiovascular disease.* Arterioscler Thromb Vasc Biol, 2010. **30**(9): p. 1802-9.

213. Majed, B.H. and R.A. Khalil, *Molecular Mechanisms Regulating the Vascular Prostacyclin Pathways and Their Adaptation during Pregnancy and in the Newborn.* Pharmacological Reviews, 2012. **64**(3): p. 540-582.
214. Guo, Y., et al., *The COX-2/PGI2 receptor axis plays an obligatory role in mediating the cardioprotection conferred by the late phase of ischemic preconditioning.* PLoS One, 2012. **7**(7): p. e41178.
215. Hocherl, K., et al., *Activation of the PGI(2)/IP system contributes to the development of circulatory failure in a rat model of endotoxic shock.* Hypertension, 2008. **52**(2): p. 330-5.
216. Villa, E., et al., *Acute effects of iloprost on blood pressure, heart rate, renal hemodynamics, diuresis, natriuresis, plasma renin activity and plasma norepinephrine in uninephrectomized hypertensive mongrel dogs.* J Hypertens Suppl, 1991. **9**(6): p. S352-3.
217. Fitzgerald, D.J., et al., *Decreased prostacyclin biosynthesis preceding the clinical manifestation of pregnancy-induced hypertension.* Circulation, 1987. **75**(5): p. 956-63.
218. Tuder, R.M., et al., *Prostacyclin synthase expression is decreased in lungs from patients with severe pulmonary hypertension.* Am J Respir Crit Care Med, 1999. **159**(6): p. 1925-32.
219. Yokoyama, C., et al., *Prostacyclin-deficient mice develop ischemic renal disorders, including nephrosclerosis and renal infarction.* Circulation, 2002. **106**(18): p. 2397-403.
220. Davis, T.L. and N.A. Sharif, *Pharmacological characterization of [(3)H]-prostaglandin E(2) binding to the cloned human EP(4) prostanoid receptor.* Br J Pharmacol, 2000. **130**(8): p. 1919-26.
221. Thibodeau, J.F., et al., *Vascular Smooth Muscle-Specific EP4 Receptor Deletion in Mice Exacerbates Angiotensin II-Induced Renal Injury.* Antioxid Redox Signal, 2016. **25**(12): p. 642-656.
222. Ross, R., *Atherosclerosis--an inflammatory disease.* N Engl J Med, 1999. **340**(2): p. 115-26.
223. Davis, R.J., et al., *EP4 prostanoid receptor-mediated vasodilatation of human middle cerebral arteries.* Br J Pharmacol, 2004. **141**(4): p. 580-5.
224. Cheng, Y., et al., *Role of Prostacyclin in the Cardiovascular Response to Thromboxane A₂.* Science, 2002. **296**(5567): p. 539-541.
225. Egan, K.M., et al., *COX-2-derived prostacyclin confers atheroprotection on female mice.* Science, 2004. **306**(5703): p. 1954-7.
226. Kobayashi, T., et al., *Roles of thromboxane A(2) and prostacyclin in the development of atherosclerosis in apoE-deficient mice.* J Clin Invest, 2004. **114**(6): p. 784-94.
227. Wharton, J., et al., *Prostacyclin analogues differentially inhibit growth of distal and proximal human pulmonary artery smooth muscle cells.* Circulation, 2000. **102**(25): p. 3130-6.
228. Banerjee, I., et al., *Determination of cell types and numbers during cardiac development in the neonatal and adult rat and mouse.* Am J Physiol Heart Circ Physiol, 2007. **293**(3): p. H1883-91.
229. Snider, P., et al., *Origin of cardiac fibroblasts and the role of periostin.* Circ Res, 2009. **105**(10): p. 934-47.
230. Camelliti, P., T.K. Borg, and P. Kohl, *Structural and functional characterisation of cardiac fibroblasts.* Cardiovasc Res, 2005. **65**(1): p. 40-51.

231. Chen, W. and N.G. Frangogiannis, *Fibroblasts in post-infarction inflammation and cardiac repair.* Biochim Biophys Acta, 2013. **4**: p. 945-53.
232. Harding, P. and D.B. Murray, *The contribution of prostaglandins versus prostacyclin in ventricular remodeling during heart failure.* Life Sciences, 2011. **89**(19): p. 671-676.
233. Chen, Y., et al., *Prostacyclin Analogue Beraprost Inhibits Cardiac Fibroblast Proliferation Depending on Prostacyclin Receptor Activation through a TGF β-Smad Signal Pathway.* PLOS ONE, 2014. **9**(5): p. e98483.
234. Gurgul-Convey, E., K. Hanzelka, and S. Lenzen, *Mechanism of Prostacyclin-Induced Potentiation of Glucose-Induced Insulin Secretion.* Endocrinology, 2012. **153**(6): p. 2612-2622.
235. Arita, S., et al., *Increased islet viability by addition of beraprost sodium to collagenase solution.* Pancreas, 2001. **23**(1): p. 62-7.
236. Sun, X. and Q. Li, *Prostaglandin EP2 receptor: Novel therapeutic target for human cancers (Review).* Int J Mol Med, 2018. **42**(3): p. 1203-1214.
237. Kennedy, C.R., et al., *Salt-sensitive hypertension and reduced fertility in mice lacking the prostaglandin EP2 receptor.* Nat Med, 1999. **5**(2): p. 217-20.
238. Matsubara, S., et al., *Heterodimerization of the prostaglandin E2 receptor EP2 and the calcitonin receptor CTR.* PLoS One, 2017. **12**(11): p. e0187711.

LIST OF PUBLICATIONS

Carvalho J, Chennupati R, Li R, Günther S, Kaur H, Zhao W, Tonack S, Kurz M, Mößlein N, Bünemann M, Offermanns S, Wettschureck N. Orphan G-protein-coupled receptor GPRC5B controls smooth muscle contractility and differentiation by inhibiting prostacyclin receptor signaling. (Manuscript in revision).

Leal J, Teixeira-Santos L, Pinho D, Afonso J, **Carvalho J**, Lourdes Bastos M, Albino-Teixeira A, Fraga S, Sousa T (2019). L-proline supplementation improves nitric oxide bioavailability and counteracts the blood pressure rise induced by angiotensin II in rats. Nitric Oxide, 2019. 82: p. 1-11.

Tischner D, Grimm M, Kaur H, Staudenraus D, **Carvalho J**, Looso M, Gunther S, Wanke F, Moos S, Siller N, Breuer J, Schwab N, Zipp F, Waisman A, Kurschus F C, Offermanns S, Wettschureck N, Single-cell profiling reveals GPCR heterogeneity and functional patterning during neuroinflammation. JCI Insight, 2017. 2(15).

Kaur H, **Carvalho J**, Looso M, Singh P, Chennupati R, Preussner J, Gunther S, Albarran-Juarez J, Tischner D, Classen S, Offermanns S and Wettschureck N. Single-cell profiling reveals heterogeneity and functional patterning of GPCR expression in the vascular system. Nat Commun. 2017, 8:15700.

Kaur H, Takefuji M, Ngai CY, **Carvalho J**, Bayer J, Wietelmann A, Poetsch A, Hoelper S, Conway SJ, Mollmann H, Looso M, Troidl C, Offermann S, Wettschureck N, Targeted Ablation of Periostin-Expressing Activated Fibroblasts Prevents Adverse Cardiac Remodeling in Mice. Circ Res, 2016. 118(12): p. 1906-17.

Reina-Couto M, Vale L, **Carvalho J**, Bettencourt P; Albino-Teixeira A, Sousa T. Resolving Inflammation in Heart Failure: Novel Protective Lipid Mediators. Current drug targets, 2016. 17(10): p. 1206-1223.

Carvalho J, Reina-Couto M, Valente MJ, Vale L, Afonso J, Carvalho F, Bettencourt P, Sousa T, Albino-Teixeira A. Impaired resolution of inflammation in human chronic heart failure. Eur J Clin Invest, 2014. 44(6): p. 527-38.

Rocha H, Ferreira R, **Carvalho J**, Vitorino R, Santa C, Lopes L, Gregersen N, Vilarinho L, Amado F. Characterization of mitochondrial proteome in a severe case of ETF-QO deficiency. J Proteomics, 2011. 75(1): p. 221-8.